A STUDY ON DURABILITY PROPERTIES OF ULTRA-HIGH PERFORMANCE CONCRETE (UHPC) UTILIZING LOCAL FINE QUARTZ SAND

BY

AHMED YOUSUF SHAREEF

A Thesis Presented to the

DEANSHIP OF GRADUATE STUDIES

KING FAHD UNIVERSITY OF PETROLEUM & MINERALS

DHAHRAN, SAUDI ARABIA

In Partial Fulfillment of the
Requirements for the Degree of

MASTER OF SCIENCE

In

CIVIL ENGINEERING

SEPTEMBER 2013

KING FAHD UNIVERSITY OF PETROLEUM AND MINERALS

DHAHRAN 31261, SAUDI ARABIA

DEANSHIP OF GRADUATE STUDIES

This thesis written by **AHMED YOUSUF SHAREEF** under the direction of his thesis advisor and approved by his thesis committee, has been presented to and accepted by the Dean of Graduate Studies, in partial fulfillment of the requirements for the degree of **MASTER OF SCIENCE IN CIVIL ENGINEERING.**

Thesis Committee

Dr. Shamshad Ahmad (Advisor)

Prof. Abul Kalam Azad (Co-advisor)

Prof. Omar S. Baghabra Al-Amoudi (Member)

Dr. Salah U. Al-Dulaijan (Member)

Dr. Ahmad Saad Al-Gahtani (Member)

16 DEC 2013

Prof. Nedal T. Ratrout
Departmental Chairman

Prof. Salam A. Zummo
Dean of Graduate Studies

23/12/13
Date

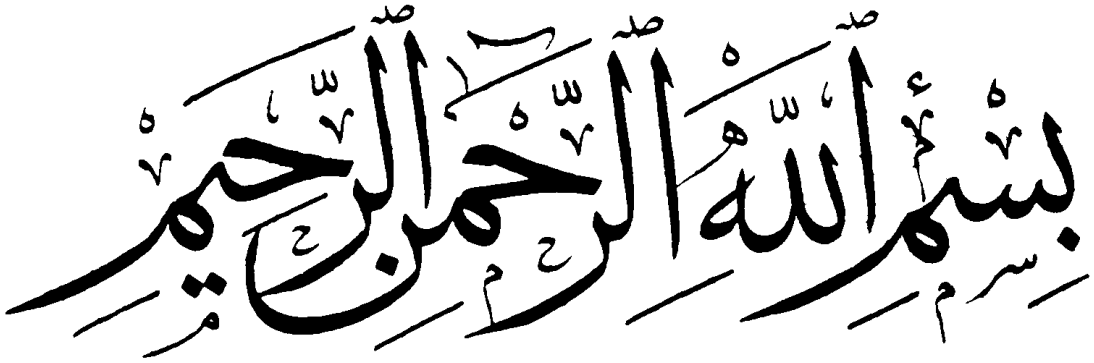

IN THE NAME OF ALLAH, THE MOST GRACIOUS, THE MOST MERCIFUL

DEDICATED

TO

MY FAMILY

ACKNOWLEDGEMENTS

All praise is due only to ALLAH subhana wa ta' aala, the sustainer of the worlds, the most merciful for granting me patience, health and knowledge to complete this work.

I would like to thank King Fahd University of Petroleum and Minerals for providing me the opportunity and financial assistance for pursuing MS program.

I acknowledge my sincere appreciation and thanks to Dr. Shamshad Ahmad for his supervision and guidance throughout this research. I am very much grateful to my co-advisor Prof. Abul Kalam Azad for his guidance and valuable time spent during all the stages of this work. I am grateful to my committee, Prof. Omar Al-Amoudi, Dr. Salah Al-Dulaijan and Dr. Ahmad Al-Gahtani for their guidance and cooperation. I am also indebted to the Department Chairman, Prof. Nedal Ratrout, and other faculty members especially Prof. Hussain Jubran Al-Gahtani and Prof. Mohammed Maslehuddin for their support.

I acknowledge the efforts and guidance of Mr. Mukarram Khan and Mr. Syed Imran Ali during the execution of my experimental work and thank them whole heartedly. I would also like to thank Mr. Mohammed Ibrahim, Mr. Mohammed Shameem and Mr. Mohammed Barry for their support during this work.

I would like to thank all my seniors and my friends Mr. Zubair, Saad Muhammad Saad khan, Umar, AbdulAzeem, Riyaz, Liaqat, Zia ul Haq, Mr. Fasi, Mr. Zabi, Mr. Minhaj and Mr. Naseer for always being there for me.

Lastly, special thanks are due to my parents for their sacrifices, efforts, prayers and encouragement during all the stages of my life.

TABLE OF CONTENTS

LIST OF TABLES

LIST OF FIGURES

THESIS ABSTRACT (ENGLISH)

Name: **AHMED YOUSUF SHAREEF**

Title: **A STUDY ON DURABILITY PROPERTIES OF ULTRA-HIGH PERFORMANCE CONCRETE (UHPC) UTILIZING LOCAL FINE QUARTZ SAND**

Degree: **MASTER OF SCIENCE**

Major Field: **CIVIL ENGINEERING**

Lack of good quality of coarse aggregates in many parts of Kingdom of Saudi Arabia is a major concern in producing high performance concrete. For the aggressive environmental conditions prevailing in the Arabian Gulf, there has been a growing interest in developing a new cementitious material possessing superior mechanical and durability properties. Reactive powder concrete, which is also called as ultra-high performance concrete (UHPC), has been recently reported to be an advanced concrete material having strength more than 150 MPa with both high ductility and durability. UHPC is prepared with high cement content, high dosage of superplasticizer, fine quartz sand, and fibers, maintaining a very low water/binder ratio. The coarse aggregate is entirely replaced by fine quartz sand which behaves as a self-placing material with excellent rheological properties.

It is found through literature review that a limited amount of research has been conducted on producing UHPC using locally available ingredients and evaluating performance of UHPC for local environmental conditions. In order to explore the possibility of producing UHPC using local fine quartz sand and evaluating the performance of the developed mixtures of UHPC, an integrated research work was conducted into two parts. First part consisted of preparing a set of 27 mixtures of UHPC according to 3^3 factorial experiment designs by varying the three key mix parameters (cement content, silica fume content and water/binder ratio) and testing the mixtures of the UHPC for mechanical properties. Second part of the work was to carry out tests on all mixtures for determining the durability properties.

This thesis is based on the second part of the project focusing on durability properties of the developed UHPC mixtures. The tests conducted to study the durability properties of UHPC mixtures included water penetration depth, chloride permeability, electrical resistivity, pH, sulfate attack, chloride diffusion coefficient and reinforcement corrosion rate tests. Very low values of water penetration depths and chloride permeability and very high values of electrical resistivity and pH recorded for all the mixtures of UHPC are indicative of high resistance of UHPC mixtures against reinforcement corrosion. The lack of evidence of active corrosion in almost all the mixtures of UHPC, as revealed by gravimetric and electrochemical monitoring for an exposure period of 15 months, also indicates the high resistance of these mixtures against reinforcement corrosion.

MASTER OF SCIENCE DEGREE
KING FAHD UNIVERSITY OF PETROLEUM AND MINERALS
Dhahran, Saudi Arabia

THESIS ABSTRACT (ARABIC)

ملخص الرسالة (باللغة العربية)

الإسم : أحمد يوسف شريف

عنوان الرسالة : دراسة خصائص الديمومة للخرسانة شديدة الصلابة باستخدام ركام ناعم محلي

التخصص : الهندسةالمدنية

الدرجة العلمية : ماجستير بالعلوم الهندسية

يؤثر نقص تواجد الركام الخشن الجيد في كثير من أنحاء المملكة على القدرة على الحصول على خرسانة بمواصفات جيدة. بسبب الظروف البيئة المحيطة القاسية في منطقة الخليج العربي فإن هناك إهتمام بالغ في تطوير مادة اسمنتية جديدة تمتلك مواصفات ميكانيكية أعلى كما أنها تمتلك خصائص الديمومة. تم توثيق خرسانة المسحوق المتفاعل والتي تسمى أيضا بالخرسانة شديدة الصلابة حديثا على أنها خطوة متقدمة في المادة الخرسانية التي تصل قوتها إلى أكثر من 150 ميجا باسكال مع إمتلاكها خصائص الليونة والديمومة. تتكون الخرسانة شديدة الصلابة من محتوى عالي من الإسمنت بالاضافة إلى مادة ملدِّنة، ركام ناعم، وألياف صناعية، مع الحفاظ على مستوى قليل من نسبة الماء المضاف مقارنة مع كمية الإسمنت. يتم إستبدال الركام الخشن كليا بالركام الناعم والذي يعمل كعامل مساعد في تشغيل الخرسانة بخصائص ريولوجية ممتازة.

من خلال الإبحاث السابقة، فإن هناك عدد محدود من الإبحاث الي تم إجرائها على الخرسانة شديدة الصلابة باستخدام مكونات محلية مع فحص أداء هذه الخرسانة في الظروف الجوية الموجودة، ومن أجل إستكشاف مدى إمكانية إنتاج هذا النوع من الخرسانة وفحص مدى فعالية هذه الخرسانه فإنه تم إجراء بحث متكامل على مرحلتين، يشمل الجزء الأول تحضير 27 عينة من الخرسانة شديدة الصلابة من خلال طريقة 3^3 تصميم التجربة ومن خلال تغيير العوامل الرئيسية الثلاثة التي تشمل نسبة الإسمنت وكمية السيليكا بالاضافة إلى نسبة الماء إلى المادة الاسمنتية، كما يشمل هذا الجزء فحص هذه العينات للحصول على الخصائص الميكانيكية. يشتمل الجزء الثاني من هذا البحث على فحص جميع العينات للحصول على خصائص الديمومة.

تم القيام بهذه الإطروحة بناء على الجزء التاني من هذا المشروع والذي يركز على تطوير خصائص الديمومة للخرسانة شديدة الصلابة. تم إجراء هذه الفحوصات لدراسة خصائص الإستادة للخرسانة شديدة الصلابة والتي تشمل عمق إختراق الماء، نفاذية الكلورايد، التوصيل الكهربائي، الرقم الهيدروجيني، وهجوم الكبريتات، معامل نشر الكلورايد، ومعدل تآكل حديد التسليح. قيم قليلة من عمق نفاذ الماء ونفاذية الكلورايد بالإضافة إلى قيم عالية للتوصيل الكهربائي والارقم اليدروجيني تم الحصول عليها لجميه هذه العينات والتي توضح قدرة هذه النوع من الخرسانة على مقاومة تآكل حديد التسليح. كما أنه لا يوجد دليل على حدوث أي تآكل نشط لجميع هذه العينات وبوسائل مراقبة ومتابعة كهربائية كيميائية لمدة 15 شهرا فإن هذه دليل ومؤشر على قدرة هذه الخرسانة على الحد من تآكل حديد التسليح.

ماجستير بالعلوم الهندسية
جامعة الملك فهد للبترول والمعادن
الظهران- المملكة العربية السعودية

CHAPTER 1

INTRODUCTION

1.1 BACKGROUND

Because of the lack of good quality coarse aggregates in many parts of the Kingdom of Saudi Arabia, it has been a challenging task to produce concrete with very high performance. Recently, advances in concrete technology have been reported in literature leading to the development of the ultra-high performance concrete (UHPC). Many a times, a combination of very low water to cementitious materials ratio, high cementitious materials content, silica fume or fly ash, steel or polymer fibers, filler materials and high dosage of superplasticizer are utilized to produce the UHPC. These developments could be utilized to produce UHPC utilizing local sand as fine aggregates.

The harsh environmental conditions prevailing in the coastal areas of the Arabian Gulf cause reinforcement corrosion that pose a serious threat to the durability of concrete structures. This causes safety problems and loss of resources. Furthermore, the local concrete also suffers from the use of marginal aggregates, leading to low strength and reduced durability. Thus, there is a need to develop UHPC utilizing local fine sand. Since the quality of coarse aggregates significantly affects the properties of the resulting concrete, the possibility of minimizing its use should be explored.

Developing a UHPC mixture, which is dense and impermeable, may improve durability in the following ways:

- High impermeability will reduce the penetration of corrosive species through concrete, thus delaying the initiation of reinforcement corrosion, and
- Since the compressive strength of UHPC is high, its bond strength and tensile strength are also expected to be increased. High tensile strength will resist the concrete cracking and high bond strength will resist the loss of load-bearing capacity of the member, even at a significant rate of reinforcement corrosion.

Therefore, there is a need for developing UHPC mixtures using the locally available materials, particularly the very good quality fine quartz sand. It is expected that the developed UHPC would be durable than the normal strength concrete, thereby significantly increasing the service-life of concrete structures subjected to harsh environmental conditions. This will save a lot of national resources and would be helpful in ensuring sustainable development.

1.2 NEED FOR THIS RESEARCH

Though enough information are available on the development of UHPC mixtures and evaluation of their mechanical properties, there is lack of data on durability properties of UHPC prepared utilizing the local fine aggregates, which is characterized as very fine with a low fineness modulus. Since the environmental conditions in many parts of the Kingdom of Saudi Arabia are very conducive for reinforcement corrosion and sulfate attack, for any new concrete material the durability study is very much needed for its acceptance.

1.3 OBJECTIVES

The general objective of this study was to study the durability properties of UHPC mixtures produced utilizing local fine quartz sand. The specific objectives are as follows:

i. To prepare a number of UHPC mixtures considering three mix variables;

ii. To assess the durability characteristics of the mixtures of UHPC;

iii. To identify optimum mixtures of UHPC based on durability performance and economic analysis;

1.4 THESIS ORGANIZATION

In order to accomplish the proposed objectives of the research a thesis organization was developed which was divided into 5 chapters. The content of each of these chapters is explained below.

Chapter 1: This chapter consists of the background of the thesis work, and a brief description for the need for this research is explained. Then, the thesis objectives are stated.

Chapter 2: In this chapter, a detailed literature review is presented. A brief description of UHPC is given. Development of UHPC (ultra-high performance concrete) is mentioned and the ingredients used therein are elaborated. Techniques adopted for optimizing the constituents of the UHPC are discussed. Mix design usually followed and the durability properties thus, obtained are summarized. Lastly, recent applications of UHPC are discussed.

Chapter 3: Chapter three presents in detail the ingredients used and their mix proportions. Mixing procedure adopted and preparation and casting of the samples are deeply

discussed. Lastly, the tests employed for UHPC, the equipment and procedures for carrying out these tests are discussed.

Chapter 4: In this chapter, the in-depth analysis and discussion of the results obtained are presented.

Chapter 5: This chapter has been dedicated to the conclusions and recommendations based on the discussion from the previous chapters.

CHAPTER 2

LITERATURE REVIEW

2.1 ULTRA HIGH PERFORMANCE CONCRETE

The ultra-high performance concrete (UHPC) also called reactive powder concrete (RPC) is relatively new generation of concrete optimized at the nano and micro-scale to provide superior mechanical and durability properties compared to conventional and high performance concretes. The Improvements in UHPC are achieved through: limiting the water-to-cementitious materials ratio (i.e., w/c < 0.20), optimizing particle packing, eliminating coarse aggregate, using specialized materials, and implementing high temperature and high pressure curing regimes. In addition, and randomly dispersed and short fibers are typically added to enhance the material's tensile and flexural strength, ductility, and toughness **[1]**.

The constituents of UHPC include: Portland cement, silica fume, quartz powder (also referred as quartz flour), sand, superplasticizer, water, and fibers. Each of the components in UHPC aids in optimizing the material properties, thus contributing to its extraordinary strength. As shown in **Figure 2.1**, the compressive strength of RPC or UHPC may be as high as 200 MPa while a normal high performance concrete has a compressive strength of around 80 MPa.

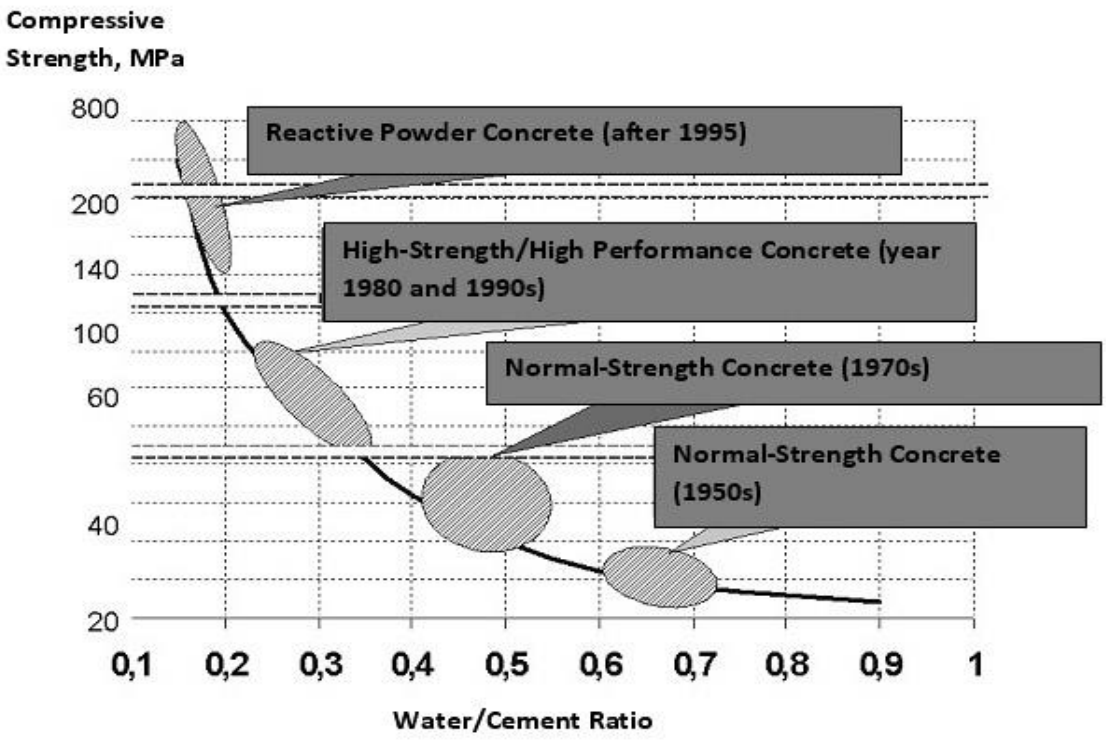

Figure 2.1: Strength comparison of various types of concrete.

Silica fume is one of the main constituents of UHPC. According to Vander Voort et al. **[2]**, silica fume in UHPC has the three main functions:

- Filling the voids in the next larger granular class, namely cement,
- Enhancing lubrication of the mix due to the perfect sphericity of the basic particles;
- Production of secondary hydrates by the pozzolanic reaction with the products from primary hydration of cement **[3]**.

The other additional constituent of UHPC is quartz powder. Quartz powder has an average diameter of 10–15 μm, approximately the same granular size as cement particles. Since quartz powder is a reactive material, it acts as an excellent paste-aggregate interface filler. For cases where heat-treatment is employed, quartz powder demonstrates

even higher reactivity. Other advantages of it include extreme hardness and availability. Sand constitutes the largest portion of UHPC with about 41 percent by weight. To obtain a highly homogeneous matrix as well as minimum void, UHPC contains finely graded sand between 150 μm to 600 μm, as shown in **Figure 2.2**.

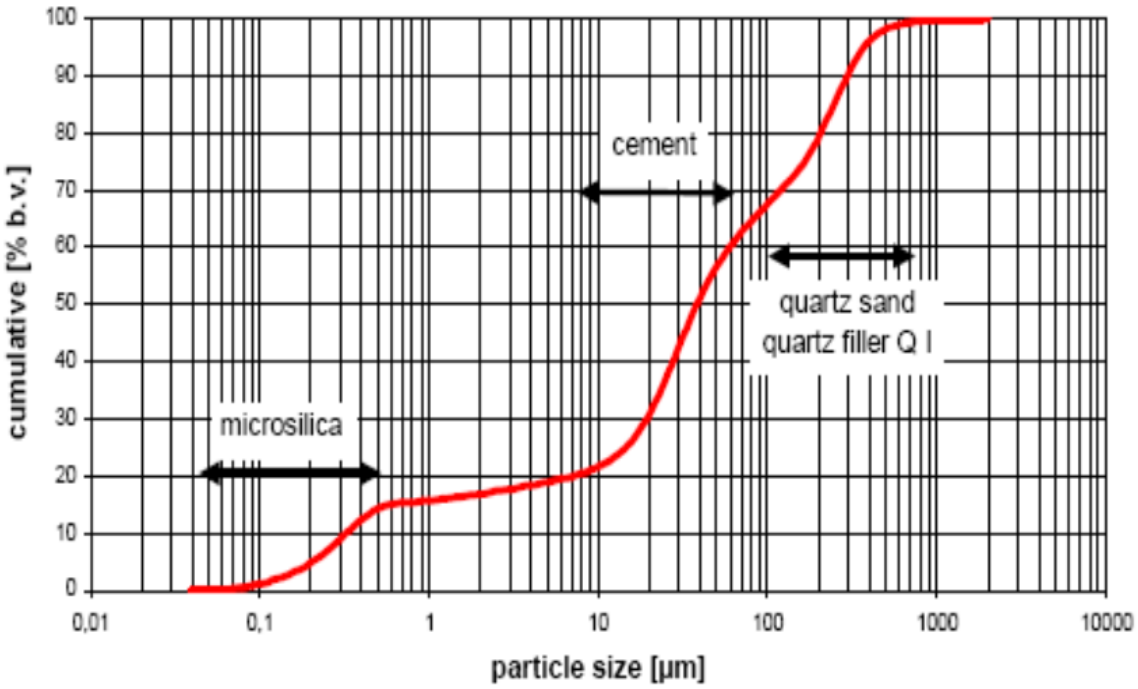

Figure 2.2: Particle Size distribution of silica fume, cement and quartz sand.

To create a gradation of particle sizes that result in a tightly packed matrix of materials the fine aggregates are carefully selected in order to minimize voids. This has the effect of creating a very durable material with low porosity and permeability. The dense microstructure also eliminates shrinkage and limits creep when heat treated during curing. Since UHPC uses a small w/cement ratio, superplasticizer is needed to increase its workability. Today's high performance superplasticizers having either a polycarboxylate (PC), NapthaleneSulfonate (NS), or Melamine Sulfonate (MS) base allow the dense, highly homogeneous mixture to be poured with the concerns of

segregation being lessened The addition of a superplasticizer helps to increase the workability.

UHPC without fibers is very strong but very brittle, consequently fibers are included to increase the tensile capacity and improve its ductility. Studies using different fiber materials, contents, sizes, and shapes have been conducted by various researchers **[4]**.

Dimensionally, the largest constituent in the mix are the steel fibers. Given the relative sizes of the sand and the fibers, the steel fibers are able to reinforce the concrete matrix on a micro level **[5]**. The addition of steel fibers helps in preventing the propagation of micro-cracks and macro-cracks and thereby limits crack width and permeability. This is the largest particle in the mix and is added at 6.2 percent by weight to the mix. Because of its size relative to the other constituents, it reinforces the concrete on the micro level and eliminates the need for secondary reinforcement in prestressed bridge girders **[6]**.

2.2 DEVELOPMENT OF UHPC

UHPC with a compressive strength of more than 150 MPa and other superior material properties is a new generation cementitious material that originated through intensive research work mostly conducted in France and Canada since 1994 **[7]**. The basic principle on which UHPC is based is to achieve a cement matrix as dense as possible (by reducing micro cracks and capillary pores in the cement matrix) and a dense transition zone between matrix and the aggregates.

Following measures are suggested to produce UHPC:

- Enhancing the homogeneity by elimination of coarse aggregates. It is well known that the transition zone between the coarse aggregate and paste matrix is often the

source of micro cracks in concrete, due to their different mechanical and physical properties. It is suggested that the maximum aggregate size in UHPC should be less than 600 μm **[3]**.

- Improving the properties of cement matrix by the addition of supplementary cementing materials, such as silica fume. The modifying effects of silica fume in concrete are attributed to its pozzolanic reaction with $Ca(OH)_2$ and filler effect in voids among cement or other component particles. In typical Portland cement based concrete, 18% silica fume, by weight of the cementitious materials, is enough for total consumption of $Ca(OH)_2$ released from cement hydration **[8]**. However, considering the filler effect the optimal share of the silica fume increases to about 30% of cement **[3]**. Therefore, the silica fume content in UHPC is normally in the range of 25-30% of the cementitious material.
- Improving the properties of cement matrix by reducing water to cementitious materials ratio.
- Enhancing the packing density of powder mixture. A mixture with a wide size distribution has a low void among the particles. This means powder mixture should be composed of a number of classes of granular powder.
- Enhancing the microstructure by post-set heat-treatment. This increases the reactivity of the cementing materials and constituents to a dense microstructure.

While UHPC shows substantially increased compressive strength and decreased porosity, it tends to be brittle. Short high carbon steel or polymer fibers of various dimensions and mechanical properties are commonly used in UHPC at various volume fractions to

improve its tensile and flexural strength, impact resistance or toughness, decrease cracking, and alter the mode of failure by increasing post cracking ductility **[9]**.

2.3 INGREDIENTS OF UHPC

Fine quartz sand (150 to 600 μm) is used as aggregate because coarse aggregate is eliminated from UHPC. An ordinary Portland cement (Type I) with low C_3A content is used as binder. Silica fume (0.1 to 1.0 μm) is generally used as supplementary cementing material. Quartz powder (smaller than 10 μm) is used as micro-filler. Super-plasticizer is used to achieve the desirable fluidity **[3, 7]**.

Richard and Cheyrezy **[3]**, have recommended the following criteria regarding the selection of ingredients of UHPC:

Sand

Sand selection parameters to be defined are:

- Mineral composition;
- Mean particle size;
- Granular range;
- Particle shape; and
- Mixture ratio by weight.

As far as mineral composition is concerned, quartz offers the following advantages:

- Very hard material;
- Excellent paste/aggregate interfaces; and
- Ready availability.

Sand with a mean particle size of about 250 μm is selected.

The particle size range is defined indirectly by the desirable maximum and minimum particle sizes. Maximum particle size is limited to 600 μm, and for the minimum value, particle sizes below 150 μm are avoided, in order to prevent interference with the largest cement particles (80-100 μm).

Fine sand is obtained by screening crushed sand, where the grains are highly angular or natural quarry sand, where the grains are more spherical. Both types of sand can be used for the UHPC. However the water demand is slightly less for natural sand, which is therefore preferable.

Cement

From the point of view of chemical composition, cements with low C_3A content (for reducing the water demand) give better results. As for particle size, it is observed that over-ground cements with a high fineness are not satisfactory, due to their high water demand. The best cement in terms of rheological characteristics and mechanical performance is high silica-modulus cement. However, this type of cement has the disadvantage of a very slow setting rate, preventing its use for certain applications. Conventional quick-setting high performance cement offers very similar mechanical performance, despite a higher water demand.

Superplasticizer

The most efficient superplasticizers are polyacrylate-based dispersing agents, but which also exhibit a retarding characteristic which can present a problem for practical applications. The conventional superplasticizers selected for their compatibility with the cement give slightly poorer results. For the low w/c ratios used for UHPCs, the optimum superplasticizer ratio is high (solid content of approximately 1.6% of cement content).

Silica fume

Silica fume used in UHPCs has three main functions, as follows:

- Filling the voids between the next larger class particles (cement);
- Enhancement of rheological characteristics by the lubrication effect resulting from the perfect sphericity of the basic particles; and
- Production of secondary hydrates by pozzolanic reaction with the lime resulting from the primary hydration.

The following parameters are used for silica fume characterization:

- Degree of particle aggregation;
- Nature and quantity of impurities;
- Basic particle size.

The main quality of a silica fume is the absence of aggregates. This leads to the use of non-compacted silica fumes. Slurry cannot be used, as the quantity of water contained in the slurry exceeds the total quantity of water required for the mixture. The most injurious impurities are carbon and alkalis.

Particle size is a secondary factor. The best results are obtained with silica fume procured from the zirconia industry, being free from impurities and totally disaggregated. However the Blaine fineness is lower than that for conventional fumes (14 m^2/g compared with 18 m^2/g). On the other hand, an impurity-free fume with a high Blaine fineness value (22 m^2/g), produced mediocre results, due to the aggregation of the finest particles.

Typically, the silica fume/cement ratio used for UHPC is 0.25. This ratio corresponds to optimum filling performance and it is close to the dosage required for complete consumption of the lime resulting from total hydration of cement. However, cement

hydration is incomplete in an UHPC, and the available quantity of silica fume is more than that required by the pozzolanic reaction.

Utilization of fly ash (FA) and ground granulated blast furnace slag (GGBFS) as an alternative to silica fume in UHPC has been reported in the literature **[10, 11]**. Test results obtained by Yazici et al. **[11]**, indicate that UHPC containing high volume binary (SF–FA or SF–GGBFS) or ternary (SF–FA–GGBFS) blends have satisfactory mechanical performance. In other words, utilization of FA and/or GGBFS in UHPC production is very effective. Cement and silica fume content can be decreased by FA and/or GGBFS replacement. Mixtures having 1.30 M CaO/SiO_2 ratio performed generally better than mixtures containing constant and high amount of SF. In other words, FA and GGBFS can be used as an alternative silica source in UHPC. Moreover, the reduction in SF content reduced the superplasticizer demand considerably. Therefore, besides the reduced heat of hydration and shrinkage, these mixtures have also important environmental benefits.

Quartz powder

Crushed crystalline quartz powder is an essential ingredient for heat-treated UHPC. Maximum reactivity during heat-treatment is obtained for a mean particle size of between 5 and 25 μm. The mean particle size of the crushed quartz used for an UHPC is l0 μm, and is therefore in the same granular class as the cement.

The ratio by weight adopted corresponds to the stoichiometric optimum for conversion of amorphous hydrates into tobermorite characterized by a C/S molar ratio of 5/6 = 0.83. This is achieved with a silica/cement ratio of 0.62. This ratio is obtained by adding silica fume and crushed quartz as a complement.

2.4 OPTIMIZATION OF UHPC MIXTURES

UHPC mixtures are obtained by optimizing several technologies: minimizing the amount of water added, using superplasticizers and a wide particle size distribution, and packing the particles to improve fluidity with minimized water additions and to optimize load-carrying capacity. Methodologies for optimizing the UHPC mixtures are reported in the literature **[12, 13]**.

Larrard and Sedran **[12]** have recommended the following approach for optimizing the UHPC mixtures using a packing model (solid suspension model):

First of all, a reference viscosity should be chosen, depending on the production method. Higher the viscosity, lower the minimum water content. However, if the mix is too sticky, the entrapped air volume will increase. Therefore, a critical viscosity should be determined for obtaining a minimal content of voids.

Secondly, the minimal matrix porosity should be looked for. This criterion leads to the determination of the silica fume/cement ratio. However, any increment of aggregate volume increases the viscosity, entailing an increase of the matrix porosity in order to keep the viscosity constant. Thus, a first attempt should be made to test different mixes having a low porosity to determine the respective influence of each parameter. For minimizing matrix porosity, it is possible to act on the size of aggregate. From this point of view, the lowest maximum size of aggregate (sand) is desirable. On the other hand, as a dense packing of the matrix is aimed at, the sand size should be high enough as compared to the maximum size of cement grains, in order to reduce the wall effect.

Therefore, mono-size sand appears to be the best solution. This is why an ultra-reactive powder concrete will be generally an ultra-high-performance mortar.

Sobolev **[13]** has presented the following approach for optimizing UHPC using the rheological and strength models:

First, the optimal SF content and SP dosage are selected according to the strength model of modified mortars: for optimal performance SF content is specified within 10–15% and SP dosage is set to 10% of SF. Second, the aggregates are optimized to fit a specific grading curve. Then w/c ratio is selected using the strength model.

2.5 MIX DESIGN

The parameters considered in the mix design of UHPC are mainly, water to binder ratio, cement content, micro silica to cement ratio, total cementitious material content, total fine aggregate content, fiber content and water to binder ratio. The ranges for these parameters have been obtained from literature survey **[3, 5, 10-27]** are as follows:

Water to total binder ratio (w/b):- 0.15-0.24

Cement content: - 800-1100 kg/m^3

Silica fume content: - 150-300 kg/m^3

Silica fume to cement ratio (SF/C): -0.15-0.35

Cement and Micro silica content: - 950-1400 kg/m^3

Quartz and Sand: - 1000-1400 kg/m^3

Fiber Content: - 190-250 kg/m^3

Fiber to total binder ratio (f/b): - 0.15-0.30

2.6 DURABILITY PROPERTIES

Roux et al **[52]** studied durability properties of RPC such as porosity, air permeability, water absorption, diffusion, and migration of chloride ions, accelerated carbonation, resistance to reinforcement corrosion, resistivity, and resistance to mechanical abrasion and compared these with the properties of two reference mixes of ordinary concrete. One with low cement content and other a high performance concrete and found that there were no pores in RPC with a diameter greater than 15 nm. The effective diffusion coefficient was 50 times less than low cement concrete. No carbonation was observed even for exposure to 100% CO2 for 90 days. The rate for reinforcement corrosion was less than 0.01µm/ yr.

Abrasion coefficient was comparable to heavy weight concrete with metallic aggregates. The resistivity for RPC was 70 times higher than that of reference concrete.

El-Dieb **[54]** produced ultra-high strength concrete (UHSC) using local available materials in the gulf region with the inclusion of steel fibers and by changing volume fractions. Different mixes were prepared to study their mechanical and durability properties. He found that fine aggregates available in UAE may be used to produce UHSC. Inclusion of steel fibers is essential to change the failure mode of UHSC from brittle to ductile. With the inclusion of steel fibers the electrical conductivity of concrete increases but this increase depend upon fraction of steel fibers. Due to dense microstructure the intrusion of external ions like Cl^- ion is very low that's why the electrical resistivity of this concrete offers a good protection of steel reinforcement against corrosion. Also, because of very low diffusion and sorptivity values UHSC shows excellent resistance against exposure conditions like sulfate attack and high chloride

content. Micro-structural studies also show dense cement paste around steel fibers and aggregates which also support the view of high durability of this concrete.

Juanhong et al **[59]** studied the durability of reactive powder concrete (RPC) and fly-ash reactive powder concrete (FRPC). With the help of X-ray diffraction and SEM the microstructure of concretes were studied. Results show that the microstructure comprises of C-S-H gel as a main composition with Ca/Si ratio less than 1.5. The crystals of $Ca(OH)_2$ and ethringite were not found. The shrinkage of RPC is approximately equal to the ordinary concrete at early ages. The coefficient of diffusion for both RPC and FRPC were about half of the ordinary high strength concrete. Carbonation depth for RPC and FRPC was almost equal to zero. Both the concretes show strong sulfate resistance, also reinforcement corrosion only takes place at the surface.

Graybeal and Tanesi **[58]** studied the durability properties of commercially available UHPC and found that it exhibits high durability properties in comparision to normal and high performance concrete. UHPC and reference concretes were cured in four different manners and was found that regardless of curing method, UHPC showed enhanced resistance to degradation due to freeze-thaw cycles and scaling deterioration. A very low chloride penetration was observed.

Graybeal and Hartmann **[57]** studied the performance of UHPC when cured under two curing regimes, ambient air cured and steam cured. Tensile and compressive strengths of concretes were found to be significantly higher than ordinary high performance concrete. Rapid chloride ion penetration test showed negligible or very low penetration of ions for both curing regimes. Abrasion test result shows that specimens cured with steam show

higher resistance than air cured specimens having maximum weight loss of 2.1 gram per abrading cycle. Similarly, UHPC showed greater resistance to freeze-thaw and scaling.

Tam et al **[56]** studied the drying shrinkage behavior and water permeability of RPC with different water-to-binder ratios and SP dosages. Drying shrinkage and water permeability for RPC was lower than that of normal concrete. This was because of the dense microstructure of RPC with relative reduced pore size and discontinuity of the voids. Higher the water to binder ratio and higher the super-plasticizer dosage will increase the drying shrinkage strains and shrinkage rate because of the fact that they tend to increase the voids in RPC as in any other conventional concrete. RPC exhibits very low water permeability, again, because of the fact that the microstructure of RPC is homogeneous and dense with discontinuity of the voids. It was also observed that increase in water to binder ratio tends to increase the water permeability but the dosage of the super-plasticizer does not have any significant effect, but excessive dosage of SP may lead to the problem of segregation which consequently leads to higher water permeability.

Filho et al **[55]** studied mechanical and durability properties of ultra-high performance fiber reinforced cement (UHPFRCC) composite and compared it with a regular grade 40 concrete and with a low environmental impact sewage sludge concrete. It was found that the average compressive strength of UHPFRCC was 162 MPa for 28 days and a tension softening behavior was observed in uni-axial tensile test. The durability performance of all the three concretes was tested by means of capillary water sorption test, gas permeability test and chloride penetration test. It was found that UHPFRCC is dense material which exhibits no permeability and porosity. The diffusion coefficients are $2x10^{-}$

^{14} m^2/s for UHPFRCC, $2.43x10^{-12}$ m^2/s for sewage sludge concrete and $3.6x10^{-12}$ m^2/s for grade 40 concrete.

Zhutovsky and Kovler **[53]** studied the effect of internal curing on durability properties of high performance concrete and reported their results as a function of water to cement ratio. HPC mixes were made with water to cement ratio ranging from 0.21 to 0.33. They used pre-saturated light-weight aggregates for internal curing and adjusted the water added during mixing so to maintain particular water to cement ratios. The results from sorptivity test indicate that internal curing tends to increase the sorptivity of the specimens and as the water to cement ratio is reduced this effect becomes more pronounced. Air permeability for all the concretes on a particular age was almost same. This implies that there is no effect of internal curing on air permeability. With the increase in water to cement ratio internal curing helps to decrease the chloride diffusivity. It was also observed that the modulus of elasticity was reduced with the introduction of internal curing and a reduction of upto 11% was observed in compressive strength of internally cured HPC as compared to conventionally cured counterpart.

In addition to improved strength and ductility, UHPC exhibits some characteristics that make it very attractive for use in a number of applications. Due to the dense cementitious matrix and small and disconnected pore structure, UHPC maintains a very low permeability: roughly 1/10 that of granite (Lafarge 2004). UHPC allows for negligible carbonation or penetration of chlorides/sulfates and also maintains a high resistance to acid attack (Perry and Zakariasen 2003).

UHPC's excellent resistance to freeze-thaw cycles also develops from the dense matrix, making it ideal for virtually any climate condition. UHPC also exhibits very low creep

and shrinkage after heat treatment when compared to conventional concretes, making the material suitable for precast/prestressed structures (Perry and Zakariasen 2003). The material can also be classified as a self-forming (self-consolidating) concrete due to the ease of flow of the material, which can be poured or pumped into place with limited or no vibration.

However, previous research demonstrated that UHPC exhibited almost no permeability and was not susceptible to chloride ingress. The very low water/cement ratio and densely packed matrix of UHPC contribute to permeability results even lower than HPC.

Bonneau et al. (1997) reported less than 10 Coulombs passing (over a six hour period) through UHPC specimens (negligible chloride ion penetrability) that were water cured at varying times and temperatures. In the U.S., additional research by Graybeal (2006a) demonstrated that UHPC had negligible chloride ion penetration when thermally treated and only very low penetration when not thermally treated. While Graybeal (2006a) demonstrated that the steel fibers did not contribute to a short circuit effect during UHPC testing, Toutanji et al. (1998) revealed that adding 0.75 in. polypropylene fibers increased the permeability of concrete and adding shorter fibers 0.50 in. reduced the permeability of the concrete. Therefore, results from rapid chloride penetration testing of UHPC should demonstrate UHPC's high resistance to chloride penetration.

Benjamin A. Graybeal (2005) show three tests were performed for each curing regime at 28 days after casting and additional three tests were performed on the Air and Tempered Steam treated regimes at 56 days. He found that the chloride ion penetrability of negligible value.

2.7 APPLICATIONS

Different applications of UHPC include: heavily (conventionally) reinforced precast elements for bridge decks; in situ applications for the rehabilitation of deteriorated concrete bridges and industrial floors **[30]**. With or without additional "passive" reinforcement it is used for precast elements and other applications like offshore bucked foundations. In addition, coarse grained UHPC with artificial or natural high strength aggregates were developed for highly loaded columns and for extremely high-rise buildings **[22]**.

Breakthroughs in application are the very first prestressed hybrid pedestrian bridge at Sherbrooke in Canada in 1997, the replacement of steel parts of the cooling tower at Cattenom and two 20.50 and 22.50 m long road bridges used by cars and trucks at Bourg-lès-Valence in France built in 2001 **[16]**. For these projects the UHPC was reinforced with about 2.5 to 3% of steel fibers (by volume) of different shape. Other footbridges with decks and/or other load bearing components made of fine grained, fiber reinforced UHPC exist in Seoul and in Japan **[14]**. A spectacular example of architectural design, taking advantage of the special benefits of UHPC, is the toll-gate of the Millau Viaduct in France. **Figure 2.3** through **Figure 2.5** shows some structures built using UHPC.

So far, the previous research shows the performance of UHPC developed using fine sand and crushed quartz powder, with particle size ranging from 45μm -600μm. But in this present study, an attempt is made to produce UHPC using local fine quartz sand meeting the particle size range criteria and at the same time being rich in silica and evaluating its durability properties.

Figure 2.3: Sherbrooke Bridge, Canada 1997.

Figure 2.4: Seonyu foot-bridge, Korea, 2003, Arch span 120 m deck, thickness 3 cm.

Figure 2.5: Toll-gate of the Millau Viaduct in France.

CHAPTER 3

METHODOLOGY OF RESEARCH

3.1 EXPERIMENTAL PROGRAM

The objective of this study was to evaluate the durability properties of UHPC mixtures produced utilizing fine local quartz sand. To achieve this objective, the following tests were conducted on specimens prepared for a total number of 27 UHPC mixtures: water penetration depth, rapid chloride permeability, electrical resistivity, pH, sulfate resistance, chloride diffusion and reinforcement corrosion rate.

3.2 MATERIALS

3.2.1 Cement

Ordinary Portland cement conforming to ASTM C 150 Type I with a specific gravity of 3.15 was used in all the concrete mixtures. Sufficient quantity of cement was procured and stockpiled safely to prevent its hardening. The chemical composition of the cement was carried out in the Central Analytical Laboratories of the Research Institute, KFUPM as shown in **Table 3-1**.

Table 3-1: Chemical Composition of Cement.

Constituent	Weight %
CaO	64.35
SiO_2	22.0
Al_2O_3	5.64
Fe_2O_3	3.80
K_2O	0.36
MgO	2.11
Na_2O	0.19
Equivalent alkalis ($Na_2O + 0.658K_2O$)	0.33
SO_3	2.10
Loss on ignition	0.7
C_3S	55
C_2S	19
C_3A	10
C_4AF	7

3.2.2 Silica fume

The chemical composition of the silica fume used is shown in **Table 3-2**. ASTM method C 114 was used to determine SiO_2 gravimetrically using Pt crucibles. Separate samples were weighed to determine oxides of Al, Ca, Na, K, Mg and sulfur and treated by EPA method 3050B. The digested extract was diluted to 100 ml and elements were determined by ICP-OES. Later the concentrations in ppm were converted to their oxides by calculation.

Table 3-2 : Chemical Composition of silica fume.

Parameters	%
Si O_2 –ASTM, C – 114	86.75
Ca/CaO	0.29/0.41
Al/Al_2O_3	0.22/0.41
Fe/Fe_2O_3	1.48/2.12
Mg/MgO	0.11/0.18
K/K2O	0.56/0.67
Na/Na_2O	0.13/0.17
Sulfur/SO3	0.31/0.77
$Na_2O+(0.658K_2O)$-%	0.62%
Loss on Ignition %, 950 ^oC – ASTM-C 114	3.35
Moisture % - 105 ^oC	0.716

3.2.3 Fine Aggregates

Local fine quartz sand with water absorption of 0.5% and specific gravity of 2.53 was used as the fine aggregate. The grading for this sand is given in **Table 3-3**.

Table 3-3: Fine aggregate grading.

Sieve Opening, mm	Cumulative % Retained
4.75	0
2.4	0
1.2	0
0.6	3.8
0.3	38.6
0.15	78.1
0.075	99.0

3.2.4 Superplasticizer

A liquid superplasticizer (commercial name: Glenium 51) was used to obtain the desired flow. Glenium 51 is polycarboxylic ether (PCE) based superplasticizer which does not contain chlorides and complies with AS 1478.1 2000 Type HWR and ASTM C 494 Types A and F The specific gravity of Glenium 51 is 1.095 kg/l with 65% water content by weight. Varying dosage of this superplasticizer was used to obtain a flow of 200 ± 2 mm for all the mixes.

3.2.5 Steel Fibers

Micro copper coated steel fibers of 0.22 mm diameter and 13 mm long with an aspect ratio l/d of 59 were utilized. These are made up of high strength steel greater than 2850 MPa and complies with ASTM A 820-90 **[31]**. These were imported from *HEBEI YU SEN*, Metal Wire Mesh Co. Ltd. China. **Figure 3.1** shows the steel fibers.

Figure 3.1: Micro copper coated steel fibers.

3.3 MIXTURE PROPORTIONS

To achieve the objectives of the study, three mix variables were considered with their three levels so as to investigate a total of 27 UHPC mixtures as per 3^3 factorial experiment design, as detailed below:

w/b ratio:	0.15, 0.175, 0.20	(3 variables)
Cement content (kg/m^3):	1000, 1100, 1200	(3 variables)
Silica fume content (% of cement):	15%, 20%, 25%	(3 variables)
Steel fiber (kg/m^3):	157	(1 variable)

Total mixtures (3×3×3×1) = 27

Absolute volume method was used to design the mixtures. The weights of constituents determined for one cubic meter of each of the UHPC mixtures are presented in **Table 3-4**.

Table 3-4: Weights of Ingredients in the Mixtures Investigated.

Mix	w/b	Cement (kg/m^3)	Silica fume (%)	Silica fume (kg/m^3)	Water (kg/m^3)	Fiber (kg/m^3)	SP (%)	SP (kg/m^3)	Sand (kg/m^3)
M1	0.15	1000	15	150	172.5	157	3.55	40.83	976.81
M2	0.15	1000	20	200	180	157	3.55	42.6	897.51
M3	0.15	1000	25	250	187.5	157	3.55	44.38	818.21
M4	0.15	1100	15	165	189.75	157	3.55	44.91	826.55
M5	0.15	1100	20	220	198	157	3.55	46.86	739.32
M6	0.15	1100	25	275	206.25	157	3.55	48.81	652.09
M7	0.15	1200	15	180	207	157	3.55	48.99	676.29
M8	0.15	1200	20	240	216	157	3.55	51.12	581.13
M9	0.15	1200	25	300	225	157	3.55	53.25	485.97
M10	0.175	1000	15	150	201.25	157	2	23	945.25
M11	0.175	1000	20	200	210	157	2	24	864.58
M12	0.175	1000	25	250	218.75	157	2	25	783.91
M13	0.175	1100	15	165	221.375	157	1.5	18.98	806.45
M14	0.175	1100	20	220	231	157	1.5	19.8	718.35
M15	0.175	1100	25	275	240.625	157	1.5	20.63	630.25
M16	0.175	1200	15	180	241.5	157	1.5	20.7	654.37
M17	0.175	1200	20	240	252	157	1.5	21.6	558.26
M18	0.175	1200	25	300	262.5	157	1.5	22.5	462.15
M19	0.20	1000	15	150	230	157	1.5	17.25	885.8
M20	0.20	1000	20	200	240	157	1.5	18	802.55
M21	0.20	1000	25	250	250	157	1.5	18.75	719.29
M22	0.20	1100	15	165	253	157	1	12.65	741.06
M23	0.20	1100	20	220	264	157	1	13.2	650.11
M24	0.20	1100	25	275	275	157	1	13.75	559.17
M25	0.20	1200	15	180	276	157	1	13.8	583.03
M26	0.20	1200	20	240	288	157	1	14.4	483.81
M27	0.20	1200	25	300	300	157	1	15	384.60

3.4 MIXING PROCEDURE

The conventional mixing method is based on BS 1881: part 125 (BSI, 1986). However, since UHPC is composed of very fine materials, the conventional mixing method is not appropriate. The following sequence in mixing of UHPC was followed based on the previous studies **[20, 21, 23]**, and as well as from the experience gained after several trials. The mixing procedure adopted is as follows:

(a) Dry mixing the powders (including cement, sand and silica fume) for about three minutes with a low speed of about 140 revolutions/minutes.

(b) Addition of half volume of water containing half amount of superplasticizer.

(c) Mixing for about three min with a high speed of about 285 revolutions/minutes.

(d) Addition of the remaining water and superplasticizer.

(e) Mixing for about ten min with a high speed of about 285 revolutions/minutes.

(f) Finally, adding steel fibers in small amounts over the course of the next two minutes into the mixture.

(g) After the fibers have been added, continue running mixer for further three minutes to ensure that the fibers are well dispersed.

The entire mixing process takes about 20-25 minutes and is specific to the constituents of the mix and the mixer, shown in **Figure 3.2**, was used. Mixing of the UHPC requires special attention to have uniform consistency. After preparation, the UHPC was poured into the molds and consolidated using a vibrating table.

Figure 3.2: Planetary Mixer (MIKRONS) used for mixing the constituents of UHPC.

As soon as mixing was completed, UHPC mix was tested for consistency. ASTM C 1437 **[32]**, standard test method for measuring flow of hydraulic cement was used for this purpose in this test. The mini slump cone is filled with UHPC mix and then it is removed slowly to allow the UHPC to flow evenly on the table and then the flow table is dropped 25 times and its average diameter is recorded. The average flow diameter of UHPC mix ranged from 180 to 220 mm.

3.5 PREPARATION AND CURING OF SPECIMENS

Specimens of UHPC were prepared and cured to carry out various tests planned in this research study. Batching of each mix was proportioned by weight. After mixing, the flow was measured and UHPC was poured in the moulds. The moulds were then vibrated until complete consolidation was achieved. After casting, the specimens were covered with plastic sheet for 24 hours and placed in the laboratory environment (22 ± 3 ^{0}C) to

minimize loss of mix water. After 24 hours, the specimens were demoulded and placed in a curing tank till the time of test. **Table 3-5** shows the type and number of specimens for each of the UHPC mixture. **Figure 3.3** shows the prepared UHPC specimens.

Table 3-5: Type and Number of Specimens Prepared and Tested.

Property	**Specimen shape and size (mm)**	**Test Standard**	**No. of specimens for each mix**
Water penetration depth	100 x 100 x 100 cube	DIN 1048	3
Chloride permeability	100 x 200 Cylinder	ASTM C 1202	3
Sulfate resistance	50 x 50 x 50 cube	Strength reduction	6
Chloride diffusion coefficient	75 × 150 mm cylinder	Fick's second law of diffusion	1
Electrical Resistivity	A centrally embedded rebar in 75 × 150 mm concrete cylinder	Two probe Wenner method	2
pH	Powder obtained from centrally embedded rebar in 75 × 150 mm concrete cylinder by drilling	pH meter	1
Reinforcement Corrosion rate	A centrally embedded rebar in 75 × 150 mm concrete cylinder	Linear polarization resistance method	3
	Number of specimens per mix		**19**
	Total number of specimens = 19 x 27 =		**513**

Figure 3.3: A set of specimens prepared from each UHPC mixture.

3.6 TESTING OF SPECIMENS

3.6.1 Water Penetration Depth

The water permeability test, which is most commonly used to evaluate the permeability of concrete, is the one specified by DIN 1048. In this test, the 100 mm concrete cubes, after 28 days of water curing, were dried under laboratory condition for 24 hour. They were thereafter dried in oven for three days at 70^0 C and then they were cooled for 1 day in the laboratory condition.

The water penetration test setup is shown in **Figure 3.4**. Samples were placed on the setup and water was applied on one face of the specimen under a pressure of five bars. This pressure was maintained constant for a period of 72 hours. After the completion of the test, the specimens were taken out and split open into two halves. The water penetration profile on the concrete surface was then marked and the maximum depth of

water penetration in three specimens was recorded and considered as an indicator of the water permeability. The depth of water penetration is a reliable durability assessment test **[60]**. The higher the depth of water penetration the lower is the durability of the concrete material. **Table 3-6** shows the classes of water penetration depth.

Table 3-6: Assessment of Concrete Permeability According to Water Penetration Depth [The Concrete Society, 1987].

Range of d	Penetration class
d < 30 mm	Low
30 mm ≤ d ≤ 60 mm	Moderate
d > 60 mm	High

Figure 3.4: Water permeability test setup

3.6.2 Rapid Chloride Permeability

The chloride permeability was determined after 28 days of water curing. For this purpose, a disk, 50 mm thick, was cut from the center of the cylindrical (75 x 150 mm) specimen. The curved surface of the disk was coated with an epoxy coating to avoid evaporation of moisture during testing. The disk specimens were saturated with water under vacuum and kept saturated for one day.

The concrete specimen was clamped between cells. During the test, a potential difference of 60 V DC was maintained across two voltage cells: upstream (cathode) and downstream (anode). The upstream cell was filled with 3% sodium chloride solution, and the downstream one was filled with 0.3 M sodium hydroxide solutions. The details of this test method are described in ASTM C 1202 [2000] and AASHTO T-277.

The voltage applied to a given resistor was monitored at every 30 min for a period of six hours with the help of a data logging system; from which the current values of each cell were calculated and the total charge passed throughout the specimen was calculated. Since a 75 mm nominal diameter specimen was used, the test results must be adjusted accordingly if the diameter of the specimen is other than 95 mm using the following relationship [62]:

$$Q_s = Q_x * (95 / x)^2$$

Where Q_s is the charge passed through the 95 mm diameter specimen, Q_x is the charge passed through x diameter specimen and x is the diameter of non-standard specimen (in this investigation, x was 75 mm). **Figure 3.5** shows the set-up used to determine the

chloride permeability in this study. **Table 3-7** shows the ASTM C 1202 classification of concrete penetrability by chloride ions based on charge passed.

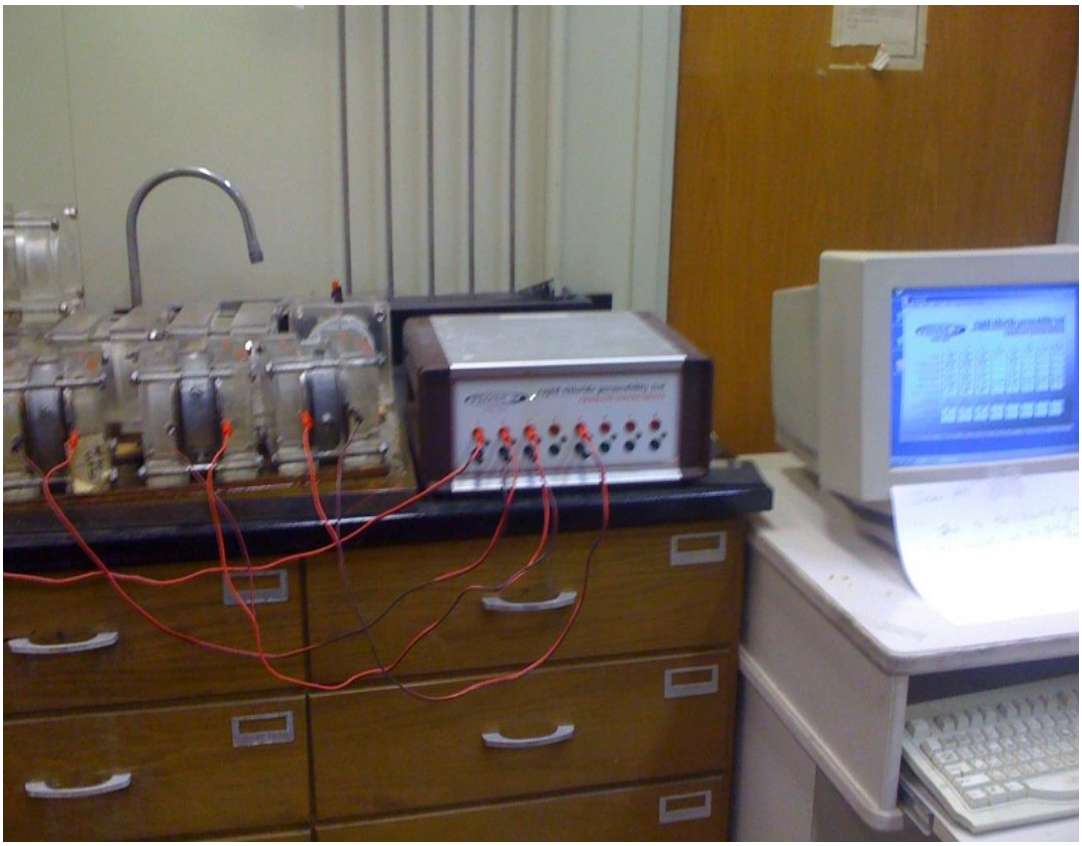

Figure 3.5: Rapid chloride permeability test set-up

Table 3-7: Chloride ion penetrability based on charge passed [62]

Charge Passed (Coulombs)	Chloride Ion Penetrability
> 4000	High
2000-4000	Moderate
1000-2000	Low
100-1000	Very Low
< 100	Negligible

3.6.3 Electrical Resistivity

Since corrosion is an electro-chemical process, the flow rate of the ions through concrete between the anodic and cathodic areas of a depassivated rebar embedded in concrete

determines the rate at which corrosion can occur in that rebar. This flow rate of ions is affected by the resistivity of the concrete **[62]**. Therefore, measuring the electrical resistivity of concrete could give some clues as to the likelihood of corrosion taking place **[61]**. **Table 3-8** shows the empirical indication of likelihood of corrosion of a depassivated rebar for various resistivity ranges of covercrete.

The performance of any concrete mixture in corrosion resistance is not only a function of its pore size and distribution, but also dependent upon its electrical resistivity. The electrical resistivity was measured on centrally embedded rebar cylindrical specimen after 28 days of curing and then exposed in 5% NaCl solution for a period of 450 days.

The electrical resistivity of UHPC mixtures was assessed using a two probe James RM-8000 resistivity meter shown in **Figure 3.6**. Using a 6 mm masonry drill bit two holes 8 mm deep were drilled with a spacing of 5 cm on the specimen. A small amount of conductive gel was inserted into each hole. The resistivity meter was connected to the two probe lead and the probes inserted into the holes. The action button on the resistivity meter was pressed which displays the apparent resistivity on the LCD.

Table 3-8: Empirical resistivity thresholds for depassivated steel [62, 65].

Resitivity Level (k-Ohm-cm)	**Likelihood of corrosion**
< 5	Very high
5-10	High
10-20	Moderate to Low
> 20	Low to Negligible

Figure 3.6: Resistivity meter measuring the electrical resistivity of UHPC specimen.

3.6.4 pH testing

pH value of all the UHPC mixes were determined by drilling out powder from centrally embedded rebar specimens which were water cured for 28 days and exposed to 5% NaCl solution for a period of 450 days. The powdered sample was passed through 150 micron size sieve (ASTM no.100 sieve) and was thoroughly mixed with distilled water in 1:1

proportion by weight. The mixture was filtered using a filter paper. The pH of the filtrate was then measured using a pH meter. **Figure 3.7** show the powdered sample drilled out from the UHPC specimen.

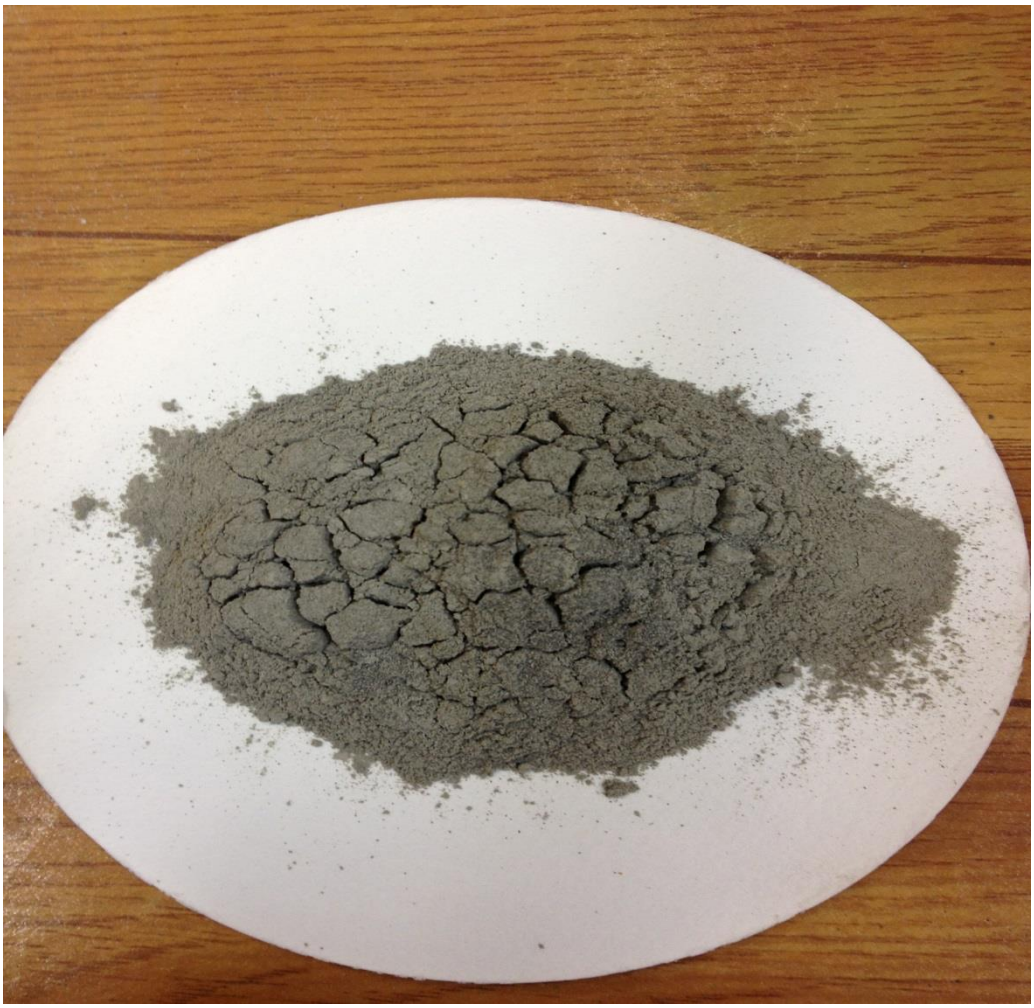

Figure 3.7: Powdered sample used for determining the pH value of UHPC specimen

3.6.5 Assessment of Sulfate Attack

Ground water and soil contaminated with sulfates (magnesium, sodium and calcium) cause concrete to crack, spall and soften. To assess the performance of all the concrete mixes, specimens, 50 mm cubes, were exposed to 5% sulfate solution (2.5% $MgSO_4$, 2.5% Na_2SO_4) after a water curing period of 28 days. After 9 months of exposure to

mixed sulfate environment, the performance of concrete specimens was evaluated through visual examination and reduction in compressive strength.

Specimens were inspected visually to see the signs of spalling and softening. After 9 months of exposure, the concrete specimens placed in water and sulfate solution were tested in compression. The relative reduction in compressive strength due to sulfate attack, denoted as sulfate deterioration factor (SDF) was calculated using the following formula.

$$SDF = \frac{100(CSW - CSS)}{CSW}$$

Where,

CSW = Average compressive strength of concrete specimens immersed in water; and

CSS = Average compressive strength of concrete specimens immersed in sulfate solution

3.6.6 Chloride Diffusion Coefficient

The chloride diffusion coefficient was determined after 28 days of water curing. After this curing period, the specimens were allowed to dry for a week and then they were coated with an epoxy resin all over leaving one circular flat surface (top) uncoated. It is expected that uniaxial (i.e. one dimensional) diffusion of chloride would occur through the uncoated surface. The coated specimens were immersed in a 5% sodium chloride solution for 12 months. First after 6 months and then after 12 months period, the specimens were cleaned and dried to remove the surface moisture and thin slices of concrete were obtained at 5, 15, 25, 35 and 45 mm by dry cutting, as shown in **Figure**

3.8. The slices were crushed and ground to a fine powder passing through ASTM No. 100 sieve.

Figure 3.8: Slices of UHPC specimen used for chloride diffusion test.

In order to determine the total chloride concentration, three grams of the powder was dissolved in hot mixture of 3 ml concentrated nitric acid and 47 ml distilled water. The solution was kept in a shaker for 24 hours, thereafter, the specimen was filtered and the filtrate was diluted to 100 ml. The chloride concentrations were plotted against the concrete depth for each specimen. The chloride profile was utilized to determine the coefficient of chloride diffusion according to Fick's second law of diffusion **[54]**, and the

solution of Fick's second low for a semi-infinite domain with a uniform concentration of C_S at the surface (x=0) that as shown below:

$$C_x = C_s \ [1 - \text{erf}\{x / \sqrt{2t.D}\})]$$

Where:

C_x is the chloride concentration at depth, x, %.

C_s is the chloride concentration at surface, %.

x is the depth from concrete surface, cm

t is the time in seconds, and

D is the effective chloride diffusion coefficient, cm^2/s.

The chloride diffusion coefficient and the surface chloride concentration were obtained using a computer program written in MATHEMATICA, based on Fick's second law of diffusion as presented in Appendix.

3.6.7 Reinforcement Corrosion

Reinforcement corrosion was evaluated by measuring the corrosion current density. The concrete specimens were partially (4 cm from the bottom) exposed to 5% NaCl solution and corrosion current density was measured every month.

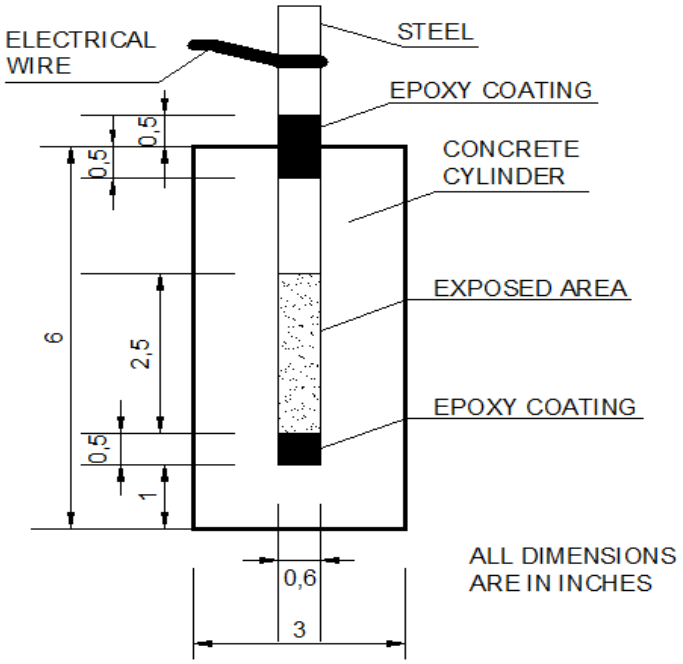

Figure 3.9: Reinforcement Corrosion Specimen.

Figure 3.10: Reinforcement corrosion specimens

The corrosion current density measurements provide an indication of the rate at which the reinforcement corrosion is progressing. This information is of great importance in knowing the extent of corrosion damage and in predicting the remaining service life, which is useful in taking decisions regarding the repair and rehabilitation works. The corrosion current density was measured according to the linear polarization resistance method (LPRM) **[67].**

In the LPRM experiments, a stainless steel plate was used as a counter electrode. The steel bar and stainless steel plate were connected to a Potentiostat/Galvanostat. The polarization resistance (R_p) was determined by conducting a linear polarization scan in the range of ±10 mV of the corrosion potential. A scan rate of 0.1 mV/s was used. The corrosion current density (I_{corr}) was determined using the Stern and Geary formula shown below **[67]**. A schematic representation of the experimental set-up utilized to measure I_{corr} on steel in the concrete specimens is shown in **Figure 3.11**. Three specimens were tested and the average I_{corr} values are reported.

$$I_{corr} = B/R_P$$

Where I_{corr} = Corrosion current density, µA/cm^2,

R_p= Polarization resistance Ω cm^2,

$$B = \frac{(\beta_a * \beta_c)}{2.3(\beta_a + \beta_c)}$$

$\beta_a$and β_c are the anodic and cathodic Tafel constants, mV/decade, respectively.

Figure 3.12 shows the corrosion current density setup.

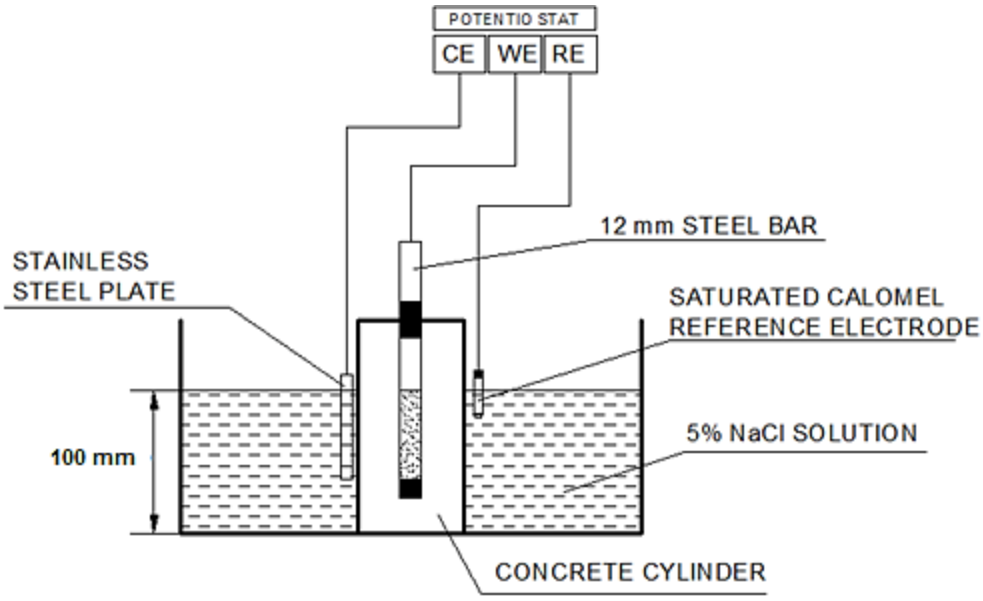

CE= Counter electrode, WE= Working electrode, RE= Reference electrode

Figure 3.11: Schematic Representation of the Corrosion Current Density Measurements.

Figure 3.12: Corrosion Current Density set-up

The Tafel constants are normally obtained by polarizing the steel to 250 mV of the corrosion potential (Tafel plot). However, in the absence of sufficient data on β_a and β_c, a value of B equal to 26 mV for steel in active condition and 52 mV for steel in passive condition is often used. Lambert et al. **[68]** reported a good correlation between corrosion rates determined using these values and the gravimetric weight loss method.

After the final reading of I_{corr} was taken (i.e. 450 days exposed) the specimens were split to remove the rebar and a thorough visual examination of the extracted rebars was done.

3.7 STATISTICAL ANALYSIS OF EXPERIMENTAL DATA

A statistical analysis of the test results was carried out to develop models relating the durability properties of the developed UHPC mixtures. Analysis of variance (ANOVA) was first carried out to assess the effect of mixture variables, such as w/b ratio, cement content, silica fume content on water penetration depth, chloride permeability, electrical resistivity and pH values of the UHPC mixtures using simple software namely, MINITAB. Secondly, based on the ANOVA results, the models for water penetration depth, chloride permeability, electrical resistivity and pH values were developed using the *least squares* method. In the ANOVA as well as in the regression models, the notations used for independent variables were as follows:

w/b: water to binder ratio

C: Cement content in kg/m^3

SF: Silica fume content (as % of the cement content)

CHAPTER 4

RESULTS AND DISCUSSION

The experimental program was discussed in Chapter 3. In this chapter, the results of the experimental work for all 27 mixtures of UHPC are presented and discussions on these results are given, thereon. Section 4.1 discusses about the trial mixtures considered to optimize various constituents of UHPC. Section 4.2 through 4.8 discusses all the durability properties studied for UHPC mixtures. In section 4.9, the indirect assessment of performance of UHPC mixtures against rebar corrosion is shown and finally the best performing mixture and the most economical mixture are shown in section 4.10 and 4.11.

4.1 TRIAL MIXTURES

Several trial mixtures were prepared to optimize various constituents of the UHPC. Firstly, the grading of sand was optimized to obtain the maximum particle packing leading to higher density and strength. To satisfy the flow criteria, the dosage of a plasticizer was optimized to meet the required flow. The Optimization of other constituents like water-binder ratio and cement and silica fumes content can be determined from the tests conducted in detail.

4.1.1 Optimization of Sand Grading

Sand constitutes about 50% of all the constituents in UHPC. To achieve the desired properties of the UHPC, it is desirable to optimize the grading of the sand. This will help

us in achieving denser microstructure with closely packed particles, thereby enhancing the performance of concrete. For this purpose, specimens for compression testing were prepared using the following mix design with only one variable, i.e. the sand grading.

Water/binder ratio = 0.20

Cement = 1000 kg/m^3

Silica fume = 150 kg/m^3 (% by cement weight)

Water = 230 kg/m^3

Sand = 977 kg/m^3

The various sand grades used were:

- Natural (ungraded)
- Passing 600 µm and Retained 150 µ
- Passing 600 µm (ASTM no. 30 sieve)
- Passing 300 µm (ASTM no. 50 sieve)
- Passing 150 µm (ASTM no. 100 sieve)
- Mixed - 1/3rd passing 600 µm, 1/3rd passing 300 µm, 1/3rd passing 150 µm

The results obtained from compression testing on the mixtures prepared using various sand grades are presented in **Table 4-1**.

7, 14, and 28-day compressive strengths for all six trial mixtures are shown in **Figure 4.1**. From the plot shown in **Figure 4.1**, it is clearly evident that the natural sand grading is giving the best results because natural sand grading fortunately belonged to a particle size distribution corresponding to highest packing. Hence, natural sand grading was used for the preparation of UHPC mixtures for detailed study.

Table 4-1: Compressive strength of UHPC specimens prepared with different sand grading.

Mix #	Sand grade	SP (%)	Flow (cm)	Density (kg/m^3)	7-Day f_c` (MPa)	14-day f_c` (MPa)	28-day f_c` (MPa)
1	Natural	1.5	20	2282	92	109	126
2	600-150	1.7	18	2239	81	102	117
3	Pass 600	1.8	16	2265	87	91	113
4	Pass 300	2.0	21.5	2260	88	96	109
5	Pass 150	2.1	17.5	2280	78	85	101
6	Mixed	1.9	19.5	2004	57	63	64

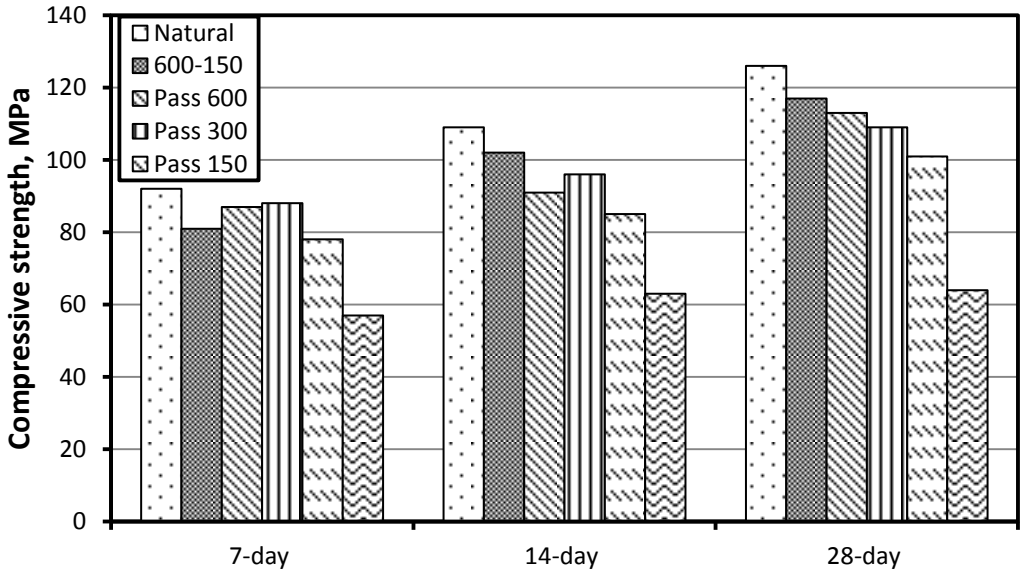

Figure 4.1: Compressive strength of UHPC specimens prepared with different sand grading.

4.1.2 Optimization of Superplasticizer

The optimization of superplasticizer dosage is very crucial for UHPC, as it provides UHPC mixtures the required flow for very low water to binder ratio. Flowability is essential for pouring UHPC mixture into the moulds and for the adequate consolidation. Several trials were carried out to optimize the superplasticizer dosage for each of the 27 UHPC mixtures to meet the targeted flow of 200 ± 20mm in each case. Results showing

the optimum superplasticizer dosages and corresponding flow for all 27 mixtures are presented in **Table 4-2.**

Table 4-2: Optimum dosages of superplasticizer for all 27 UHPC mixtures to meet flow criteria of 200 ± 20mm.

Mix ID	w/b	Cement (kg/m^3)	Silica fume (%)	Silica fume (kg/m^3)	Water (kg/m^3)	Optimum SP dosage (%)	Flow (cm)	28-day compressive strength (MPa)
M-1	0.15	1000	15	150	172.5	3.6	18	132
M-2	0.15	1000	20	200	180	3.6	18	135.6
M-3	0.15	1000	25	250	187.5	3.6	18	136.9
M-4	0.15	1100	15	165	189.75	3.6	20	132
M-5	0.15	1100	20	220	198	3.6	21	136.3
M-6	0.15	1100	25	275	206.25	3.6	19	138.9
M-7	0.15	1200	15	180	207	3.6	20	132.8
M-8	0.15	1200	20	240	216	3.6	20.5	135
M-9	0.15	1200	25	300	225	3.6	20.5	137
M-10	0.175	1000	15	150	201.25	2	22	129.4
M-11	0.175	1000	20	200	210	2	20	133.3
M-12	0.175	1000	25	250	218.75	2	22	135
M-13	0.175	1100	15	165	221.38	1.5	18.5	128.4
M-14	0.175	1100	20	220	231	1.5	20.5	130
M-15	0.175	1100	25	275	240.63	1.5	19	133
M-16	0.175	1200	15	180	241.5	1.5	22.5	130
M-17	0.175	1200	20	240	252	1.5	20	134
M-18	0.175	1200	25	300	262.5	1.5	20	136
M-19	0.2	1000	15	150	230	1.5	22	121.5
M-20	0.2	1000	20	200	240	1.5	21.5	126.2
M-21	0.2	1000	25	250	250	1.5	22	128
M-22	0.2	1100	15	165	253	1	19	123.3
M-23	0.2	1100	20	220	264	1	18.8	125.7
M-24	0.2	1100	25	275	275	1	19	128.3
M-25	0.2	1200	15	180	276	1	21	128
M-26	0.2	1200	20	240	288	1	20	132.2
M-27	0.2	1200	25	300	300	1	19	135

From **Table 4-2**, it is evident that the optimum superplasticizer dosage was 3.6% by weight of the cementitious material for all mixtures with a w/b ratio of 0.15. For mixtures with w/b ratio of 0.175, optimum superplasticizer dosage was in the range of 1.5% to 2% of the cementitious material. The optimum dosage of superplasticizer was in the range of 1% to 1.5% in the UHPC mixtures with a w/b ratio of 0.20. As expected, it is evident that the requirement of superplasticizer increases with the decrease in the w/b ratio.

4.2 WATER PENETRATION DEPTH

The water penetration depths of UHPC specimens belonging to all 27 mixtures, measured after 28 days of water curing are presented in **Table 4-3**. As observed from **Table 4-3**, there is decrease in water penetration depth with the increase in cement content. Also, with the increase in silica fume content, the water penetration depth decreased, while it was opposite for the water to binder ratio because by decreasing the w/b ratio, a decrease in water penetration depth was observed. The lowest depth was noted in the UHPC specimen with highest cement content in combination with highest silica fume content and lowest water to binder ratio of this study. While the greatest depth achieved was in UHPC with lowest cement content in combination with lowest silica fume content and highest water to binder ratio. All the mixtures of UHPC followed consistent trend and all of them were classified as low penetration depths.

4.2.1 Effect of w/b ratio, cement content and silica fume content on water penetration depth

The variations of water penetration depth with silica fume content and w/b ratio are shown in **Figure 4.2** through **Figure 4.4**, for cement contents 1000, 1100 and 1200 kg/m^3, respectively. As can be seen from **Figures 4.2** through **4.4**, the water penetration

depth decreased significantly with the increase in silica fume content and decrease in w/b ratio.

Table 4-3: Average water penetration depth for UHPC mixtures

Mix ID	w/b	Cementing Blend		Water penetration depth (mm)
		Cement (kg/m^3)	SF (%)	
M-1	0.15	1000	15	8.3
M-2	0.15	1000	20	6.3
M-3	0.15	1000	25	4.7
M-4	0.15	1100	15	6.7
M-5	0.15	1100	20	3.7
M-6	0.15	1100	25	4.7
M-7	0.15	1200	15	5.3
M-8	0.15	1200	20	4.7
M-9	0.15	1200	25	3.3
M-10	0.175	1000	15	10.7
M-11	0.175	1000	20	9.7
M-12	0.175	1000	25	7.7
M-13	0.175	1100	15	8.7
M-14	0.175	1100	20	7.0
M-15	0.175	1100	25	5.7
M-16	0.175	1200	15	8.3
M-17	0.175	1200	20	5.3
M-18	0.175	1200	25	5.7
M-19	0.2	1000	15	13.3
M-20	0.2	1000	20	11.3
M-21	0.2	1000	25	9.7
M-22	0.2	1100	15	12.7
M-23	0.2	1100	20	9.7
M-24	0.2	1100	25	8.7
M-25	0.2	1200	15	10.3
M-26	0.2	1200	20	9.0
M-27	0.2	1200	25	7.7

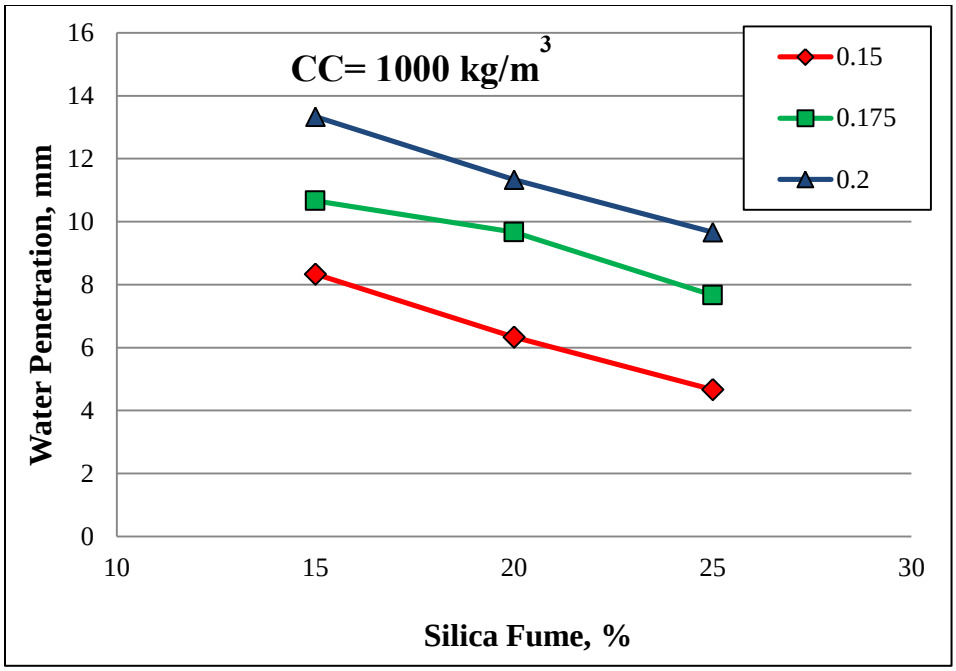

Figure 4.2: Water penetration depth for CC: 1000 kg/m^3 for different w/b ratios and silica fume.

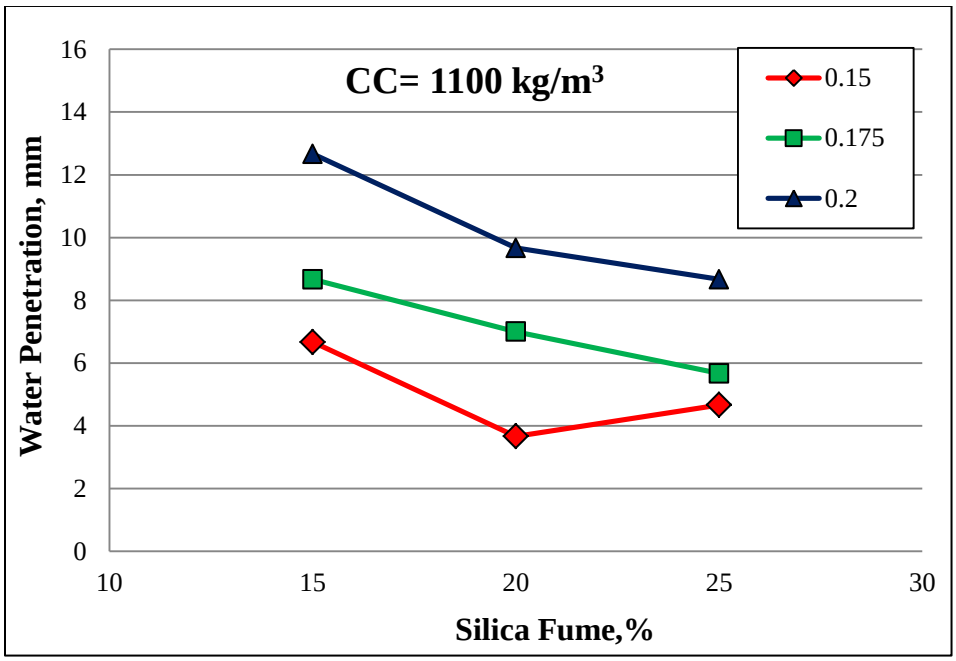

Figure 4.3: Water Penetration depth for CC: 1100 kg/m^3 for different w/b ratios and silica fume.

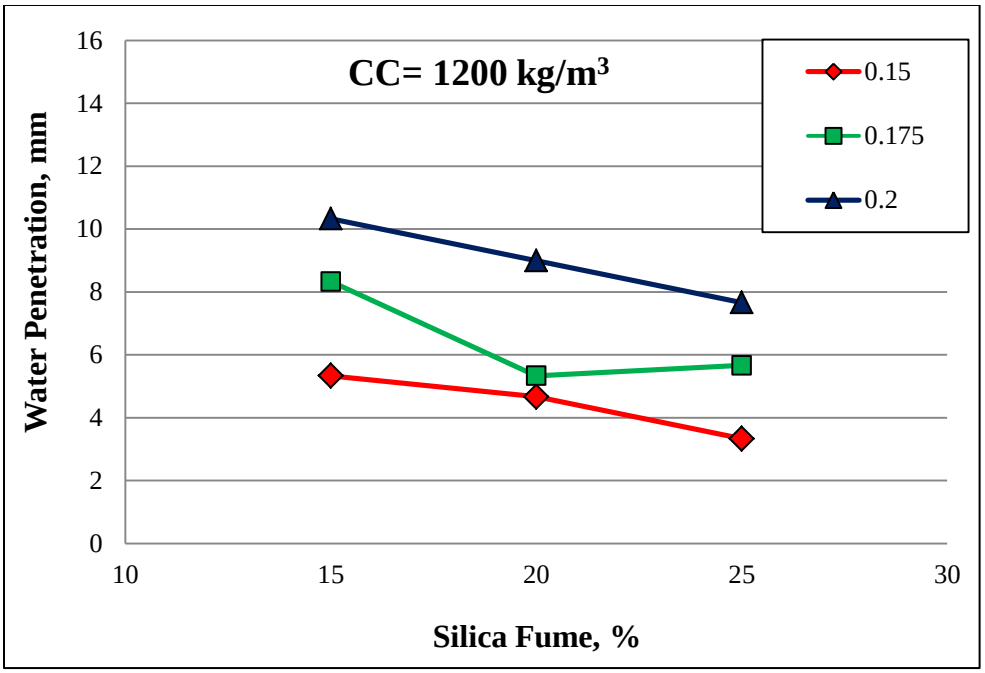

Figure 4.4: Water Penetration depth for CC: 1200 kg/m^3 for different w/b ratios and silica fume.

4.2.2 Water permeability ratings based on measured values of water penetration depths

The 28-day water penetration depth (WPD) values for the UHPC mixtures were plotted in **Figure 4.5** through **Figure 4.7**, for water to binder ratios of 0.15, 0.175 and 0.2, respectively, for rating the permeability of UHPC mixtures according to the criteria as specified in Table 3-6. As can be seen from **Figure 4.5** through **Figure 4.7**, all the UHPC mixtures can be rated with the **low permeability (i.e., WPD < 30 mm)**. The reason behind low permeability of the UHPC mixtures can be attributed to dense microstructure of UHPC having very fine pores which are mostly segmented. The positive effect of lower w/b ratio on water permeability is evident from **Figure 4.5**,

Figure 4.6 and **Figure 4.7**.

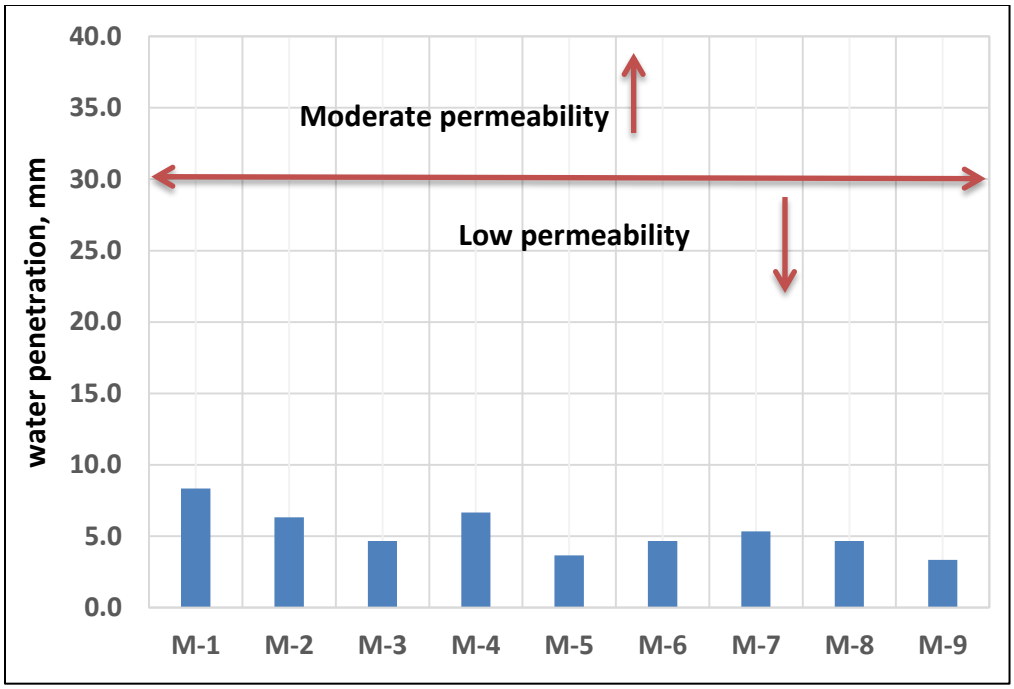

Figure 4.5: Classification of water permeability based on penetration in mm for mixes 1 through 9 (w/b=0.15).

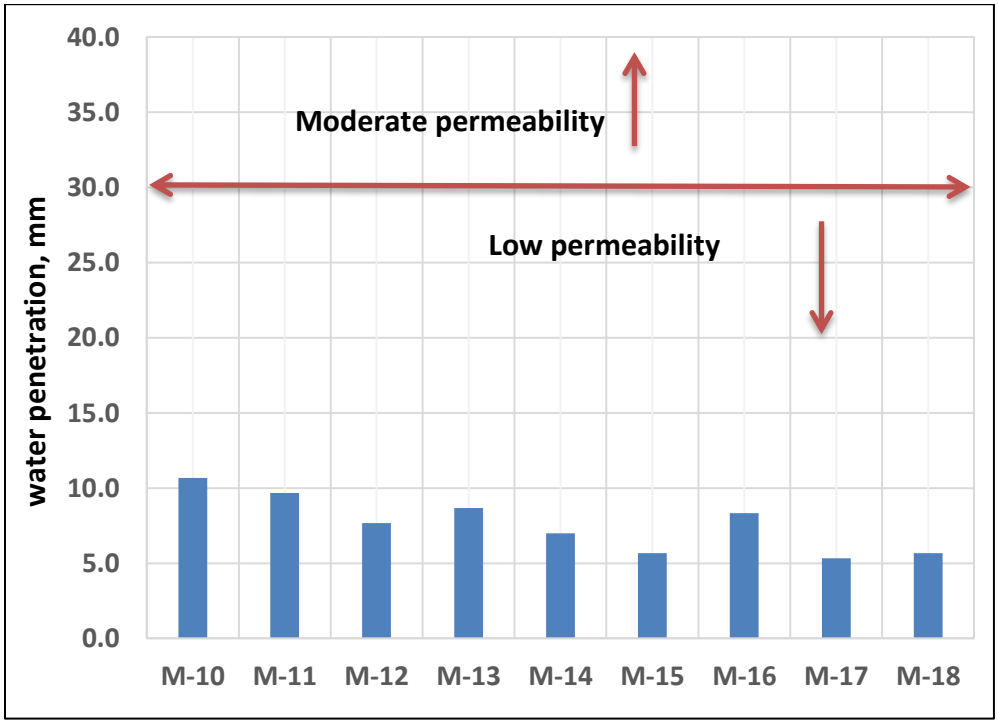

Figure 4.6: Classification of water permeability based on penetration in mm for mixes 10 through 18 (w/b=0.175).

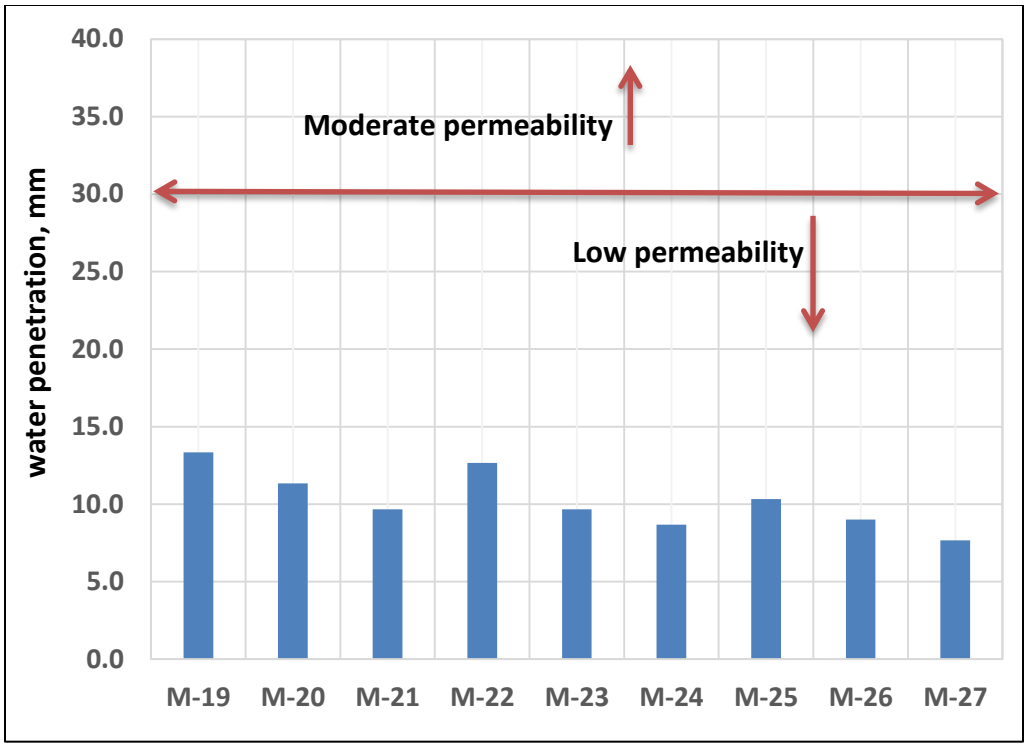

Figure 4.7: Classification of water permeability based on penetration in mm for mixes 19 through 27 (w/b=0.2).

4.2.3 Comparison of water permeability with other types of concrete studied at KFUPM

Table 4-4, shows the relative comparison between water penetration depths of UHPC with other types of concretes studied in different research projects conducted at KFUPM. Although there may not be a clear comparison made between these studies due to the difference in all the major factors involving in mix design but still it can be seen that UHPC showed much lower water penetration depths than other concretes in use. The most important thing to be noted which is clearly seen in **Table 4-3** that the water penetration depths for all the UHPC specimens were consistently low and very few crossed 10 mm penetration. **Figure 4.8** shows the comparison of minimum and maximum water penetration depths for different types of concrete studied at KFUPM.

Table 4-4: Comparison of water penetration depth of UHPC with other types of concrete

Type of concrete	w/b	Cement Content (kg/m^3)	Admixtures	28- d compressive strength, MPa	Water Penetration Depth (mm)
UHPC	0.15	1200	25% SF	137 (max)	3.3 (min)
	0.2	1000	15% SF	121.5 (min)	13.3 (max)
SCC [69]	0.3	400	10% SF +10% LSP	78.3 (max)	6.6 (min)
	0.3	400	15% CKD + 5% MK	46.0 (min)	21 (max)
Ternary [70]	0.4	370	7% SF + 25% FA	53.9 (max)	20.3 (min)
	0.4	370	2.5% SF + 10% FA	48.4 (min)	43 (max)

LSP= Lime stone powder, MK= Metakaolin, FA= Fly ash, CKD= Cement kiln dust

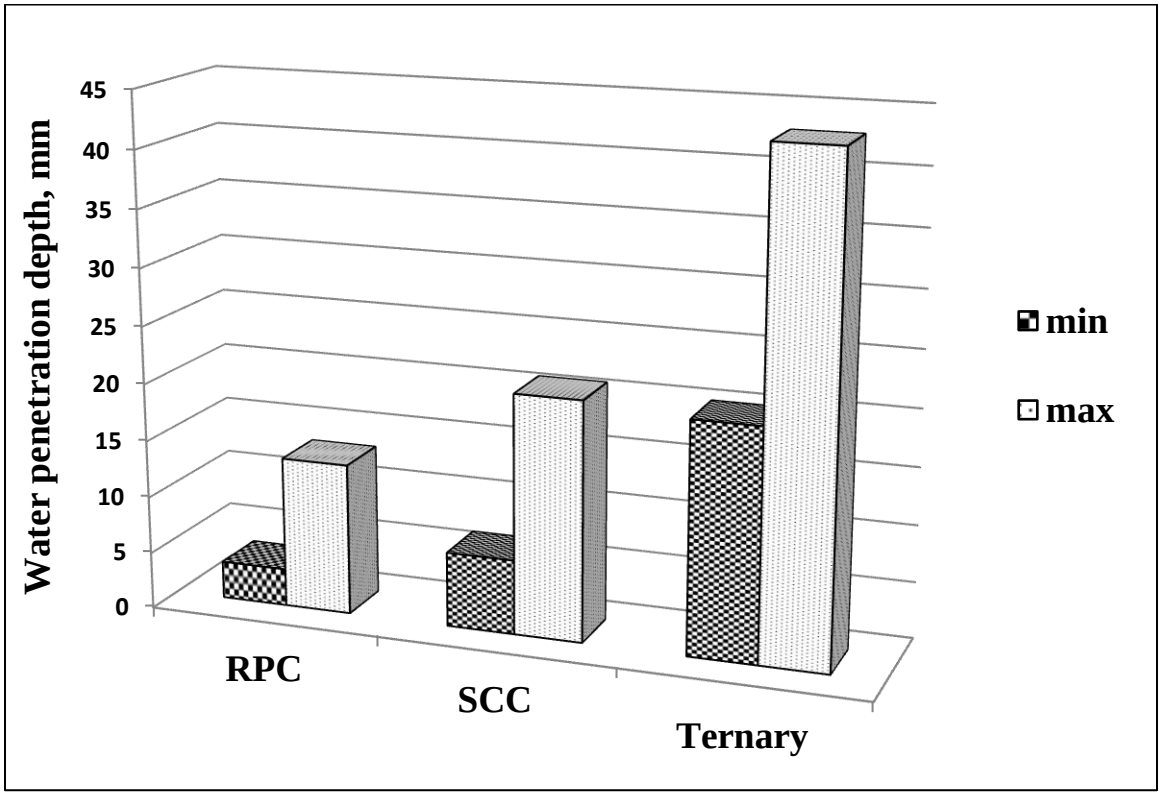

Figure 4.8: Comparison of minimum and maximum water penetration depths obtained for different types of concrete.

4.2.4 Statistical Analysis for Water Penetration Depth

Data in **Table 4-3** was utilized to develop relationship between the parameter (water penetration depth) and w/b ratio, cementitious material content and silica fume content. The ANOVA for water penetration depth, for which a general linear model was developed, is given below:

ANOVA for Water Penetration Depth, WP vs. C, w/b, SF

Factor	Type	Levels	Values
C	fixed	3	1000, 1100, 1200
w/b	fixed	3	0.150, 0.175, 0.200
SF	fixed	3	150, 200, 250

Analysis of Variance for WP, using Adjusted SS for Tests

Source	DF	Seq SS	Adj SS	Adj MS	F	P
C	2	121.742	107.336	53.668	34.96	0.000
w/b	2	304.760	303.573	151.787	98.88	0.000
SF	2	104.983	104.983	52.492	34.19	0.000
Error	69	105.923	105.923	1.535		
Total	75	637.408				

S = 1.23900 R-Sq = 83.38% R-Sq(adj) = 81.94%

P-values indicate that all three factors have significant effect on WPD. F-ratios indicate that the w/b ratio has most significant effect.

The regression equation relating the water penetration depth to the w/b ratio, cementitious material content, and silica fume content is given below.

$$WP = 12.1 - 0.0144\ C + 98.9\ w/b - 0.0285\ SF$$

A good fit of this model is noted by a $R^2 = 0.82$.

The above model indicates that WPD is increasing with w/b ratio and decreasing with C and SF contents.

4.3 CHLORIDE PERMEABILITY

The average values of the rapid chloride permeability (in terms of charge passed through the specimens) after 28 days of water curing of all 27 mixtures of UHPC are presented in **Table 4-5**.

Table 4-5: Rapid Chloride Permeability of UHPC specimens

Mix ID	w/b	Cementing Blend		Average charge passed, Coulombs
		cement (kg/m^3)	SF (%)	
M-1	0.15	1000	15	81
M-2	0.15	1000	20	76
M-3	0.15	1000	25	65
M-4	0.15	1100	15	53
M-5	0.15	1100	20	45
M-6	0.15	1100	25	39
M-7	0.15	1200	15	33
M-8	0.15	1200	20	21
M-9	0.15	1200	25	20
M-10	0.175	1000	15	140
M-11	0.175	1000	20	133
M-12	0.175	1000	25	128
M-13	0.175	1100	15	108
M-14	0.175	1100	20	96
M-15	0.175	1100	25	87
M-16	0.175	1200	15	73
M-17	0.175	1200	20	65
M-18	0.175	1200	25	59
M-19	0.2	1000	15	242
M-20	0.2	1000	20	210
M-21	0.2	1000	25	207
M-22	0.2	1100	15	182
M-23	0.2	1100	20	160
M-24	0.2	1100	25	139
M-25	0.2	1200	15	125
M-26	0.2	1200	20	99
M-27	0.2	1200	25	89

As observed from **Table 4-5**, like water permeability, the chloride permeability was also found to decrease with decrease in w/b ratio and increase in cement and silica fume contents. Lowest charge passed was noted in the UHPC specimen with highest cement content in combination with highest silica fume content and lowest w/b ratio. While, the highest charge passed was recorded in UHPC with lowest cement content in combination with lowest silica fume content and highest w/b ratio.

4.3.1 Effect of w/b ratio, cement content and silica fume content on chloride permeability

The variations of chloride permeability with silica fume content and w/b ratio are shown in **Figure 4.9** through **Figure 4.11**, for cement contents 1000, 1100 and 1200 kg/m^3, respectively. As can be seen from **Figure 4.9** through **Figure 4.11**, the chloride permeability decreased significantly with the increase in silica fume content and decrease in w/b ratio. It can be noted that the decrease in chloride permeability with increase in silica fume content is more significant in case of the mixtures with w/b ratio of 0.2 as compared to the w/b ratios of 0.15 and 0.175, indicating more effectiveness of silica fume at higher w/b ratio.

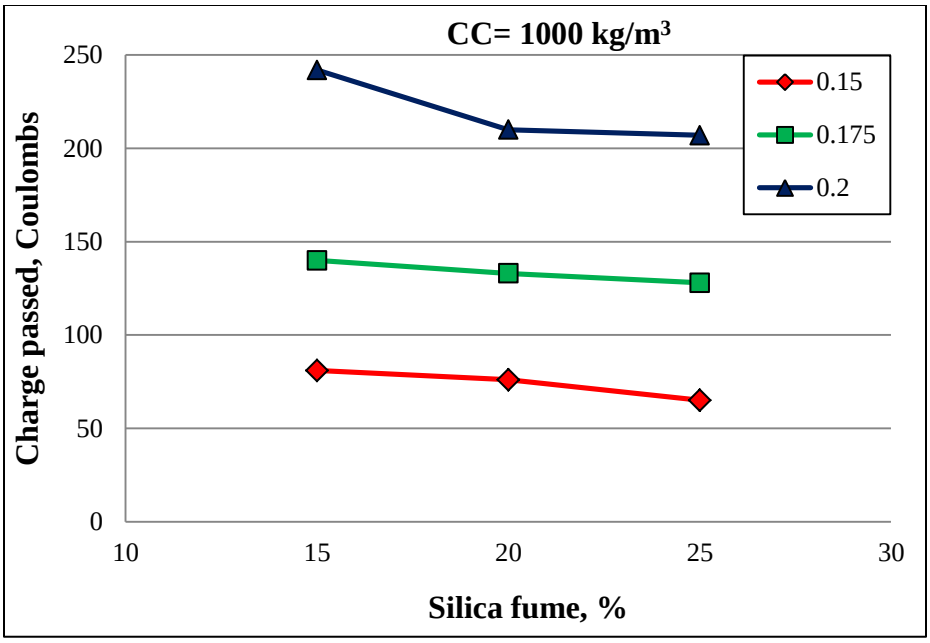

Figure 4.9: Charge passed in specimens with CC: 1000 kg/m^3 for different w/b ratios and silica fume content.

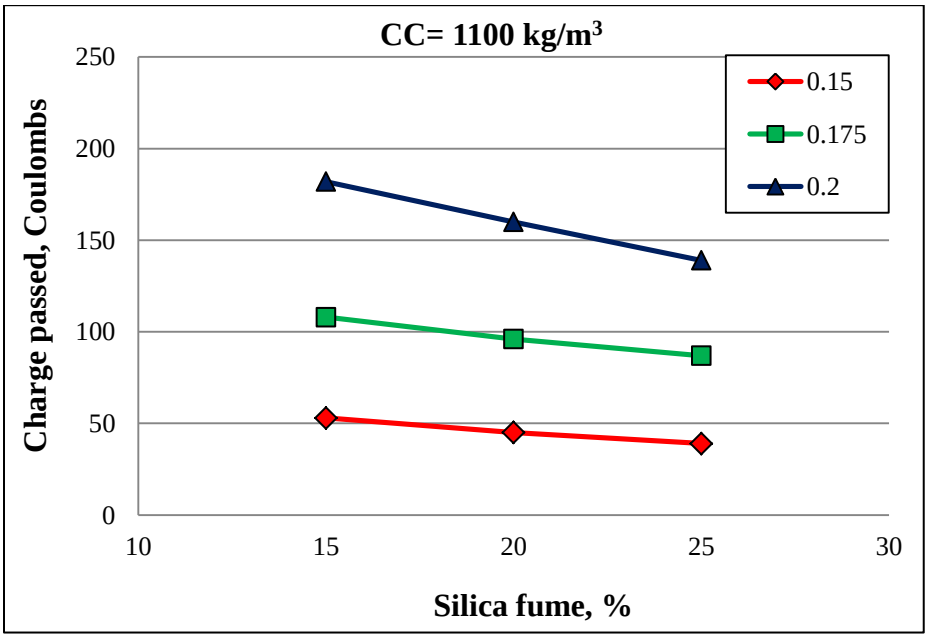

Figure 4.10: Charge passed in specimens with CC: 1100 kg/m^3 for different w/b ratios and silica fume content.

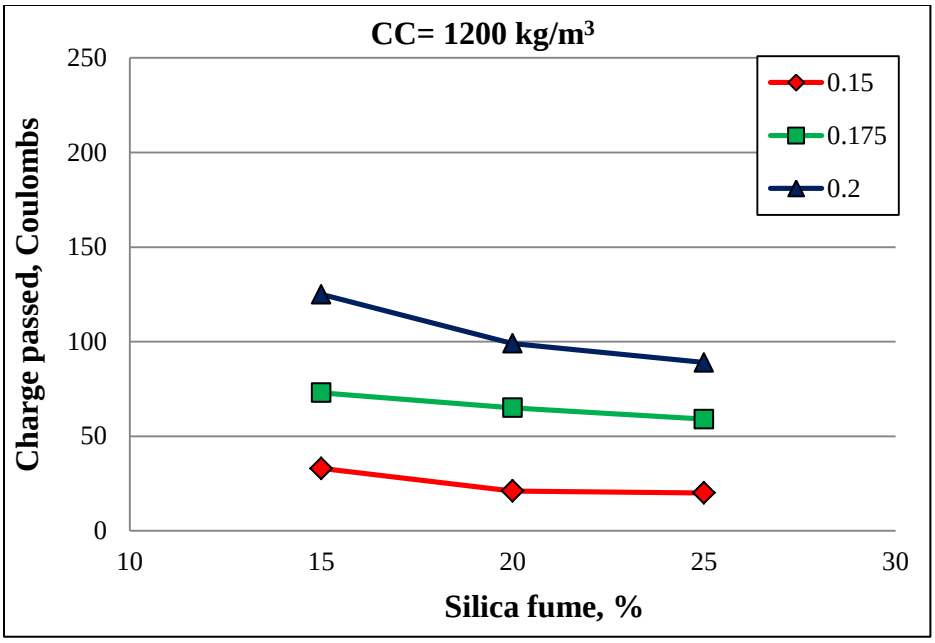

Figure 4.11: Charge passed in specimens with CC: 1200 kg/m^3 for different w/b ratios and silica fume content.

4.3.2 Chloride permeability ratings based on measured values of charge passed

The 28-day chloride permeability measured for all 27 mixtures, in terms of charges passed, were plotted in three groups for w/b ratios of 0.15, 0.175 and 0.2, respectively, as shown in **Figure 4.12** through **Figure 4.14**, for rating the chloride permeability of UHPC mixtures according to ASTM C 1202, as presented in **Table 3-7**. As can be seen from **Figure 4.12** through **Figure 4.14**, all the UHPC mixtures can be rated with the **very low or negligible** chloride permeability. The reason behind very low or negligible chloride permeability of the UHPC mixtures can be attributed to dense microstructure of UHPC having very fine pores which are mostly segmented. The positive effect of lower w/b ratio on chloride permeability is evident from **Figure 4.12** through **Figure 4.14**.

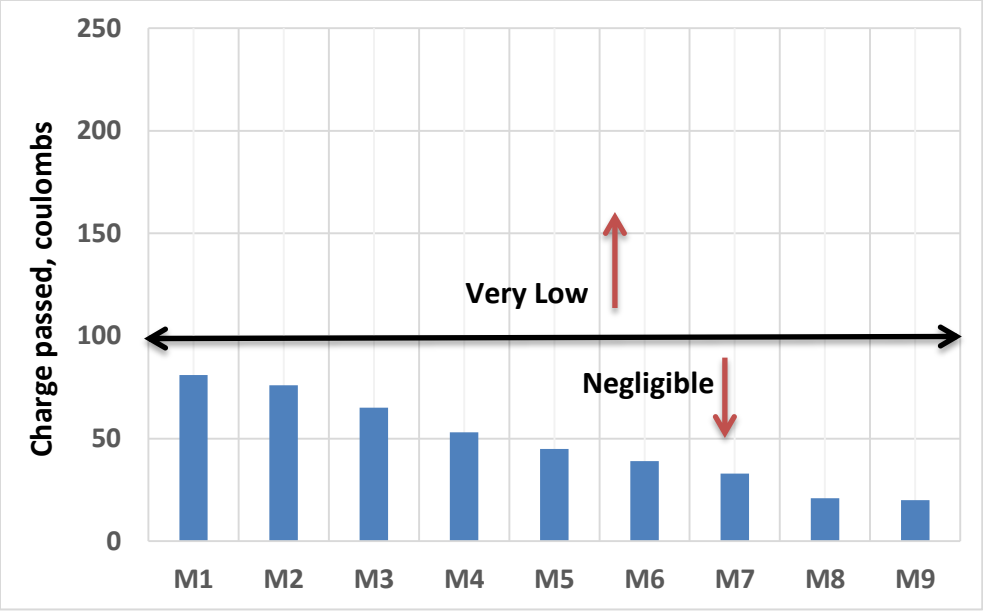

Figure 4.12: Classification of chloride permeability based on charge passed for mixes 1 through 9 (w/b=0.15).

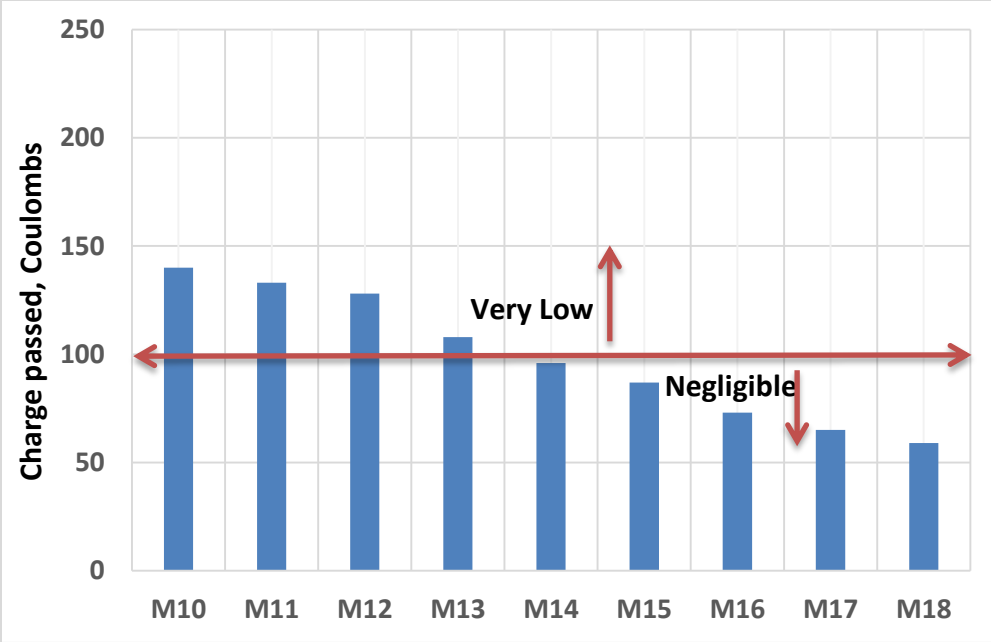

Figure 4.13: Classification of chloride permeability based on charge passed for mixes 10 through 18 (w/b=0.175).

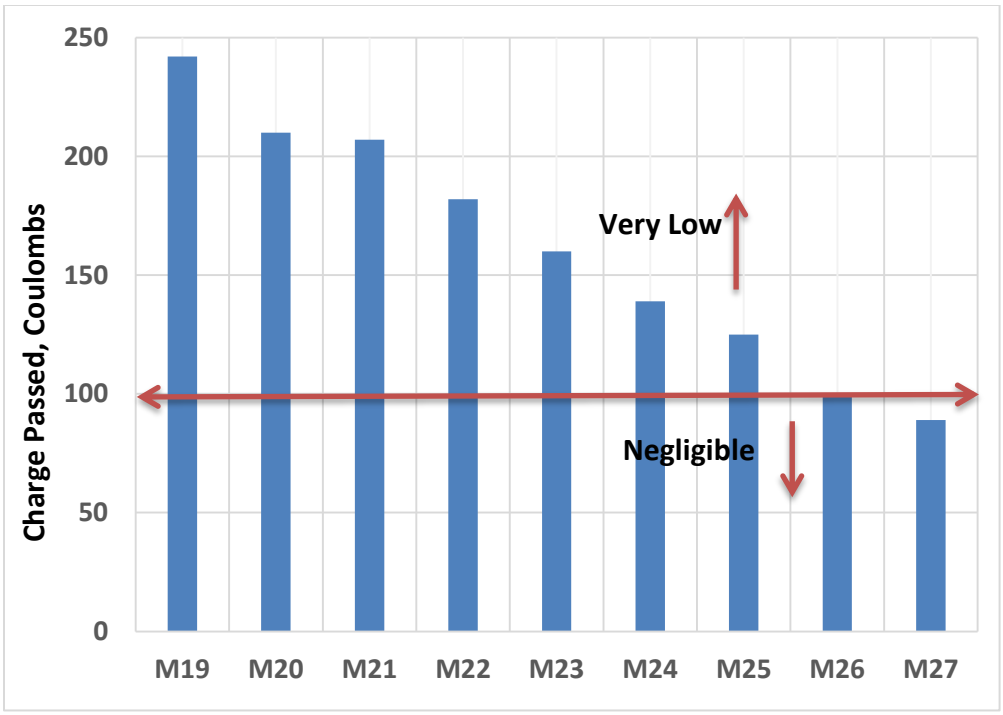

Figure 4.14: Classification of chloride permeability based on charge passed for mixes 19 through 27 (w/b=0.2).

4.3.3 Comparison of chloride permeability with other types of concrete studied at KFUPM

Table 4-6, shows the relative comparison between chloride permeability of UHPC with other types of concretes studied under different research projects conducted at KFUPM. Although, due to the difference in all the major factors involving in mix design there may not be a clear comparison made between these studies but still it can be seen that UHPC showed lower chloride permeability than other concretes. **Figure 4.15** shows the comparison of minimum and maximum charge passed through different types of concrete prepared in KFUPM research projects.

Table 4-6: Comparison of Chloride permeability of UHPC with other types of concrete.

Type of concrete	w/b	Cement Content (kg/m^3)	Admixtures	28-day compressive strength, MPa	Charge Passed, Coulombs
UHPC	0.15	1200	25% SF	137 (max)	20 (min)
	0.2	1000	15% SF	121.5 (min)	242 (max)
SCC **[69]**	0.3	400	10% SF +10% LSP	78.3 (max)	92 (min)
	0.3	400	10% NP + 10% BHD	46.0 (min)	1665 (max)
Binary **[75]**	0.35	400	7.5% SF	48.1 (max)	782 (min)
	0.5	350	20% FA	23.7 (min)	3548 (max)
Ternary **[70]**	0.4	370	7% SF + 25% FA	53.9 (max)	695 (min)
	0.4	370	2.5% SF + 10% FA	48.4 (min)	1549 (max)
Quaternary **[74]**	0.4	370	50% C + 5% SF + 25% FA + 20% Clay	42.0 (max)	805 (min)
	0.4	370	50% C + 5% SF + 30% NP + 15% BHD	36.62 (min)	3178 (max)

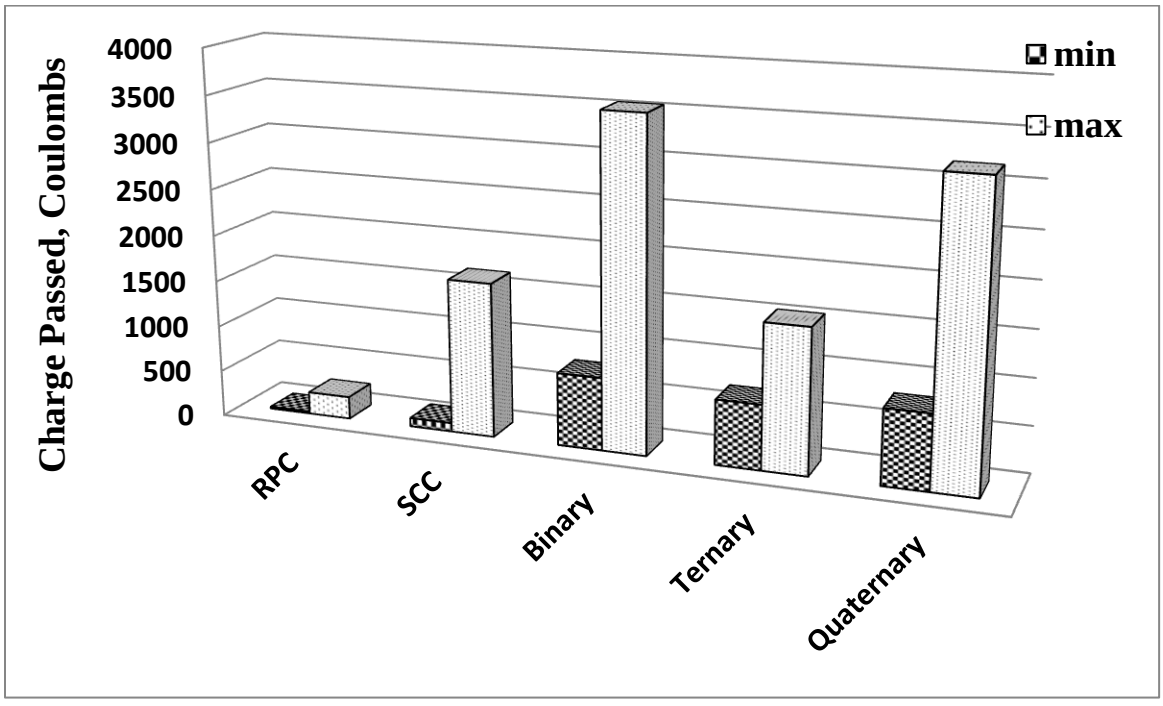

Figure 4.15: Comparison of minimum and maximum chloride permeability for different types of concrete.

4.3.4 Statistical Analysis for Chloride Permeability

Data in **Table 4-5** was utilized to develop relationship between the parameter (Charge Passed) and w/b ratio, cementitious material content and silica fume content. The ANOVA for charge passed in a chloride permeability test, for which a general linear model was developed, is given below:

ANOVA for Charge Passed, CP vs. C, w/b, SF

Factor	Type	Levels	Values
w/b	fixed	3	0.150, 0.175, 0.200
C	fixed	3	1000, 1100, 1200
SF	fixed	3	15, 20, 25

Analysis of Variance for CP, using Adjusted SS for Tests

Source	DF	Seq SS	Adj SS	Adj MS	F	P
w/b	2	58016	58016	29008	138.25	0.000
C	2	27110	27110	13555	64.60	0.000
SF	2	2379	2379	1189	5.67	0.011
Error	20	4196	4196	210		
Total	26	91701				

S = 14.4852 R-Sq = 95.42% R-Sq(adj) = 94.05%

P-values indicate that all three factors have significant effect on chloride permeability. However, SF has very little effect. F-ratios indicate that the w/b ratio has most significant effect.

The regression equation relating the charge passed to the w/b ratio, cementitious material content, and silica fume content is given below.

$$CP = 178 - 0.388\ C + 2267\ w/b - 2.27\ SF$$

A good fit of this model is noted by a $R^2 = 0.95$.

The above model indicates that CP is increasing with w/b ratio and decreasing with C and SF contents.

4.4 ELECTRICAL RESISTIVITY

The electrical resistivity of UHPC specimens was measured after 28 days of curing. The electrical resistivity of UHPC specimens prepared with varying mixture design variables are presented in **Table 4-7**.

Table 4-7: Average electrical resistivity for UHPC mixtures

Mix ID	w/b	Cementing Blend		Electrical Resistivity (k-Ohms-cm)
		cement (kg/m^3)	SF (%)	
M-1	0.15	1000	15	44.5
M-2	0.15	1000	20	54.7
M-3	0.15	1000	25	63.4
M-4	0.15	1100	15	55.5
M-5	0.15	1100	20	63.5
M-6	0.15	1100	25	67.5
M-7	0.15	1200	15	60.0
M-8	0.15	1200	20	66.4
M-9	0.15	1200	25	78.8
M-10	0.175	1000	15	36.9
M-11	0.175	1000	20	39.7
M-12	0.175	1000	25	41.0
M-13	0.175	1100	15	37.4
M-14	0.175	1100	20	44.3
M-15	0.175	1100	25	45.5
M-16	0.175	1200	15	38.0
M-17	0.175	1200	20	45.0
M-18	0.175	1200	25	67.7
M-19	0.2	1000	15	26.7
M-20	0.2	1000	20	28.7
M-21	0.2	1000	25	29.9
M-22	0.2	1100	15	31.8
M-23	0.2	1100	20	37.3
M-24	0.2	1100	25	39.9
M-25	0.2	1200	15	35.2
M-26	0.2	1200	20	42.5
M-27	0.2	1200	25	62.9

Just like water penetration depth and chloride permeability all the UHPC specimens showed same trend for electrical resistivity. While the electrical resistivity decreased with increase in w/b ratio, there was increase in electrical resistivity with the increase in cement and silica fume contents. Lowest electrical resistivity was noted in the UHPC mixture with lowest cement content in combination with lowest silica fume content and highest water to binder ratio considered in this study. While, the greatest electrical resistivity was in UHPC with highest cement content in combination with highest silica fume content and lowest water to binder ratio.

4.4.1 Effect of w/b ratio, cement content and silica fume content on electrical resistivity

The variations of electrical resistivity with silica fume content and w/b ratio are shown in **Figure 4.16** through **Figure 4.18**, for cement contents 1000, 1100 and 1200 kg/m^3, respectively. As can be seen from **Figure 4.16** through **Figure 4.18**, the electrical resistivity of UHPC mixtures increased significantly with the increase in silica fume content and decrease in w/b ratio.

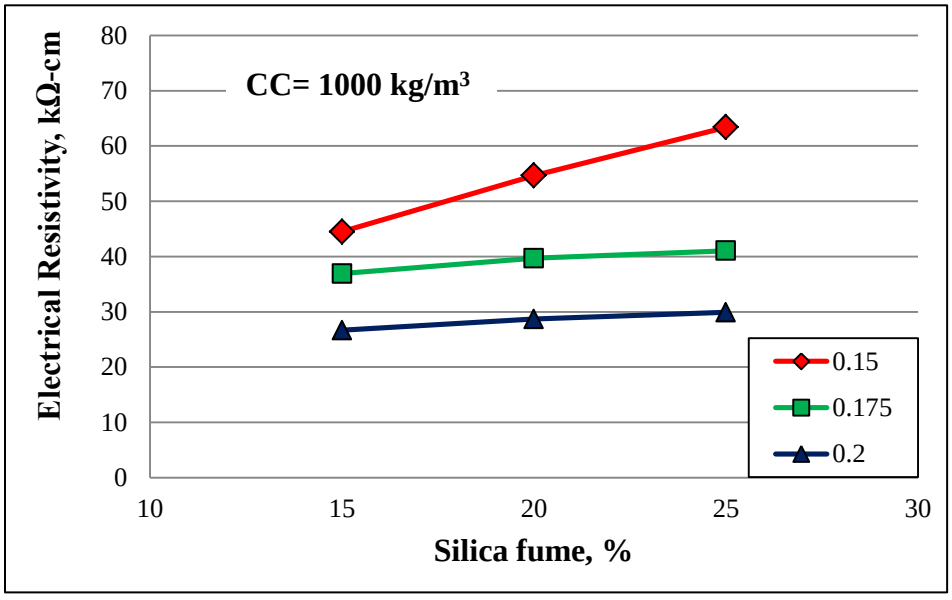

Figure 4.16: Electrical Resistivity for CC: 1000 kg/m^3 for different w/b ratios and silica fume.

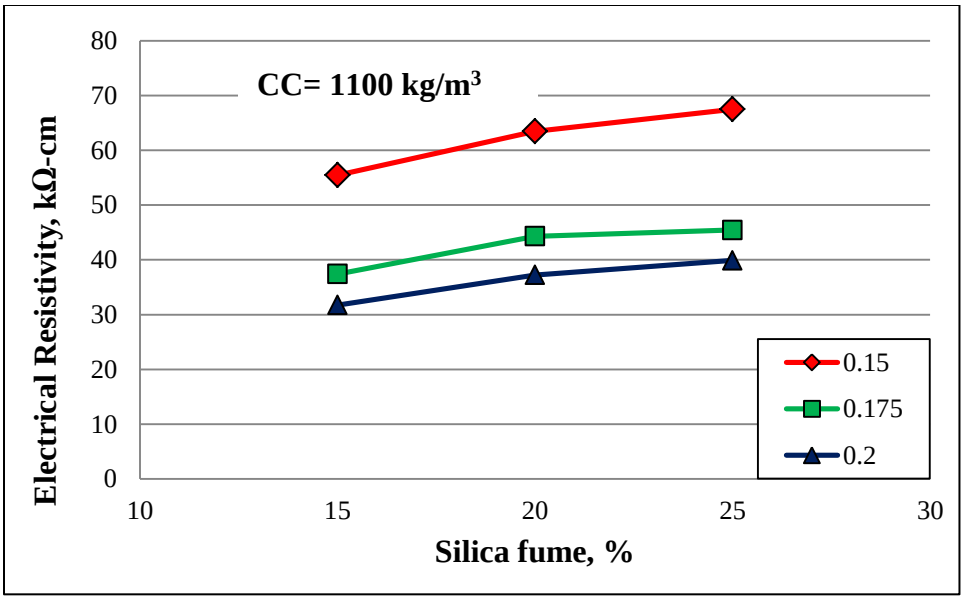

Figure 4.17: Electrical Resistivity for CC: 1100 kg/m^3 for different w/b ratios and silica fume.

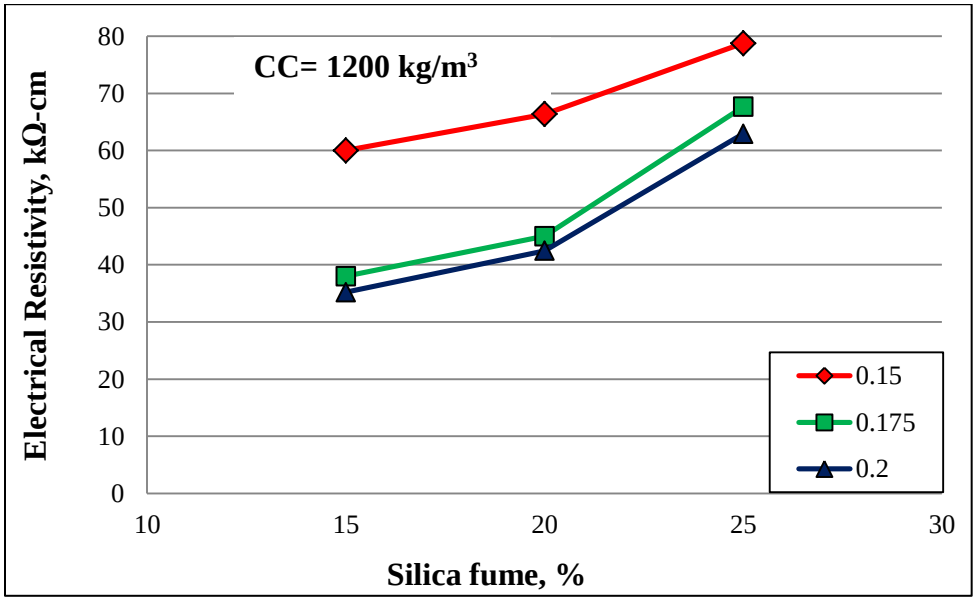

Figure 4.18: Electrical Resistivity for CC: 1200 kg/m^3 for different w/b ratios and silica fume.

4.4.2 Rating of corrosion risk based on electrical resistivity

The resistivity measured for all 27 mixtures were plotted in three groups for w/b ratios of 0.15, 0.175 and 0.2, respectively, as shown in **Figure 4.19** through **Figure 4.21**, for rating the risk of reinforcement corrosion for UHPC mixtures according to the criteria, as presented in **Table 3-8**. Going by the criteria in **Table 3-8**, the reinforcement corrosion risk for all the mixtures of UHPC may be rated as **low to negligible** (since all mixtures had electrical resistivity greater than 20 k-Ohm-cm, as shown in **Figure 4.19** through **Figure 4.21**). The reason behind very high resistivity of the UHPC mixtures can be attributed to dense microstructure of UHPC having very fine pores which are mostly segmented. The positive effect of lower w/b ratio on concrete resistivity is evident from **Figure 4.19** through **Figure 4.21**.

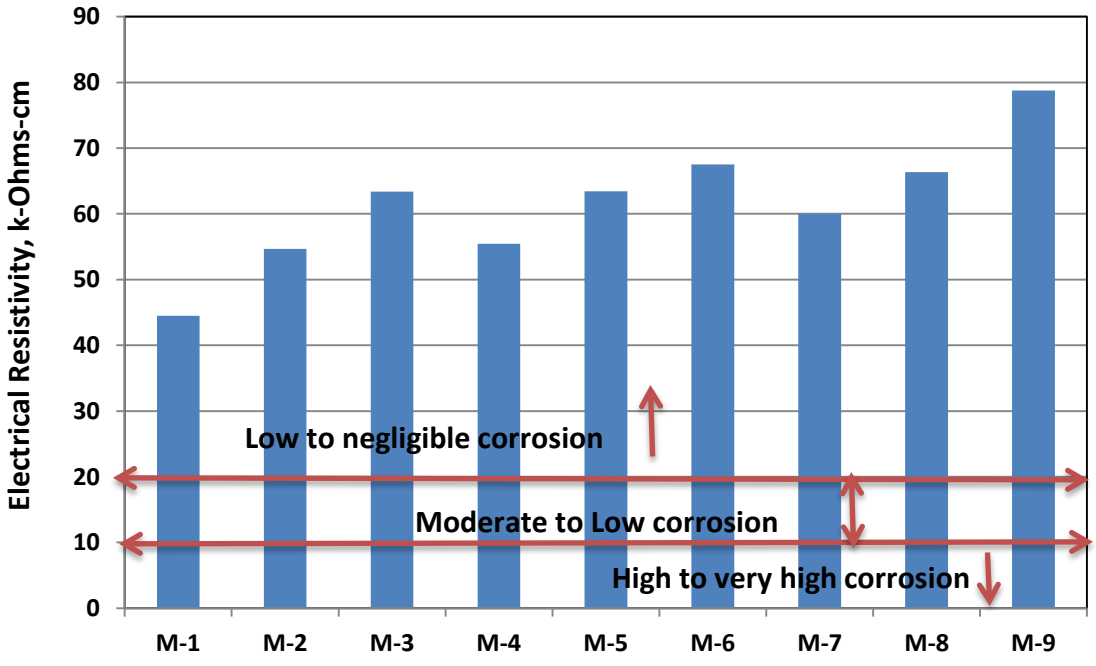

Figure 4.19: Classification of probability of corrosion based on electrical resistivity for mixes 1 through 9 (w/b=0.15).

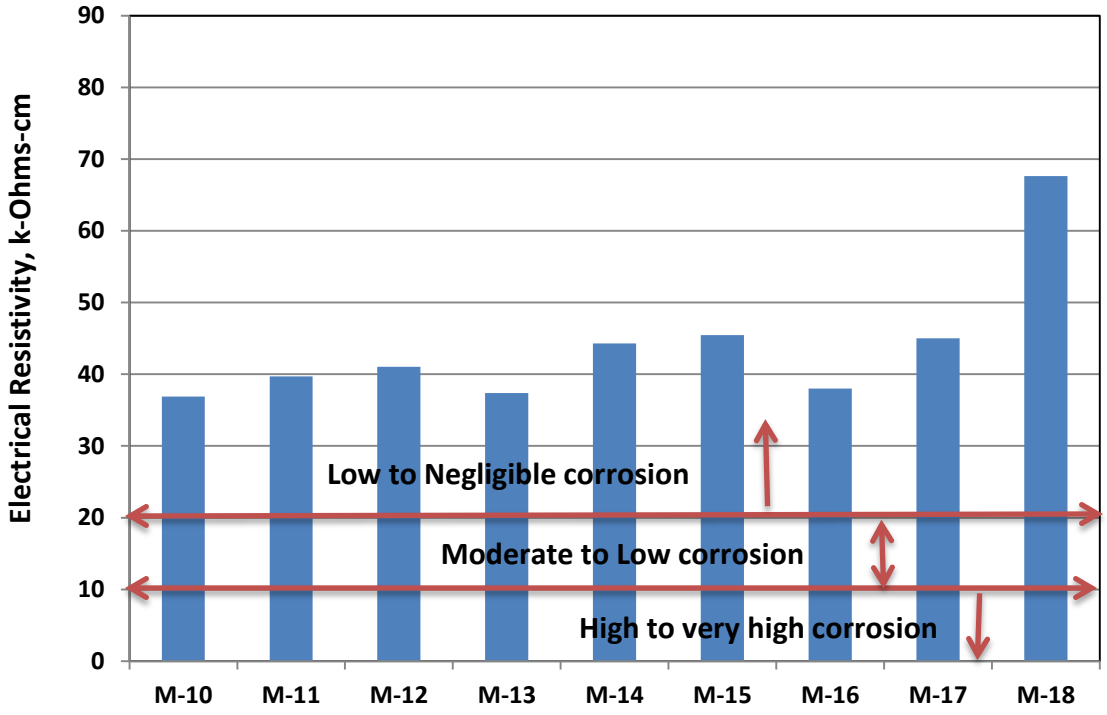

Figure 4.20: Classification of probability of corrosion based on electrical resistivity for mixes 10 through 18 (w/b=0.175).

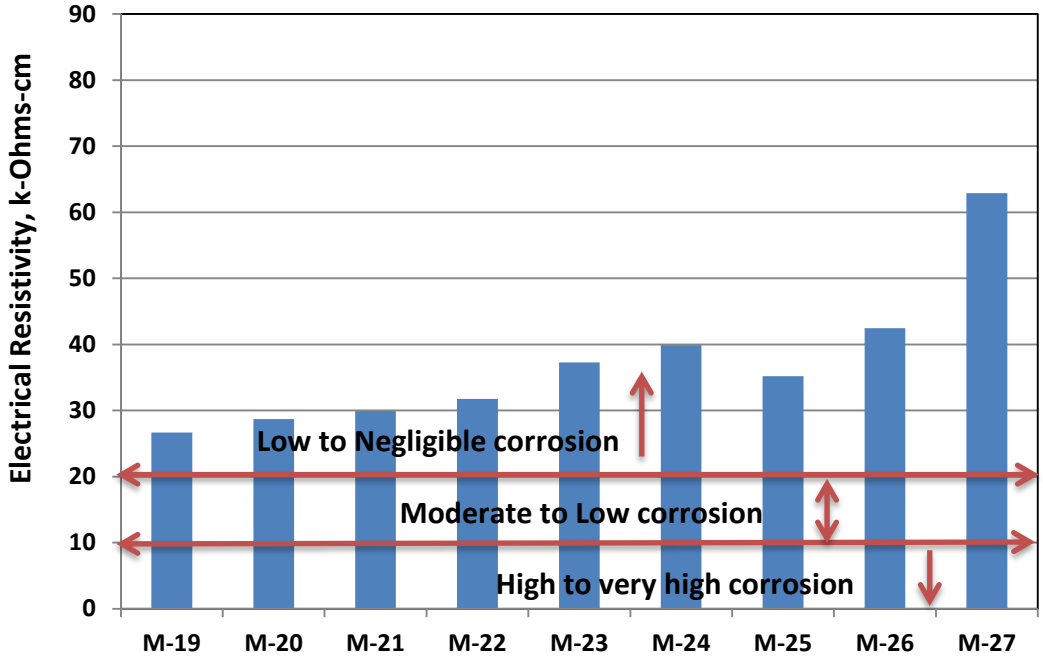

Figure 4.21: Classification of probability of corrosion based on electrical resistivity for mixes 19 through 27 (w/b=0.2).

4.4.3 Statistical Analysis for electrical resistivity

Data in **Table 4-7** was utilized to develop relationship between the parameter and w/b ratio, cementitious material content and silica fume content. The ANOVA for electrical resistivity, for which a general linear model was developed, is given below:

ANOVA for ER vs. C, w/b, SF

```
Factor  Type   Levels  Values
w/b     fixed       3  0.150, 0.175, 0.200
C       fixed       3  1000, 1100, 1200
SF      fixed       3  15, 20, 25

Analysis of Variance for ER, using Adjusted SS for Tests

Source  DF   Seq SS  Adj SS  Adj MS       F      P
w/b      2   5700.7  5700.7  2850.3  107.25  0.000
C        2   1912.9  1912.9   956.5   35.99  0.000
SF       2   1909.5  1909.5   954.7   35.92  0.000
Error   47   1249.1  1249.1    26.6
Total   53  10772.2

S = 5.15535   R-Sq = 88.40%   R-Sq(adj) = 86.92%
```

P-values indicate that all three factors have effect on ER. F-ratios indicate that the w/b ratio has most significant effect on ER

The regression equation relating the electrical resistivity value to the w/b ratio, cementitious material content, and silica fume content is given below.

$$ER = 23.9 - 487\ w/b + 0.0727\ C + 1.45\ SF$$

A good fit of this model is noted by a $R^2 = 0.85$.

The above model indicates that ER is decreasing with w/b and increasing with C and SF contents.

4.5 pH

The pH values of UHPC specimens prepared with varying mixture design variables are presented in **Table 4-8**. It is seen that by increasing the cement content, the pH of UHPC increased. But with the increase in silica fume content or water to binder ratio the pH of the UHPC starts to decrease. However, in all the cases, pH value was much higher than the threshold limit of 10 for initiation of corrosion of rebar.

Table 4-8: pH of UHPC mixtures

Mix ID	w/b	Cementing Blend		pH
		cement (kg/m^3)	SF (%)	
M-1	0.15	1000	15	12.829
M-2	0.15	1000	20	12.708
M-3	0.15	1000	25	12.547
M-4	0.15	1100	15	12.935
M-5	0.15	1100	20	12.789
M-6	0.15	1100	25	12.613
M-7	0.15	1200	15	13.012
M-8	0.15	1200	20	12.936
M-9	0.15	1200	25	12.721
M-10	0.175	1000	15	12.758
M-11	0.175	1000	20	12.602
M-12	0.175	1000	25	12.425
M-13	0.175	1100	15	12.854
M-14	0.175	1100	20	12.741
M-15	0.175	1100	25	12.467
M-16	0.175	1200	15	12.892
M-17	0.175	1200	20	12.775
M-18	0.175	1200	25	12.615
M-19	0.2	1000	15	12.715
M-20	0.2	1000	20	12.614
M-21	0.2	1000	25	12.412
M-22	0.2	1100	15	12.768
M-23	0.2	1100	20	12.674
M-24	0.2	1100	25	12.462
M-25	0.2	1200	15	12.764
M-26	0.2	1200	20	12.732
M-27	0.2	1200	25	12.543

4.5.1 Effect of w/b ratio, cement content and silica fume content on pH of UHPC specimens

From **Figure 4.22** through **Figure 4.24** it was observed that the pH of all the UHPC mixtures varied between 13.01 and 12.41. It is also observed that with the increase in cement content the pH of UHPC mixtures increased. With the increase in w/b ratio the decrease in pH is noted, this trend is more obvious in UHPC mixtures with higher cement content. Also, with the increase in silica fume content a decrease in pH was observed for all the UHPC mixtures due to the fact that addition of silica fume reduces pH of concrete due to consumption of calcium hydroxide in secondary hydration (i.e., in formation of C-S-H gel as a result of reaction between silica fume and calcium hydroxide liberated from the primary hydration).

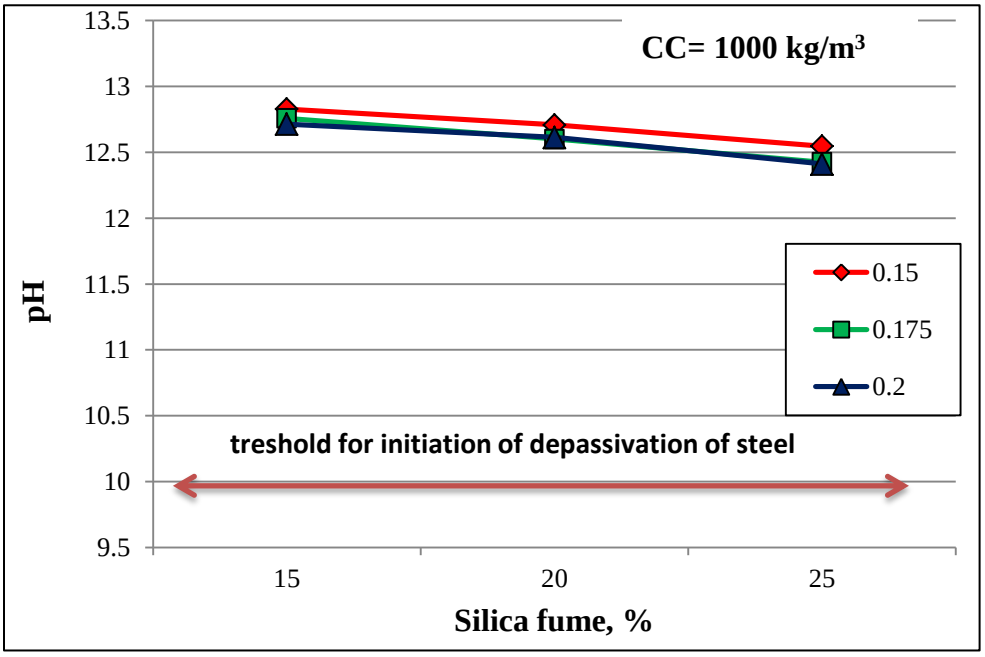

Figure 4.22: pH for CC: 1000 kg/m^3 for different w/b ratios and silica fume.

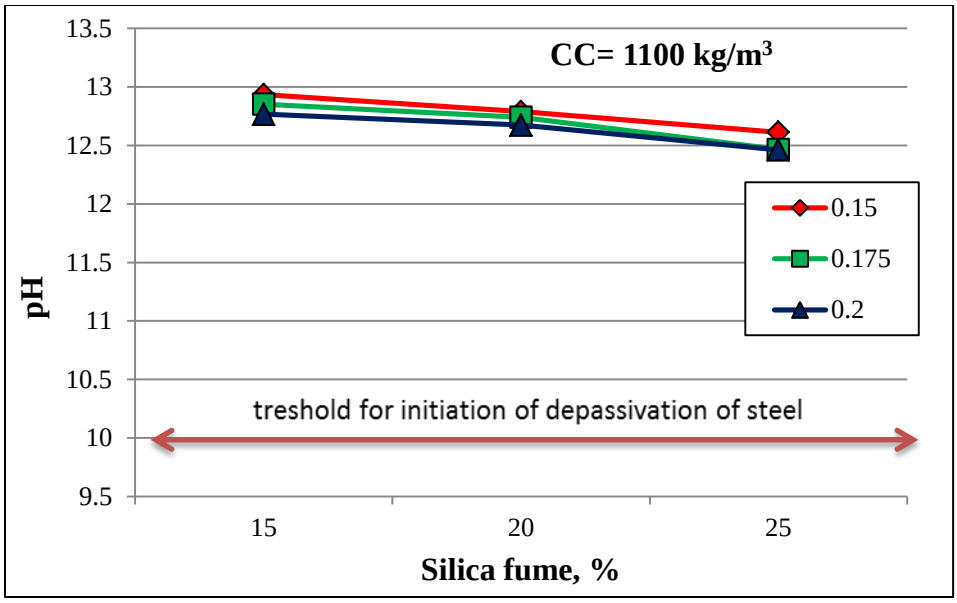

Figure 4.23: pH for CC: 1100 kg/m^3 for different w/b ratios and silica fume.

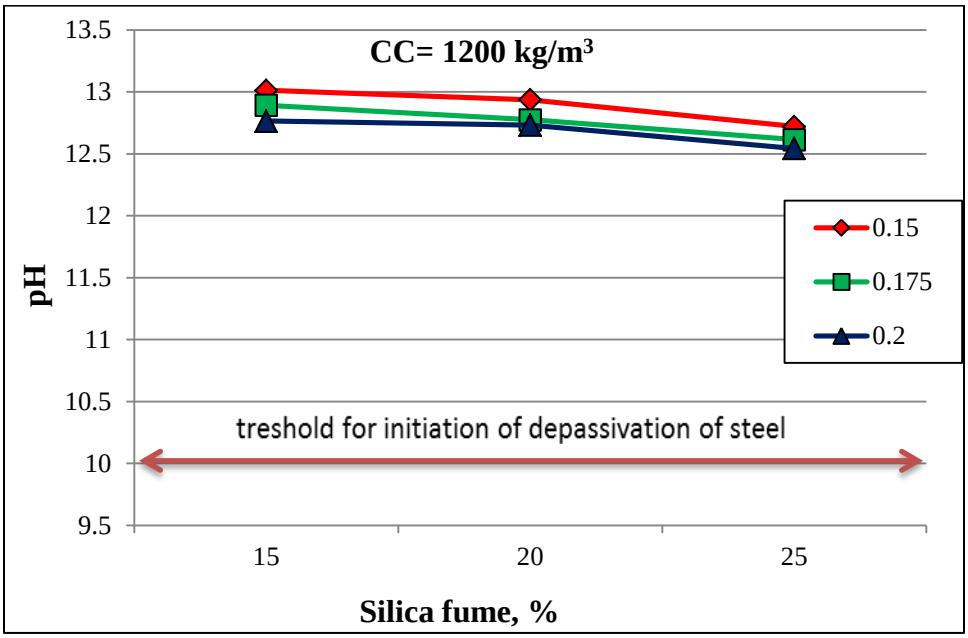

Figure 4.24: pH for CC: 1200 kg/m^3 for different w/b ratios and silica fume.

4.5.2 Low corrosion risk of UHPC mixtures based on their measured pH values

From the plots of pH values for all 27 mixtures in three groups, as shown in **Figure 4.25** through **Figure 4.27**, it can be seen that, unless chloride concentration on the rebar surface reaches to a threshold value, there is no chance of corrosion initiation in any mixture because pH value in all the mixtures are well above the threshold value of 10. Further, due to a very high pH of the UHPC mixtures, the Cl^-/OH^- ratio at a given concentration of chloride ions will be relatively lower delaying the corrosion initiation until a higher concentration of chloride ions is built-up on the rebar surface to an extent that the Cl^-/OH^- ratio crosses its threshold limit of 0.60.

.

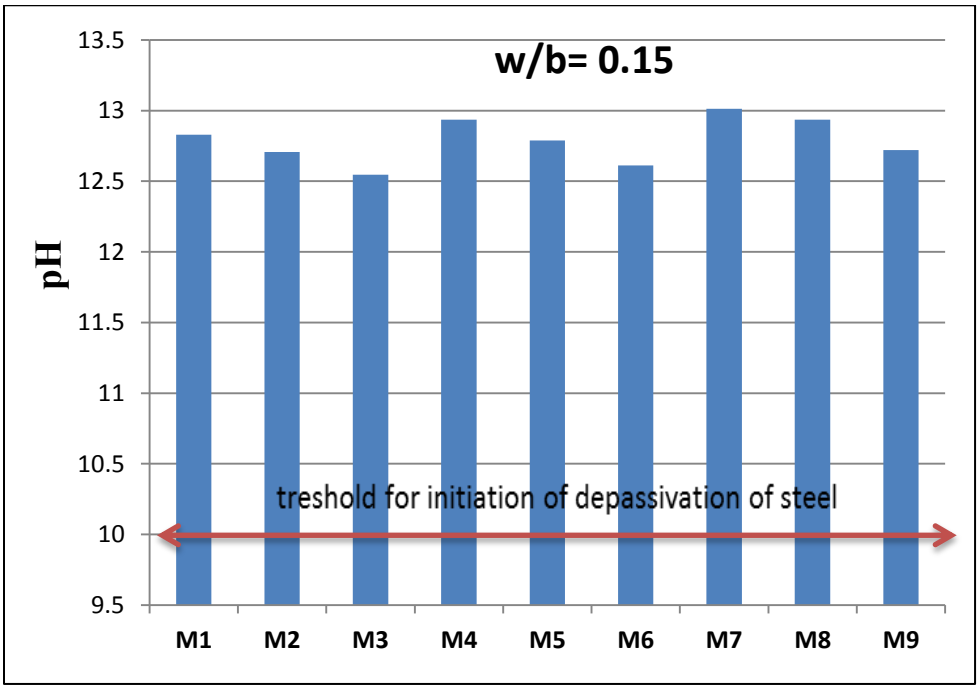

Figure 4.25: pH for water to binder ratio equal to 0.15

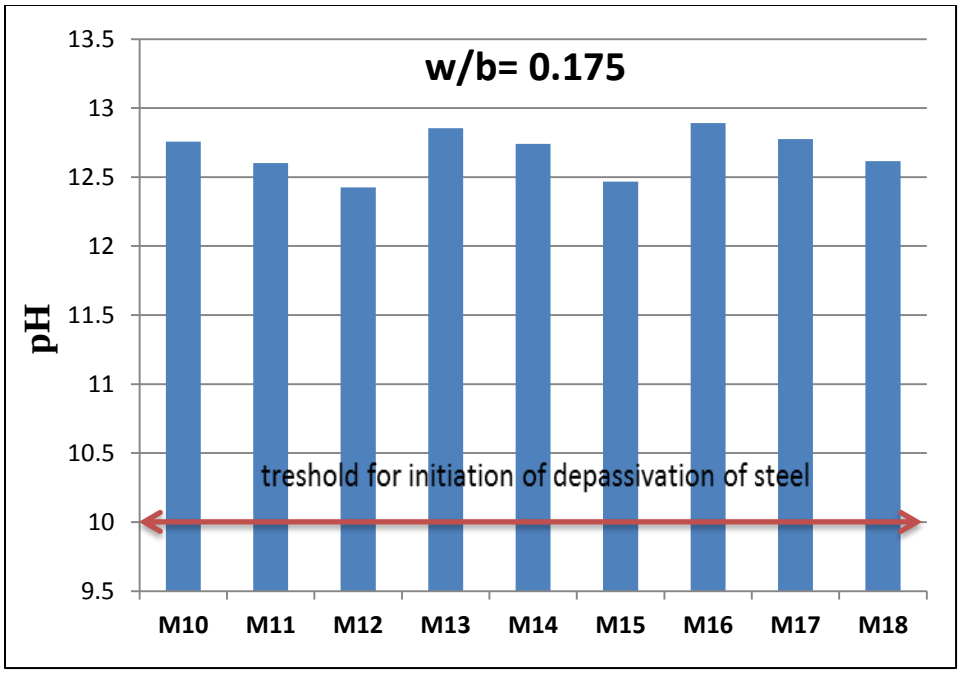

Figure 4.26: pH for water to binder ratio equal to 0.175

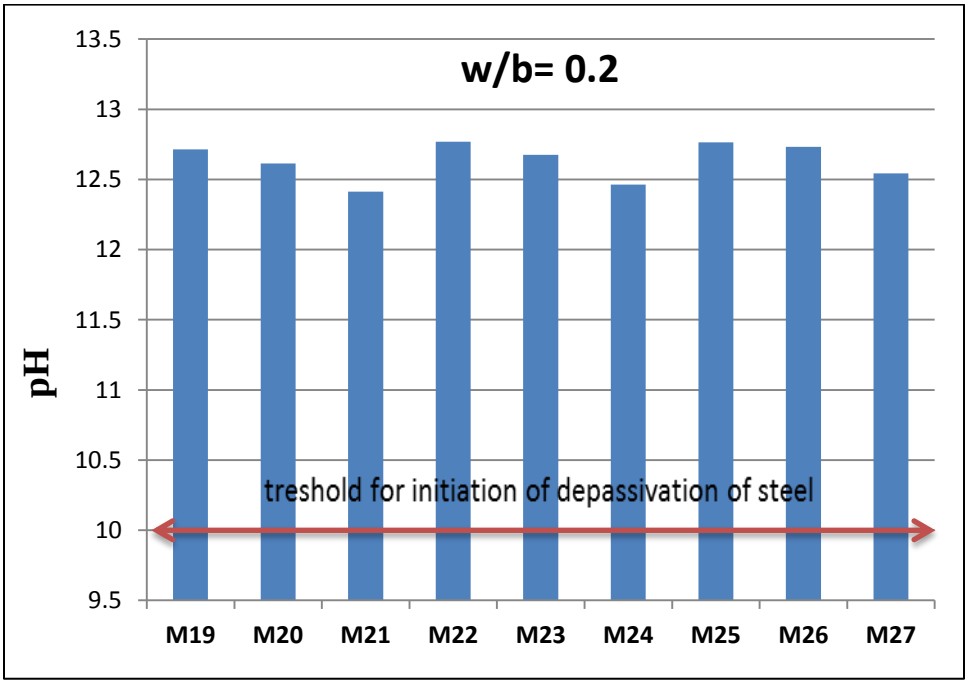

Figure 4.27: pH for water to binder ratio equal to 0.2

4.5.3 Statistical Analysis for pH values

Data in **Table 4-8** was utilized to develop relationship between the parameter (pH) and w/b ratio, cementitious material content and silica fume content. The ANOVA for pH, for which a general linear model was developed, is given below:

ANOVA for pH vs. C, w/b, SF

```
Factor  Type   Levels  Values
w/b     fixed       3  0.150, 0.175, 0.200
C       fixed       3  1000, 1100, 1200
SF      fixed       3  15, 20, 25

Analysis of Variance for pH, using Adjusted SS for Tests

Source  DF   Seq SS   Adj SS   Adj MS       F      P
w/b      2  0.14714  0.14714  0.07357   49.97  0.000
C        2  0.10133  0.10133  0.05066   34.41  0.000
SF       2  0.49427  0.49427  0.24713  167.85  0.000
Error   20  0.02945  0.02945  0.00147
Total   26  0.77218

S = 0.0383710   R-Sq = 96.19%   R-Sq(adj) = 95.04%
```

P-values indicate that all three factors have effect on pH. F-ratios indicate that the SF content has most significant effect on pH.

The regression equation relating the pH value to the w/b ratio, cementitious material content, and silica fume content is given below.

$$pH = 13.1 - 3.46\ w/b + 0.00075\ C - 0.0328\ SF$$

A good fit of this model is noted by a $R^2 = 0.93$.

The above model indicates that pH is decreasing with w/b ratio and SF content and increasing with C content.

4.6 SULFATE RESISTANCE

4.6.1 Visual Inspection

A thorough visual inspection was carried out on all the mixtures after nine months of exposure to sulfate solution, to evaluate the visible signs of softening, cracking and spalling in the UHPC specimen. Sulfate attack on concrete is primarily attributed to sodium, magnesium and calcium sulfate salts. Due to limited solubility of calcium salts in water at normal temperature (approximately 1400mg/l SO_4^{2-}), sulfate attack is then normally ascribable to presence of magnesium and sodium sulfates. **Figure 4.28** show typical UHPC specimens subjected to sulfate attack after nine months immersion in 2.5% sodium sulfate and 2.5% magnesium sulfate solution.

Figure 4.28: UHPC specimens after 9 months of exposure in sulfate solution.

Results of the visual examination revealed that all the specimens of UHPC were in good condition, in that there was no evidence of spalling and cracking neither on the surface of the specimen nor at the corners. Also, all the specimens retained their toughness and no signs of softening were seen whatsoever. Although there were no severe deterioration

signs seen on the surface, small pitch marks were seen on the specimens prepared with a water to binder ratio of 0.2 and having a cement content of 1000 kg/m^3 with a varying silica fume content of 15, 20 and 25%.

4.6.2 Compressive strength loss

After 9 months of exposure in mixed sulfate environment, all the UHPC mixtures were tested for compressive strength loss by testing the specimens in compression testing machine. These results were then compared with the compressive strength of the specimens which were water cured for the same period of time i.e. 9 months. Strength deterioration factor (SDF) was calculated in terms of percentage strength loss of specimens exposed to sulfate environment when compared with specimens which were water cured. **Table 4-9** shows the comparison of compressive strengths of UHPC mixtures cured in water and exposed to sulfates and also the deterioration factor caused by these sulfates. As observed from **Table 4-9**, the strength deterioration factor (SDF) of UHPC mixtures did not show a clear trend of variation.

4.6.3 Effect of cement content, silica fume content and w/b ratio on sulfate attack of UHPC mixtures

The variations of strength deterioration factor (SDF) with silica fume content and w/b ratio are shown in **Figure 4.29** through **Figure 4.31**, for cement contents 1000, 1100 and 1200 kg/m^3, respectively. As can be seen from **Figure 4.29** through **Figure 4.31**, the strength deterioration factor of UHPC mixtures did not show a clear trend of variation due to short duration of exposure to sulfate environment.

Table 4-9: Sulfate deterioration factor (SDF) and compressive strengths

Mix ID	Strength after exposure in sulfate solution for 9 months (MPa)	Strength after exposure in water for 9 months (MPa)	SDF (%)
M-1	137.50	142.80	3.71
M-2	141.75	146.40	3.18
M-3	143.70	147.73	2.73
M-4	134.43	146.55	8.27
M-5	137.00	149.40	8.30
M-6	140.00	149.30	6.23
M-7	138.00	146.80	5.99
M-8	143.30	149.50	4.15
M-9	143.87	151.50	5.04
M-10	131.57	138.00	4.66
M-11	134.25	143.20	6.25
M-12	138.00	146.00	5.48
M-13	130.10	143.23	9.17
M-14	133.77	148.23	9.76
M-15	138.33	149.50	7.47
M-16	134.00	143.30	6.49
M-17	141.00	149.00	5.37
M-18	140.00	150.00	6.67
M-19	123.70	137.15	9.81
M-20	125.40	136.00	7.79
M-21	130.00	137.25	5.28
M-22	126.00	136.00	7.35
M-23	130.00	137.30	5.32
M-24	132.00	144.70	8.78
M-25	127.00	137.00	7.30
M-26	129.27	137.20	5.78
M-27	141.00	144.93	2.71

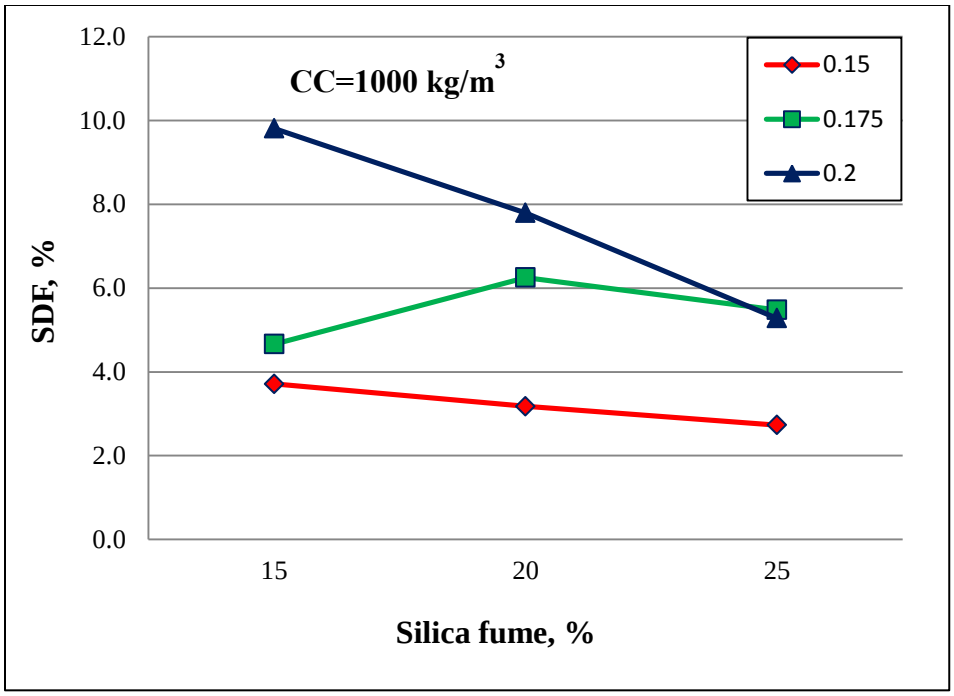

Figure 4.29: SDF for CC: 1000 kg/m^3 and varying w/b and SF percentages.

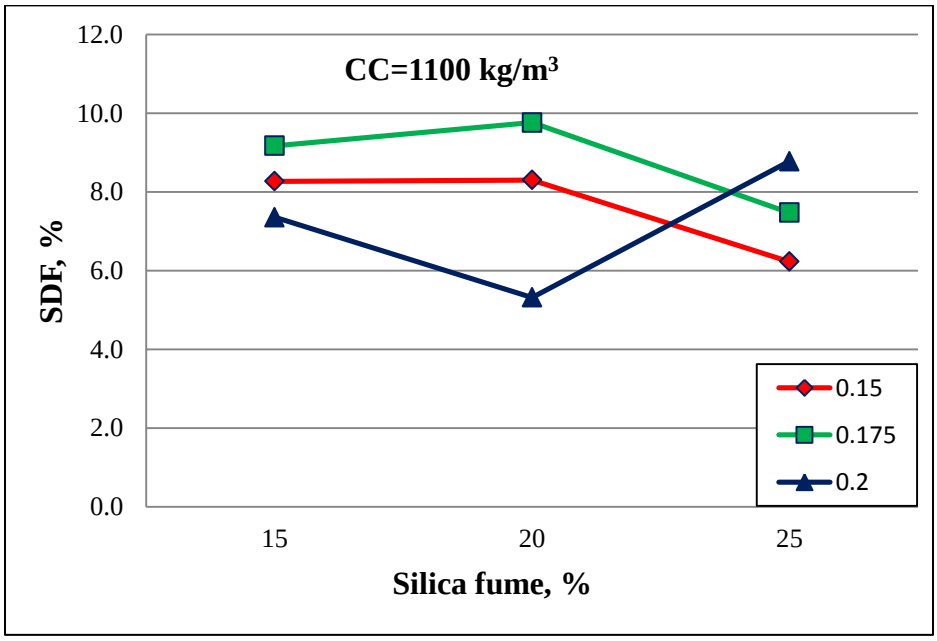

Figure 4.30: SDF for CC: 1100 kg/m^3 and varying w/b and SF percentages.

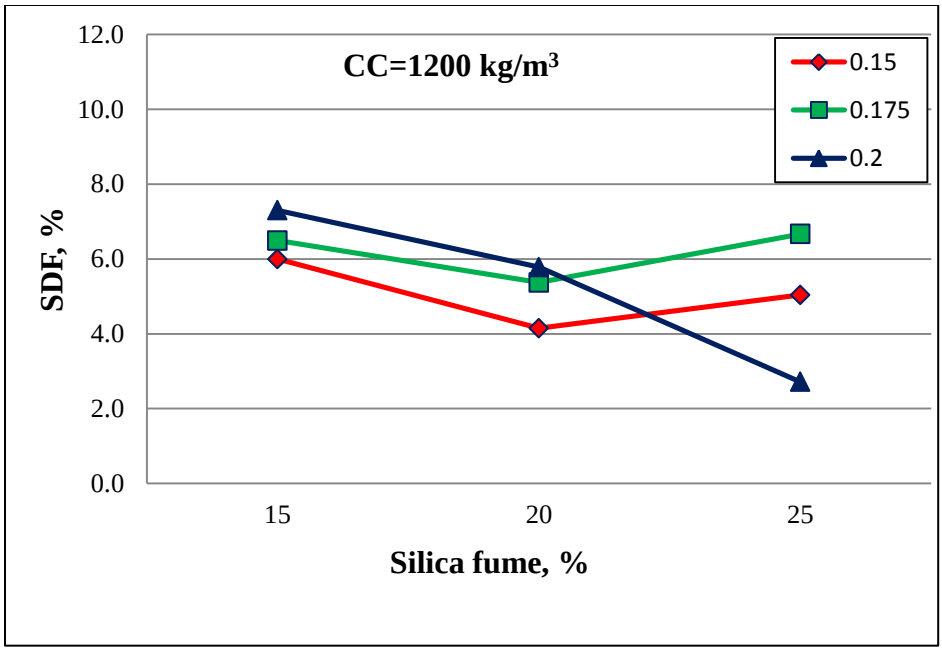

Figure 4.31: SDF for CC: 1200 kg/m^3 and varying w/b and SF percentages.

In general, the Sulfate Deterioration Factor (SDF) for the UHPC mixtures after 9 months of exposure to mixed sulfate environment is low (less than 10%). There is no clear influence of cement content, silica fume content or water to binder ratio on SDF of UHPC specimens. Some of the mixtures showed SDF values close to 10%, which is considered high for conventional concrete but for UHPC, keeping in mind higher cement and silica fume content and absence of coarse aggregate, this 10% strength loss is considered low. Also, sulfate attack is being associated with cement paste and not with aggregates this 10% loss of strength may be classified low. Further, much more importantly, the use of SF as a cement replacement material can aggravate strength loss when the source of sulfate ions is magnesium **[76].**

4.7 CHLORIDE DIFFUSION COEFFICIENT

The chloride concentrations were determined after exposing the concrete specimens to 5% NaCl solution for a period of six months. The chloride profiles, as shown in **Figure 4.32** through **Figure 4.40**, were utilized to determine the chloride diffusion coefficients according to Fick's second law of diffusion.

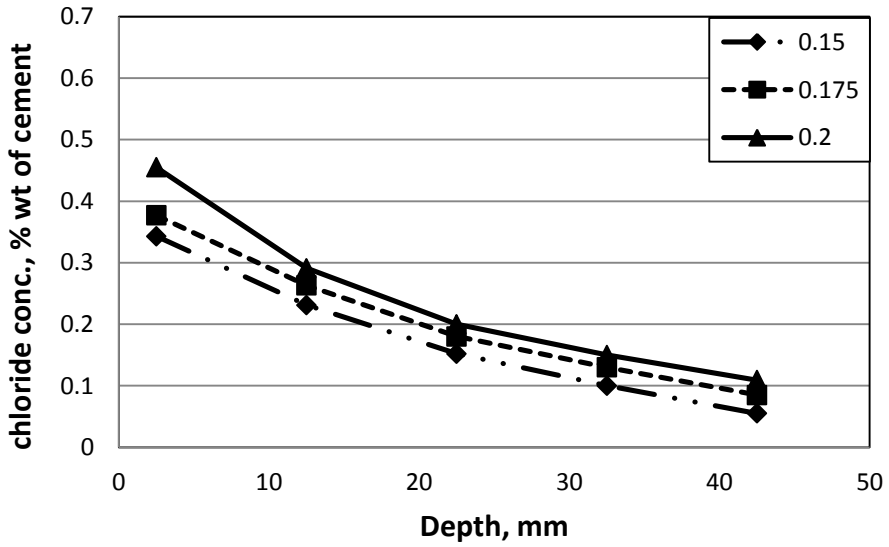

Figure 4.32: Chloride profile for CC: 1000 kg/m^3 and SF: 15% with varying w/b ratio

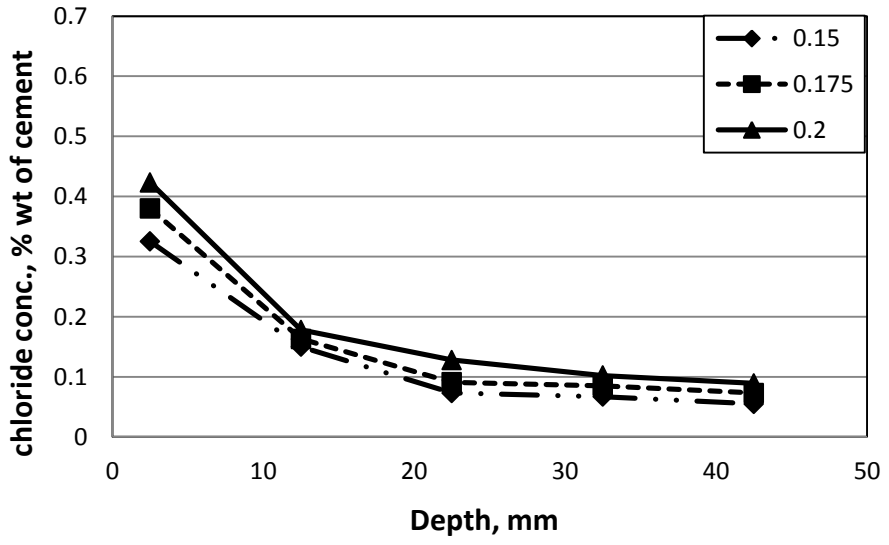

Figure 4.33: Chloride profile for CC: 1000 kg/m^3 and SF: 20% with varying w/b ratio

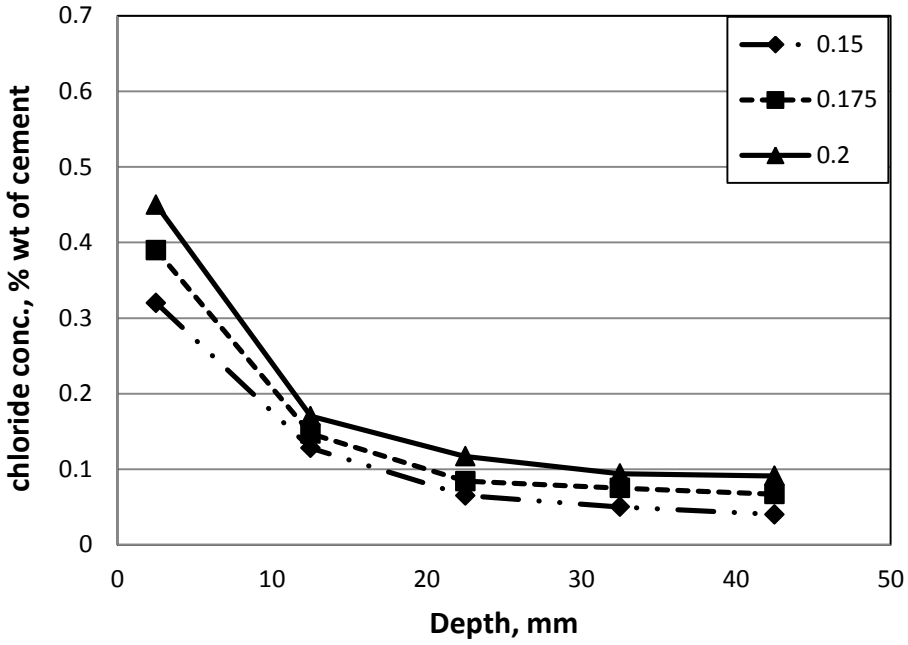

Figure 4.34: Chloride profile for CC: 1000 kg/m^3 and SF: 25% with varying w/b ratio

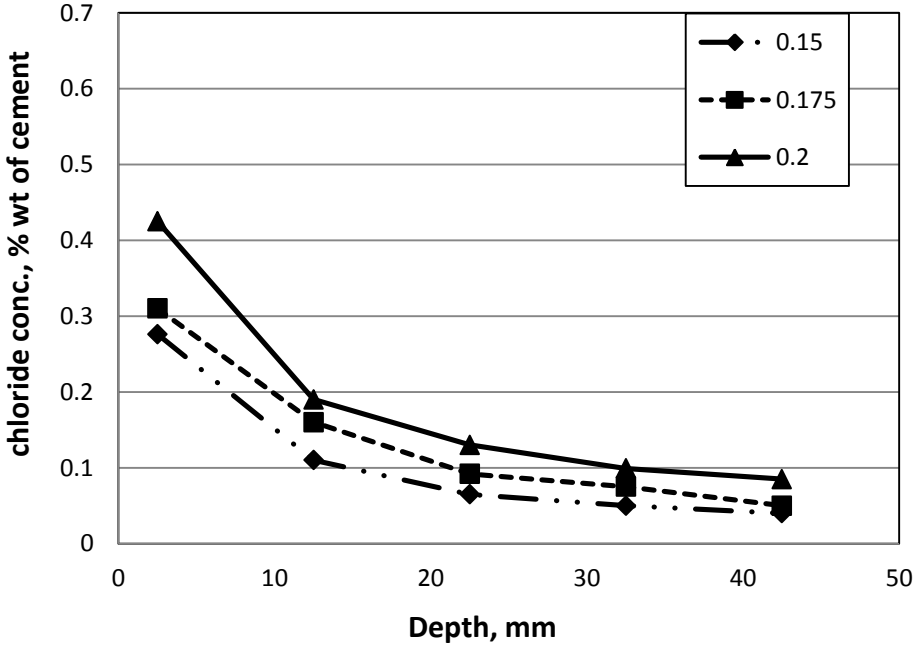

Figure 4.35: Chloride profile for CC: 1100 kg/m^3 and SF: 15% with varying w/b ratio

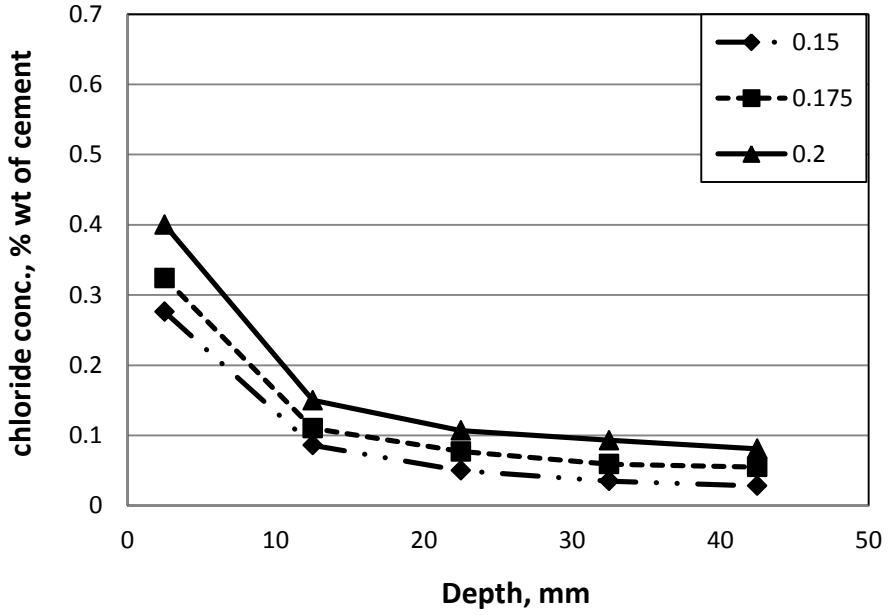

Figure 4.36: Chloride profile for CC: 1100 kg/m^3 and SF: 20% with varying w/b ratio

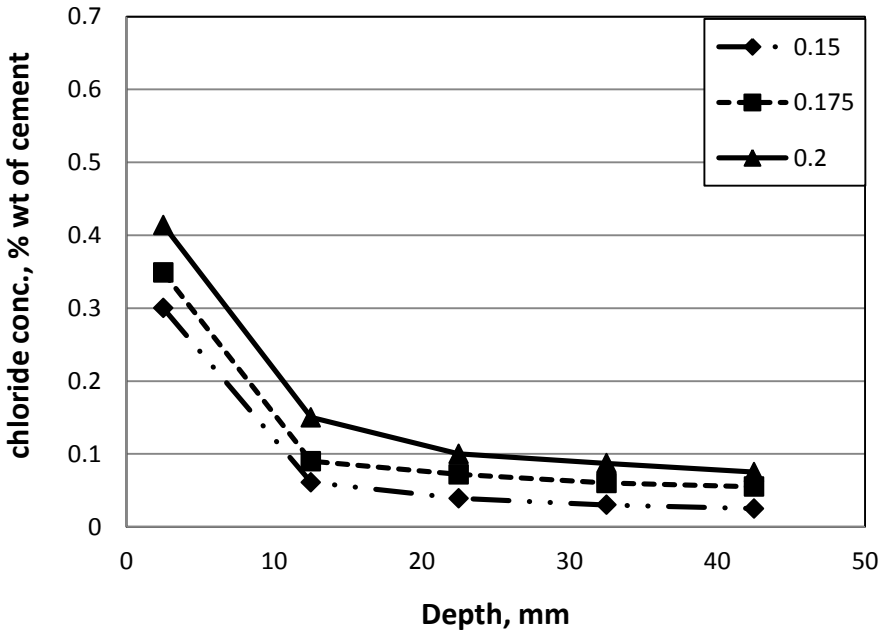

Figure 4.37: Chloride profile for CC: 1100 kg/m^3 and SF: 25% with varying w/b ratio

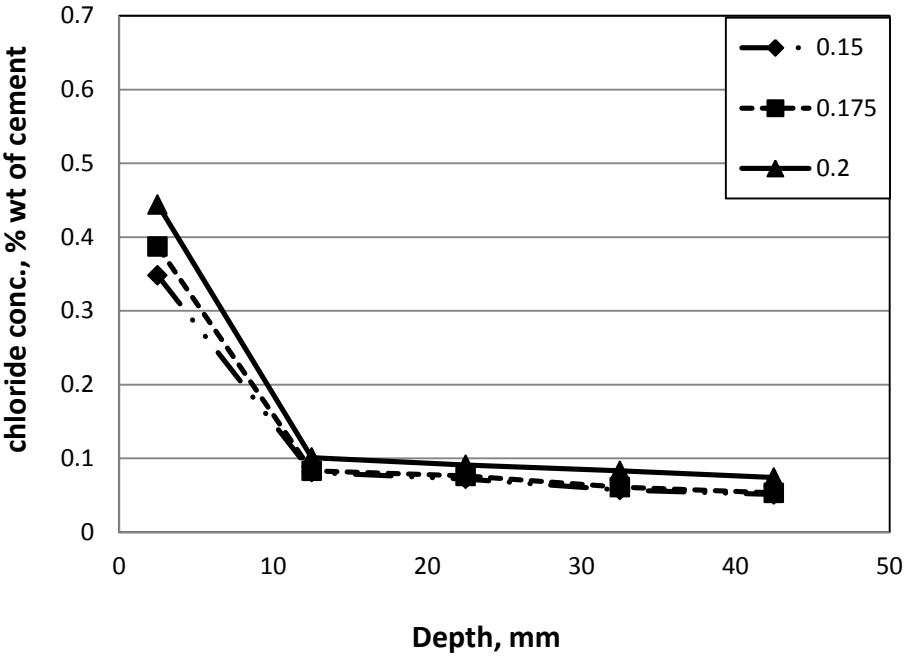

Figure 4.38: Chloride profile for CC: 1200 kg/m^3 and SF: 15% with varying w/b ratio

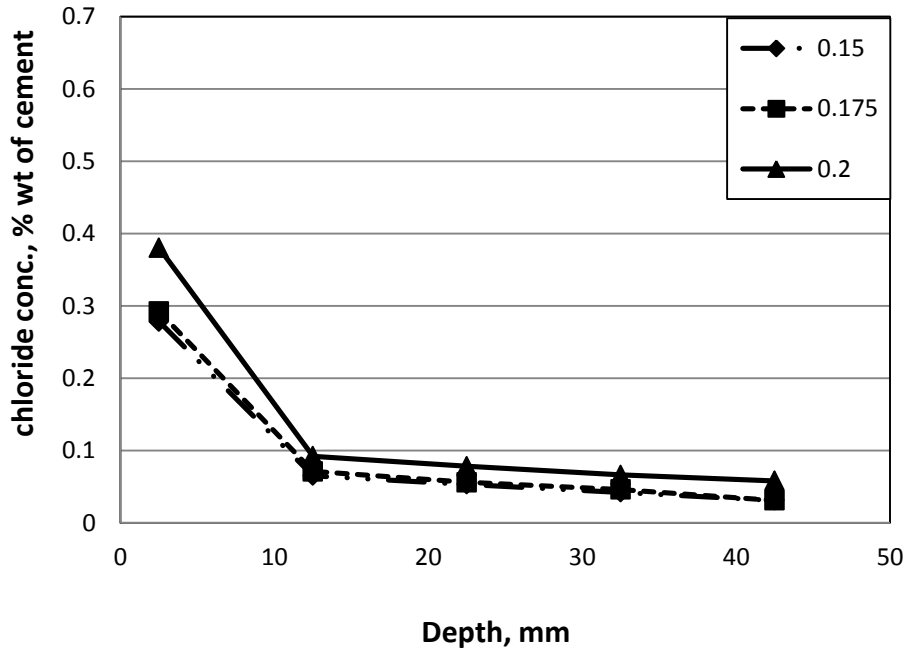

Figure 4.39: Chloride profile for CC: 1200 kg/m^3 and SF: 20% with varying w/b ratio

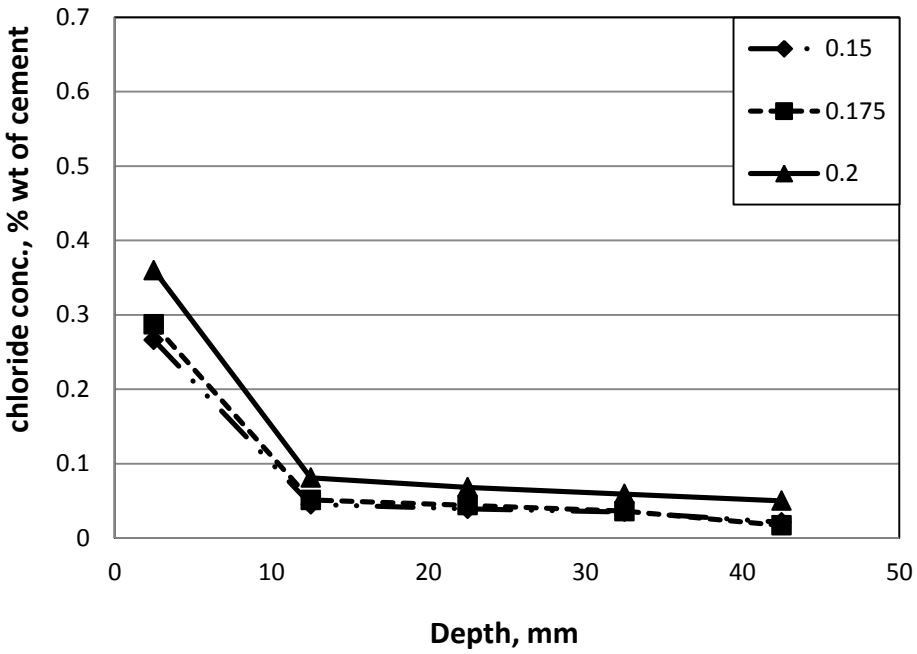

Figure 4.40: Chloride profile for CC: 1200 kg/m^3 and SF: 25% with varying w/b ratio

4.7.1 Chloride diffusion coefficient of UHPC mixtures

The chloride surface concentration by percentage weight of cement (C_s) and chloride diffusion coefficients (D_e) for UHPC specimens is presented in **Table 4-10**. The chloride diffusion coefficients were calculated using a computer program written in MATHEMATICA, based on Fick's second law of diffusion, presented in Appendix. The accuracy in estimating chloride diffusion coefficients might have got affected due to inaccurate measurement of chloride concentration on the surface of the specimens. As seen in **Figure 4.41**, the top slice which had some of the fibers protruding out from the surface got corroded during the exposure period and when the test was carried out using spectrophotometry, the top slices gave unrealistic readings of surface concentration and

resulted in diffusion coefficients values with lesser degree of accuracy. Therefore, it is essential either to remove rust from the sample before measuring chloride concentration or use other method of measurement of chloride concentration which would not be affected by the presence of rust.

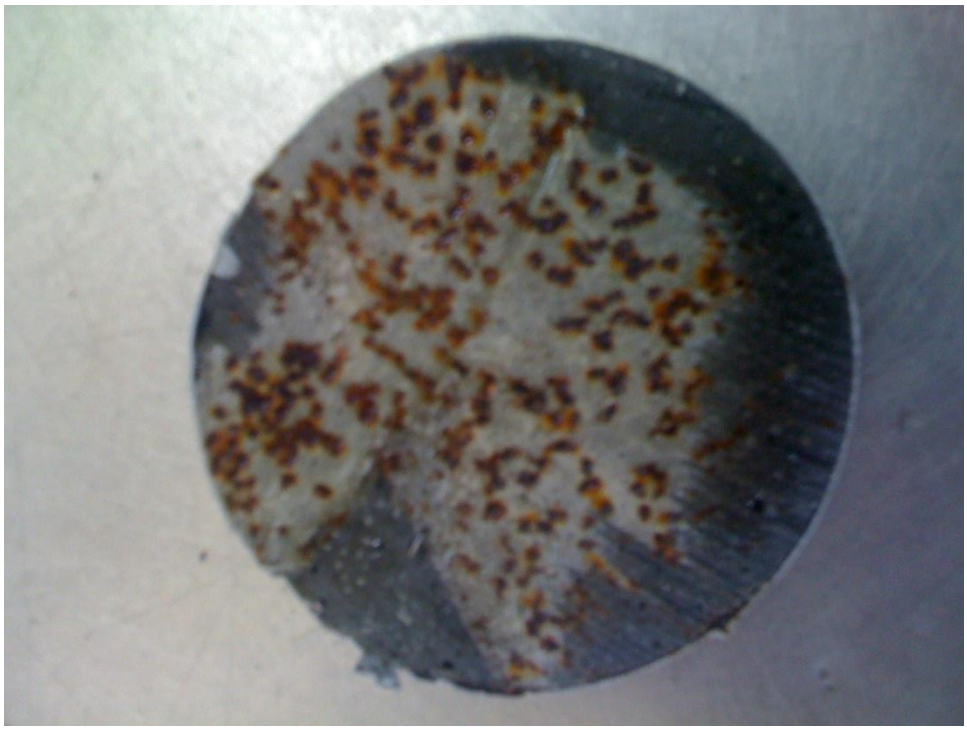

Figure 4.41: Top slice showing corroded fibers.

As can be observed from **Table 4-10**, the chloride diffusion coefficients of the UHPC mixtures varied from 2.46 to 32.38 × 10^{-8} cm^2/sec. The range of chloride diffusion coefficients of the UHPC mixtures is very much similar to that of normal concrete mixtures. The reason behind no substantial decrease of chloride diffusion coefficients of the UHPC mixtures, unlike the case of water permeability, may be attributed to the inaccuracy in the measurement of chloride concentration on the surface due to presence of rust in the sample for measurement of chloride concentration using spectrophotometry.

Table 4-10: Chloride diffusion coefficients for UHPC specimens.

Mix ID	C_s	$D_e \times 10^{-8}$ (cm^2/sec)
M-1	0.361	26.65
M-2	0.341	12.84
M-3	0.35	8.81
M-4	0.293	10.67
M-5	0.317	5.64
M-6	0.377	2.88
M-7	0.412	4.19
M-8	0.333	3.95
M-9	0.342	2.46
M-10	0.391	33.99
M-11	0.389	13.9
M-12	0.415	9.86
M-13	0.318	17.85
M-14	0.344	9.37
M-15	0.403	4.99
M-16	0.47	3.56
M-17	0.346	4.2
M-18	0.366	2.6
M-19	0.46	32.38
M-20	0.415	18.21
M-21	0.456	13.26
M-22	0.423	18.02
M-23	0.398	14.73
M-24	0.428	11.43
M-25	0.528	4.07
M-26	0.445	4.48
M-27	0.434	3.74

4.7.2 Effect of cement content, silica fume content and w/b ratio on chloride diffusion coefficients of UHPC specimens

The variations of chloride diffusion coefficient with silica fume content and w/b ratio are shown in **Figure 4.42** through **Figure 4.44**, for cement contents 1000, 1100 and 1200 kg/m^3, respectively. As can be seen from **Figure 4.42** through **Figure 4.44**, the chloride diffusion coefficient decreased significantly with the increase in silica fume content and decrease in w/b ratio. It can be noted that the decrease in chloride permeability with increase in silica fume content is more significant in case of the mixtures with w/b ratio of 0.2 as compared to the w/b ratios of 0.15 and 0.175, indicating more effectiveness of silica fume at higher w/b ratio. It is interesting to note that the effects of w/b ratio and silica fume content on chloride diffusion coefficient are insignificant at cement content of 1200 kg/m^3, as seen from **Figure 4.44**.

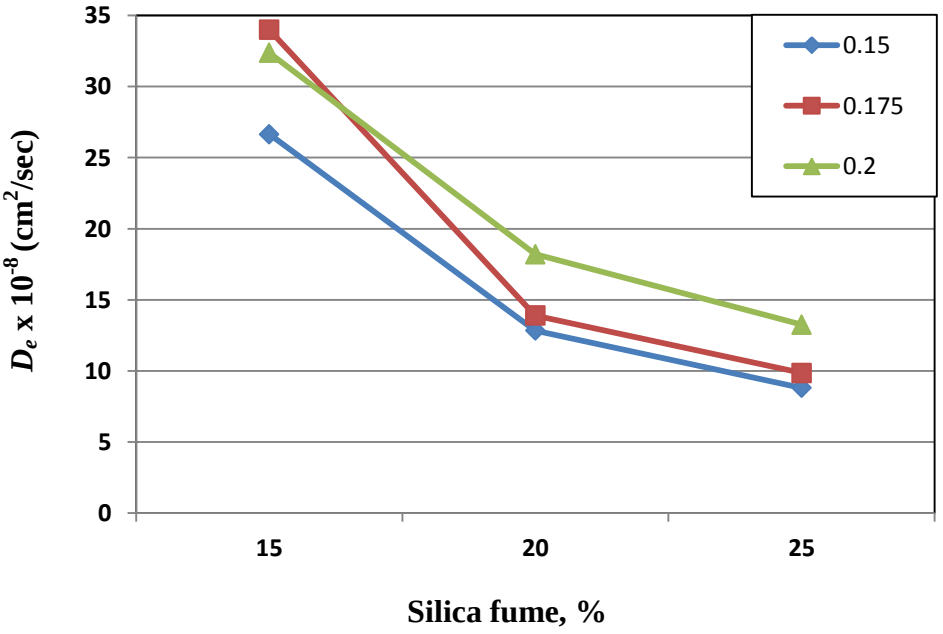

Figure 4.42: Chloride diffusion coefficient for CC: 1000 kg/m^3 for different w/b ratios and silica fume.

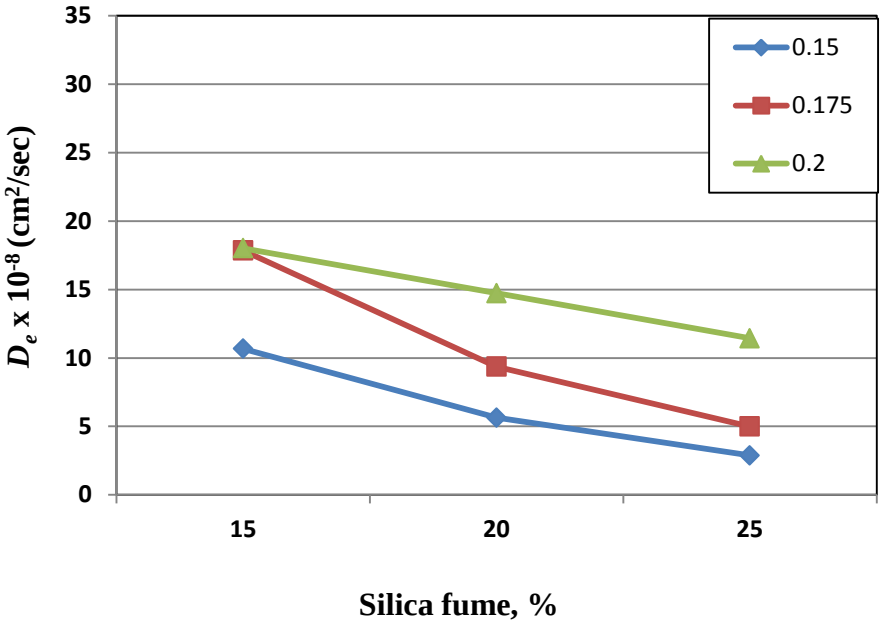

Figure 4.43: Chloride diffusion coefficient for CC: 1100 kg/m^3 for different w/b ratios and silica fume.

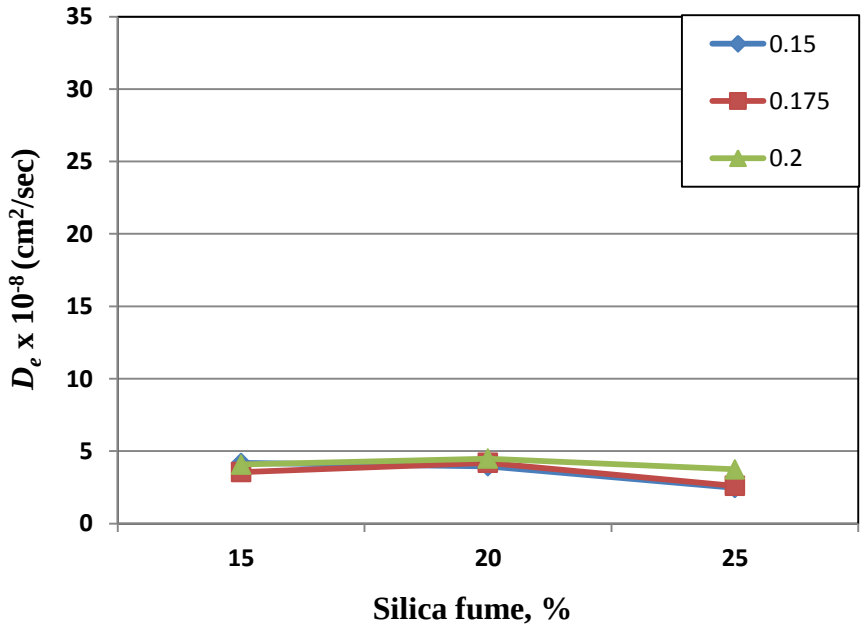

Figure 4.44: Chloride diffusion coefficient for CC: 1200 kg/m^3 for different w/b ratios and silica fume.

4.7.3 Statistical Analysis for Chloride diffusion coefficient

Data in **Table 4-10** was utilized to develop relationship between the parameter (D_e) and w/b ratio, cementitious material content and silica fume content. The ANOVA for chloride diffusion coefficient, for which a general linear model was developed, is given below:

ANOVA for Chloride diffusion coefficient, D_e vs. C, w/b, SF

Factor	Type	Levels	Values
w/b	fixed	3	0.150, 0.175, 0.200
C	fixed	3	1000, 1100, 1200
SF	fixed	3	15, 20, 25

Analysis of Variance for D_e x 10^{-8} (cm^2/sec), using Adjusted SS for Tests

Source	DF	Seq SS	Adj SS	Adj MS	F	P
w/b	2	99.17	99.17	49.58	2.44	0.112
C	2	1040.06	1040.06	520.03	25.63	0.000
SF	2	488.64	488.64	244.32	12.04	0.000
Error	20	405.83	405.83	20.29		
Total	26	2033.70				

S = 4.50458 R-Sq = 80.04% R-Sq(adj) = 74.06%

P-values indicate that only C and SF have effect on D_e. F-ratios indicate that the C content has most significant effect on D_e.

The regression equation relating the diffusion coefficient to the w/b ratio, cementitious material content, and silica fume content is given below.

$$\mathbf{D_e \times 10^{-8} (cm^2/sec) = 98.4 + 93.8\ w/b - 0.0759\ C - 1.01\ SF}$$

A good fit of this model is noted by a $R^2 = 0.80$.

The above model indicates that D is decreasing with C and SF contents and slightly increasing with w/b ratio.

4.8 REINFORCEMENT CORROSION

4.8.1 Corrosion current density

The plots of corrosion current density (I_{corr}) values, measured after different exposure periods, for the UHPC mixtures prepared with cement contents of 1000, 1100 and 1200 kg/m^3; silica fume contents of 15, 20 and 25%; and w/b ratios of 0.15, 0.175 and 0.2 are shown in **Figure 4.45** through **Figure 4.53**. It can be observed from these plots of I_{corr} values with exposure time that the I_{corr} is fluctuating within a range of 0 to 0.3 μA/cm^2. Except for a few cases, I_{corr} values were much below the threshold value of 0.3 μA/cm^2 for initiation of active corrosion of rebars. It can be concluded that the active corrosion is not initiated in any mixture even after an exposure period of 15 months as almost in each case I_{corr} value was less than the threshold value of 0.3 μA/cm^2. Furthermore, it is to be noted that since active rebar corrosion for no any mixture of UHPC had been observed, the effects of the three mixture parameters cannot be quantified.

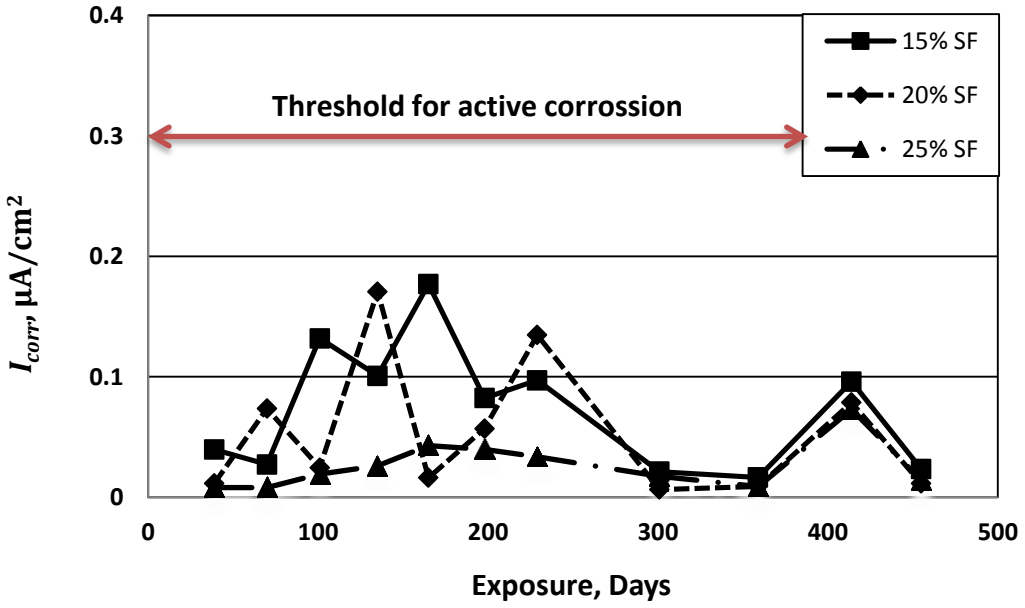

Figure 4.45: Corrosion current density on steel with CC: 1000 kg/m^3 and w/b: 0.15 with varying silica fume content.

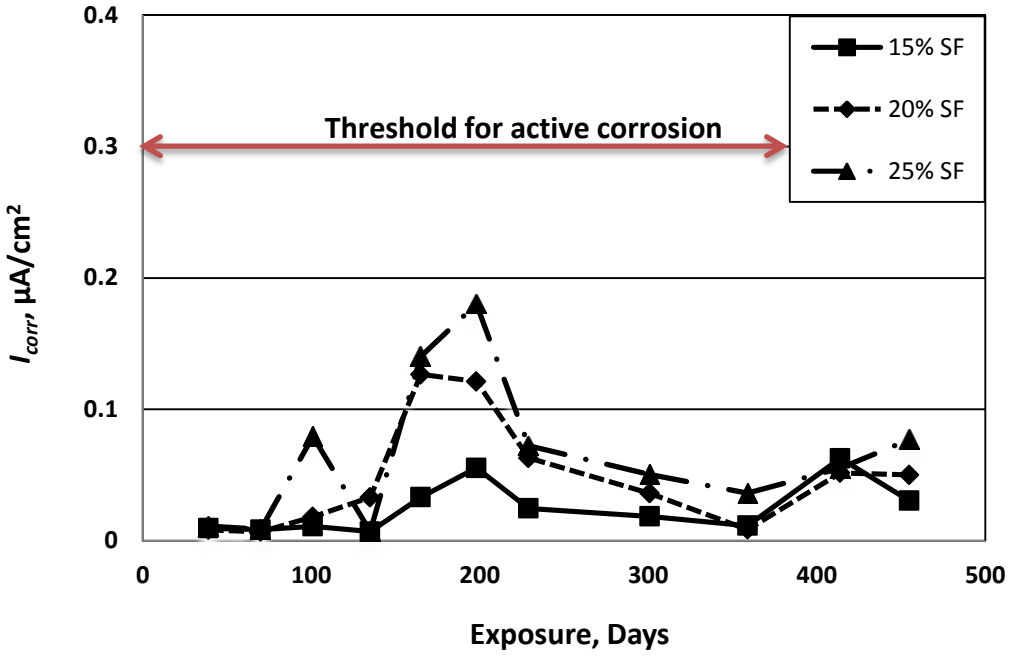

Figure 4.46: Corrosion current density on steel with CC: 1000 kg/m^3 and w/b: 0.175 with varying silica fume content.

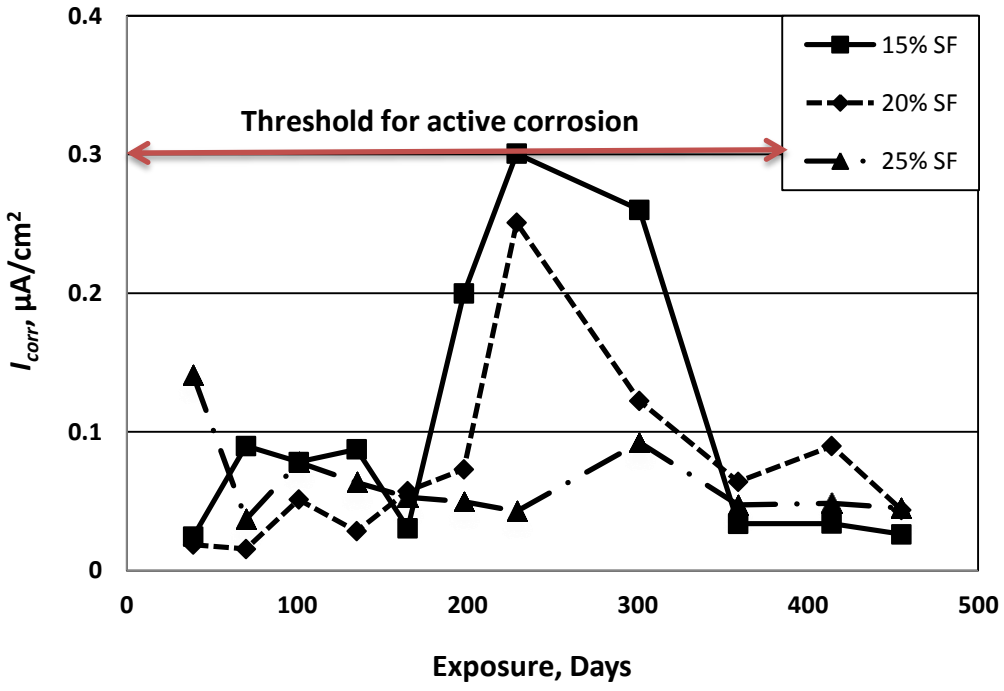

Figure 4.47: Corrosion current density on steel with CC: 1000 kg/m^3 and w/b: 0.2 with varying silica fume content.

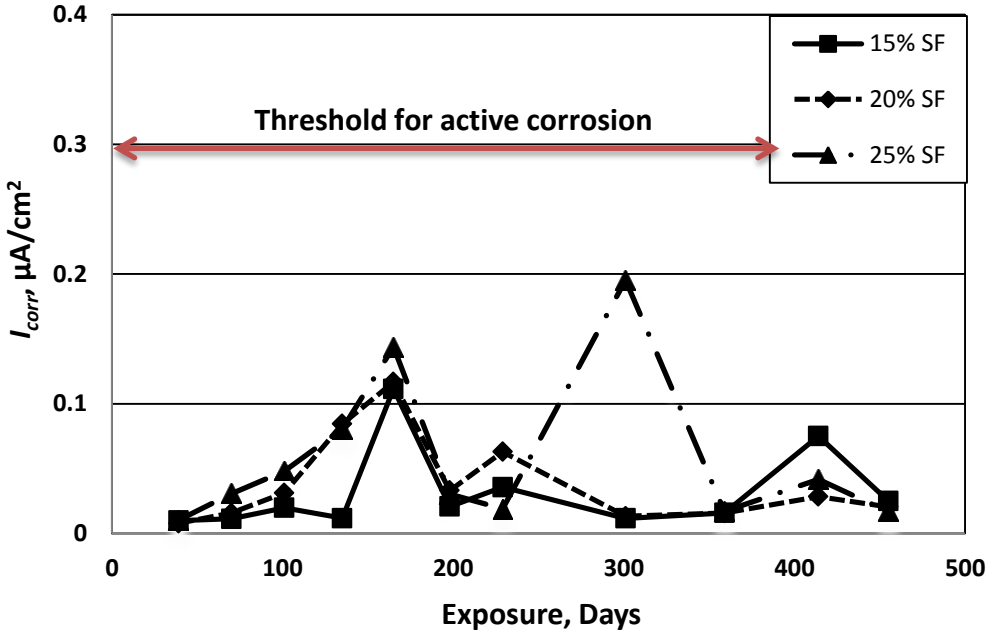

Figure 4.48: Corrosion current density on steel with CC: 1100 kg/m^3 and w/b: 0.15 with varying silica fume content.

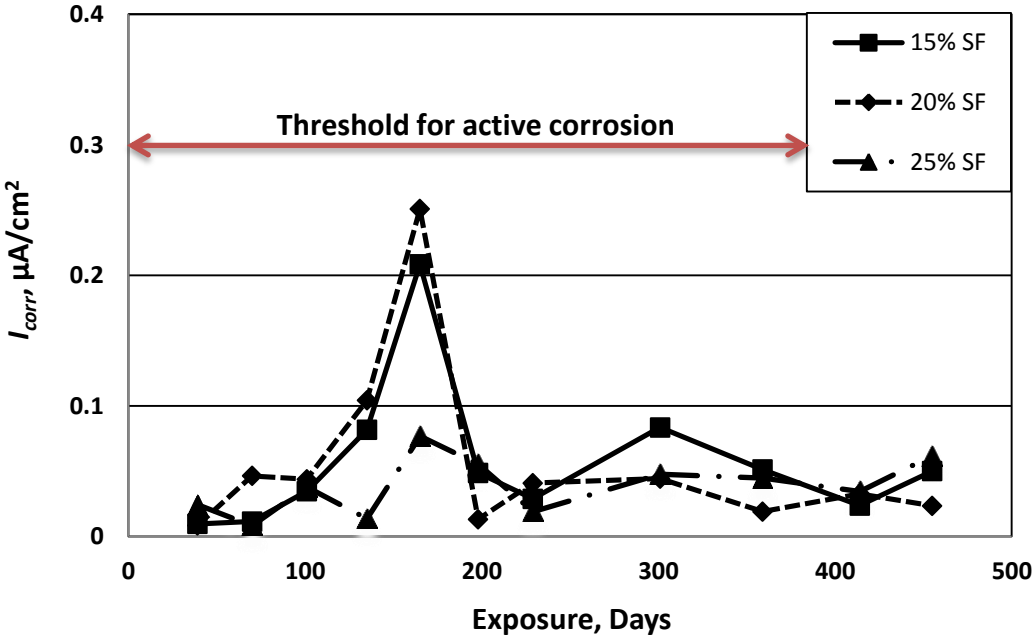

Figure 4.49: Corrosion current density on steel with CC: 1100 kg/m^3 and w/b: 0.175 with varying silica fume content.

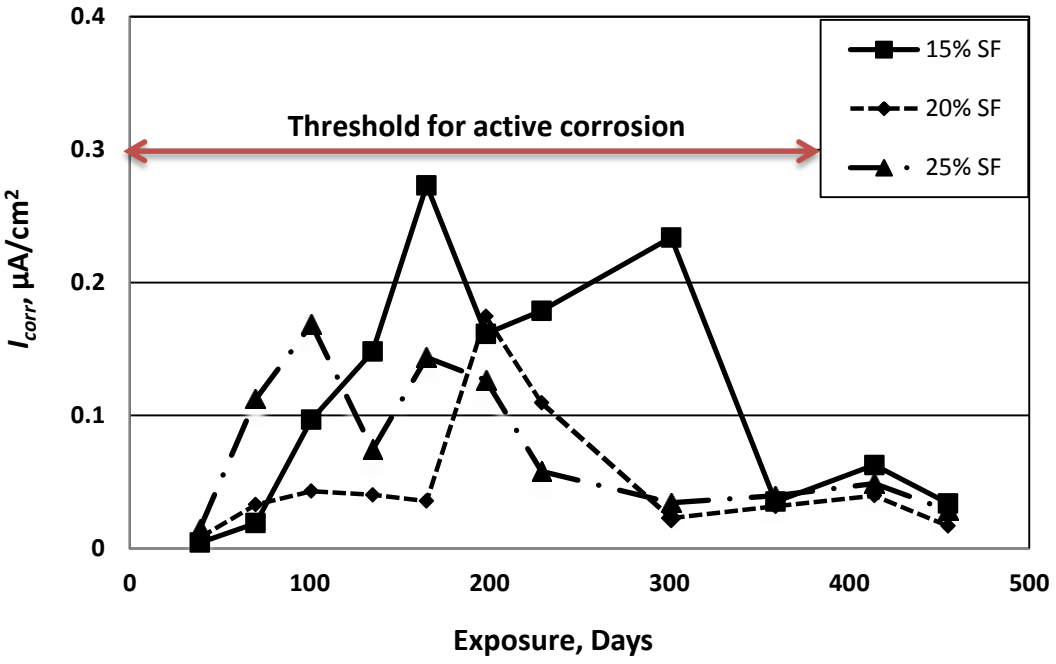

Figure 4.50: Corrosion current density on steel with CC: 1100 kg/m^3 and w/b: 0.2 with varying silica fume content.

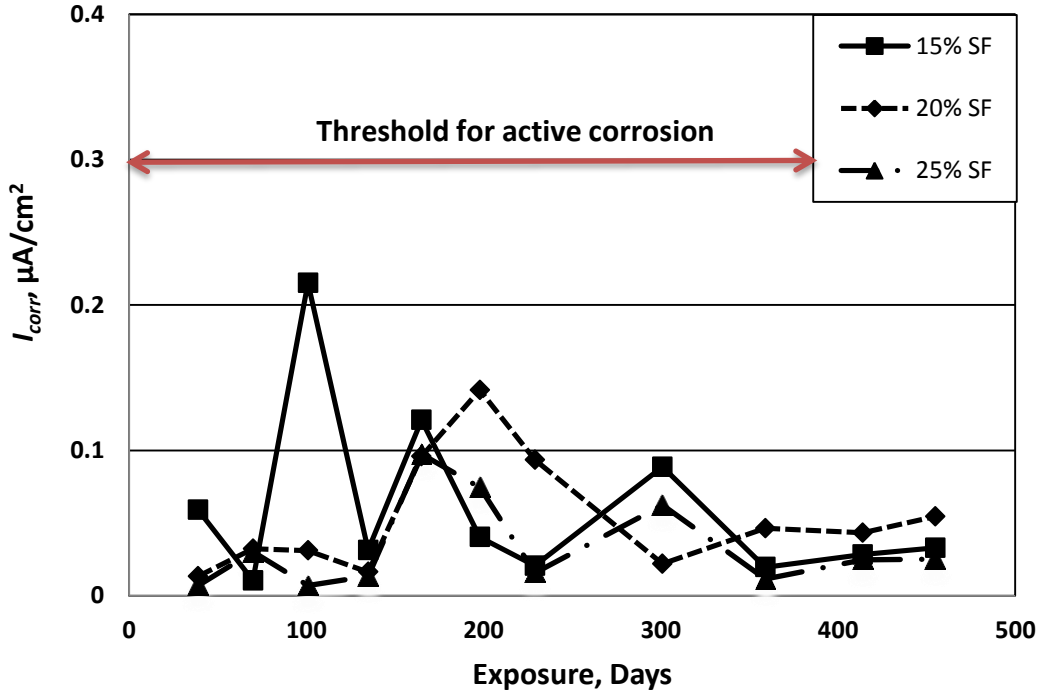

Figure 4.51: Corrosion current density on steel with CC: 1200 kg/m^3 and w/b: 0.15 with varying silica fume content.

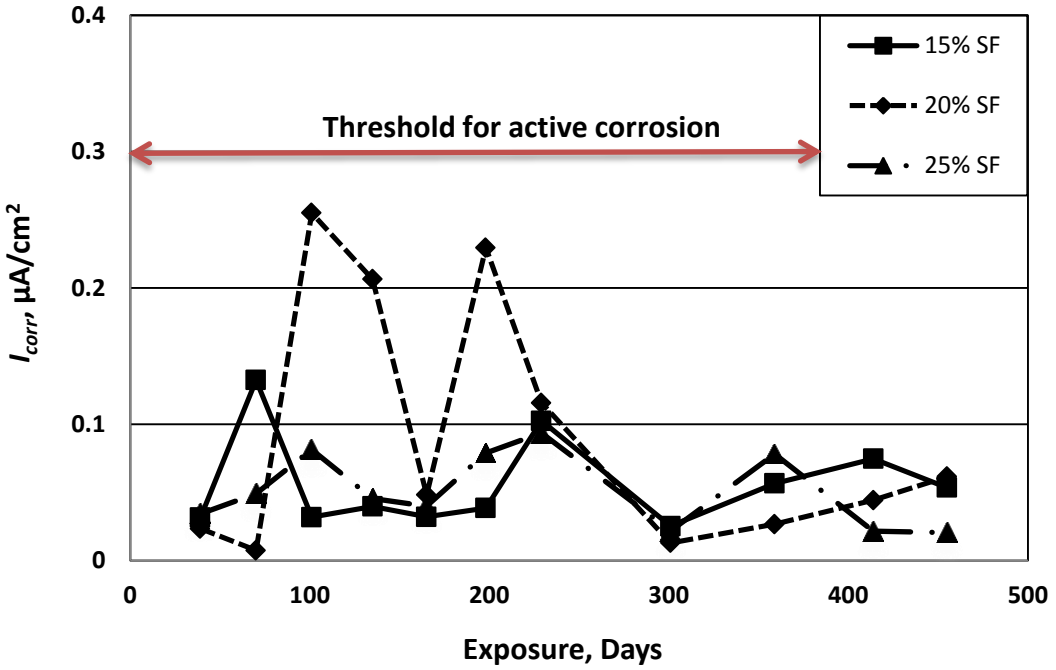

Figure 4.52: Corrosion current density on steel with CC: 1200 kg/m^3 and w/b: 0.175 with varying silica fume content.

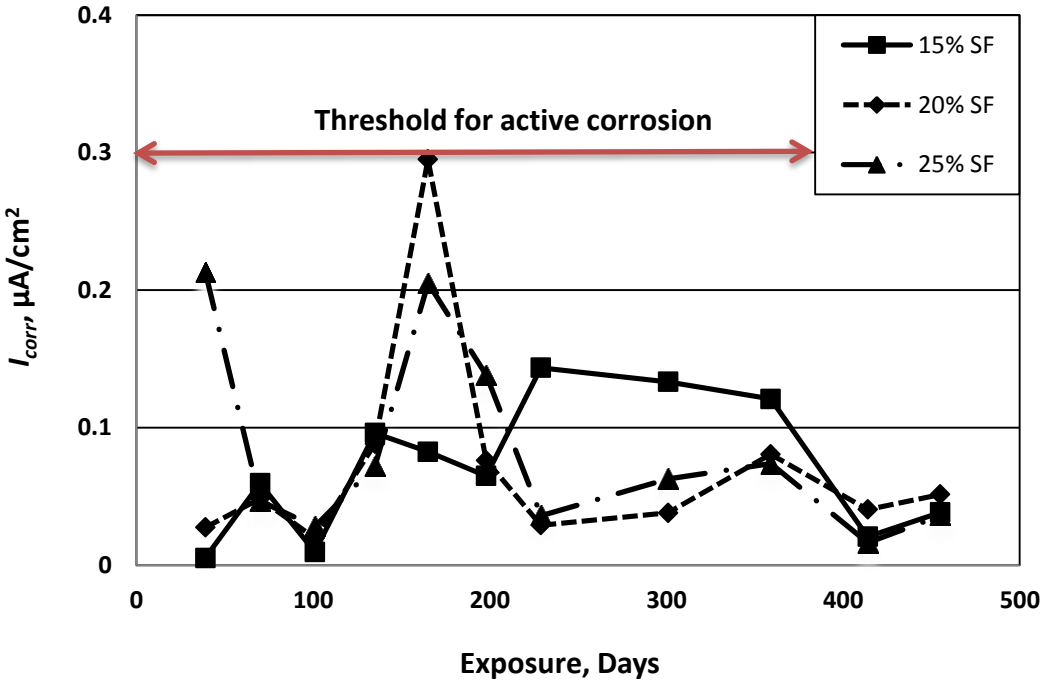

Figure 4.53: Corrosion current density on steel with CC: 1200 kg/m^3 and w/b: 0.2 with varying silica fume content.

4.8.2 Visual Examination

After 450 days of exposure to the 5% NaCl solution, the bars were extracted from the specimens to confirm that all the rebars embedded in UHPC mixtures are free from corrosion as indicated by monitoring I_{corr}. **Figure 4.54** through **Figure 4.61** show the rebars which were extracted from UHPC mixtures showing no signs of corrosion on the part of the rebar which was embedded in concrete and allowed to corrode. The UHPC mixture prepared with water to binder ratio of 0.2, cement content of 1000 kg/m^3 and silica fume content of 15% (mix no. 19) showed very little sign of corrosion, as shown in **Figure 4.59**. In this particular case I_{corr} was equal to the threshold value of 0.30 µA/cm^2.

Figure 4.54: Reinforcement bar embedded in UHPC cylinder showing no signs of corrosion for mix # 1

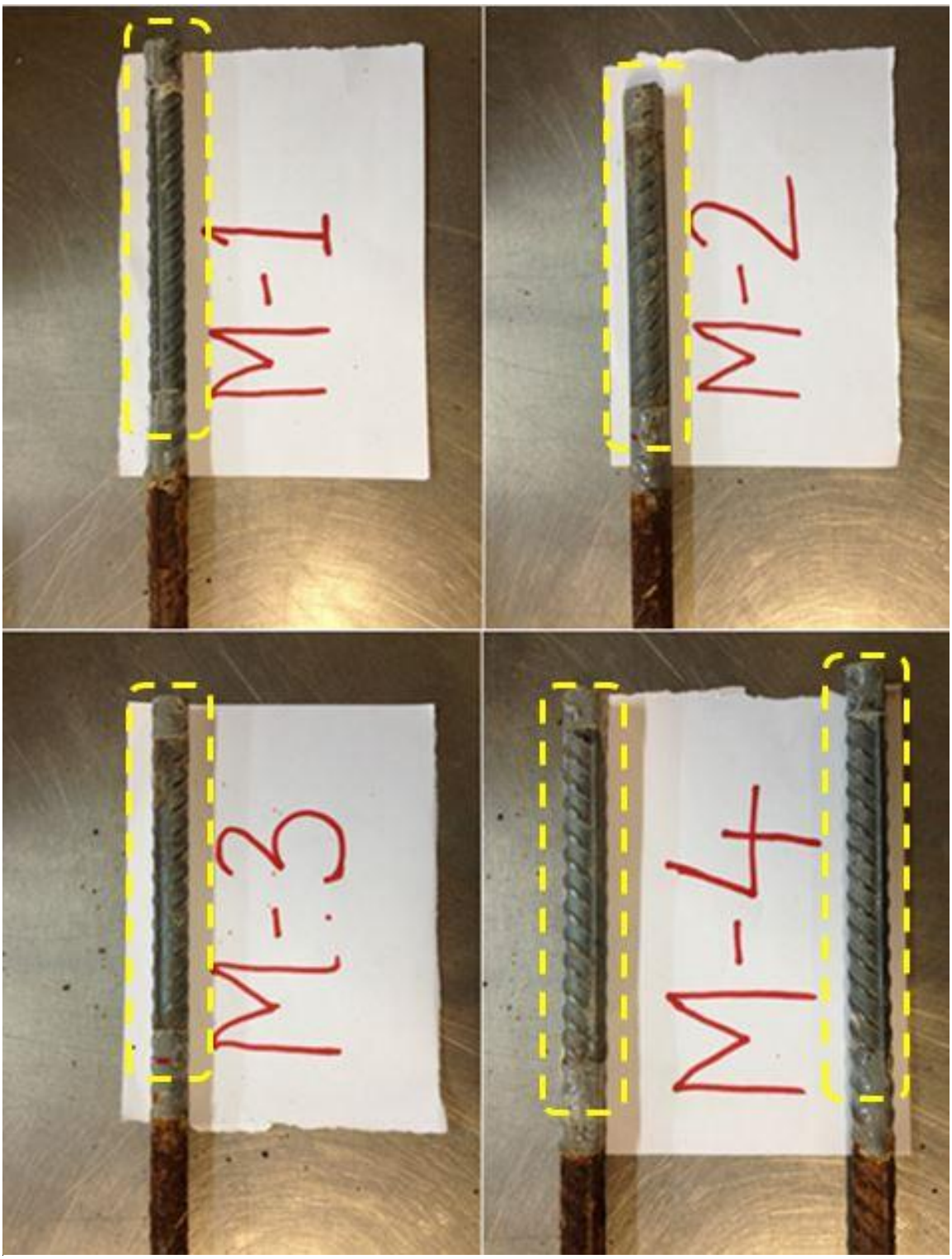

Figure 4.55: Highlighted portion of the rebar was embedded in concrete (Mixes no.1 to 4)

Figure 4.56: Highlighted portion of the rebar was embedded in concrete (Mixes no.5 to 8)

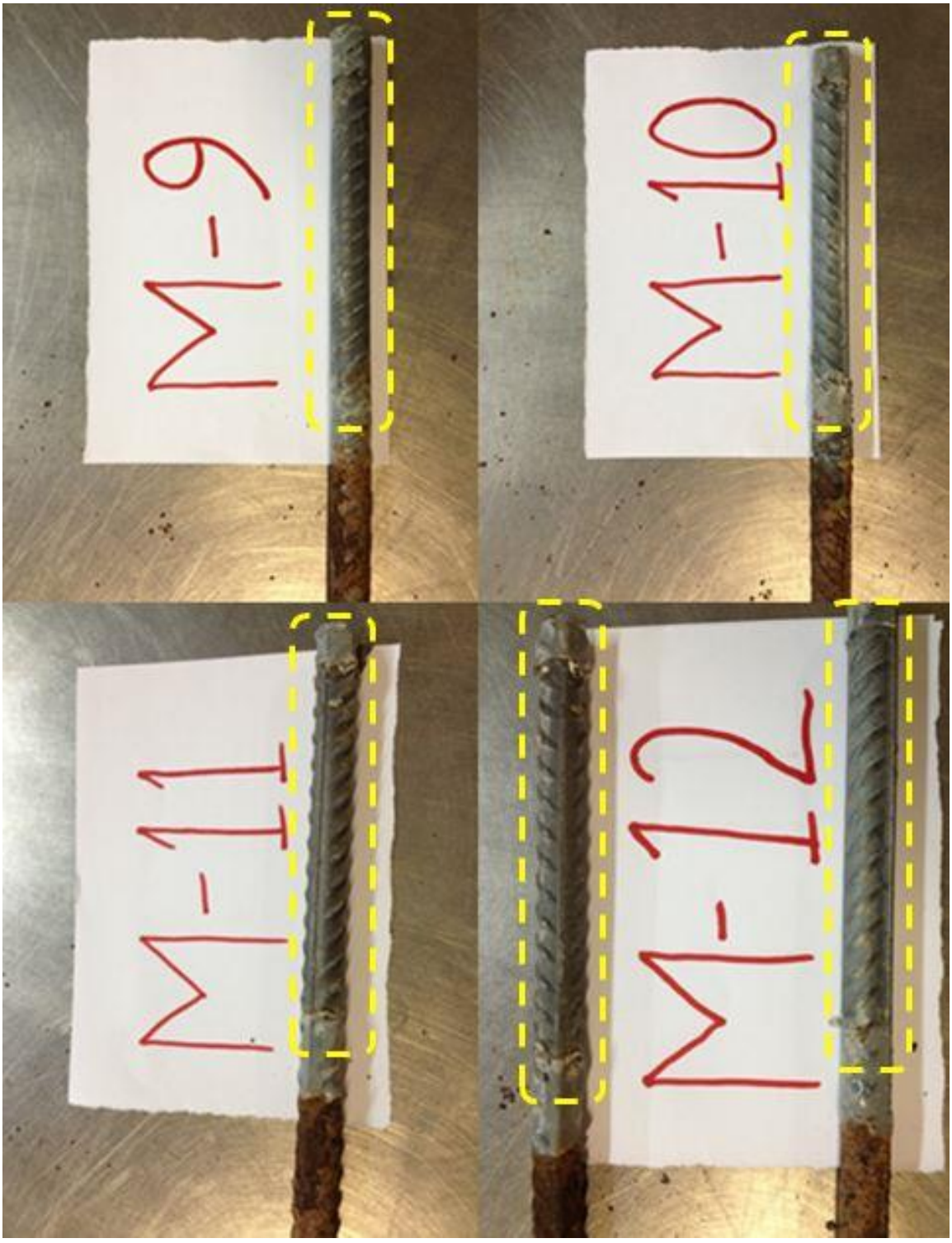

Figure 4.57: Highlighted portion of the rebar was embedded in concrete (Mixes no.9 to 12)

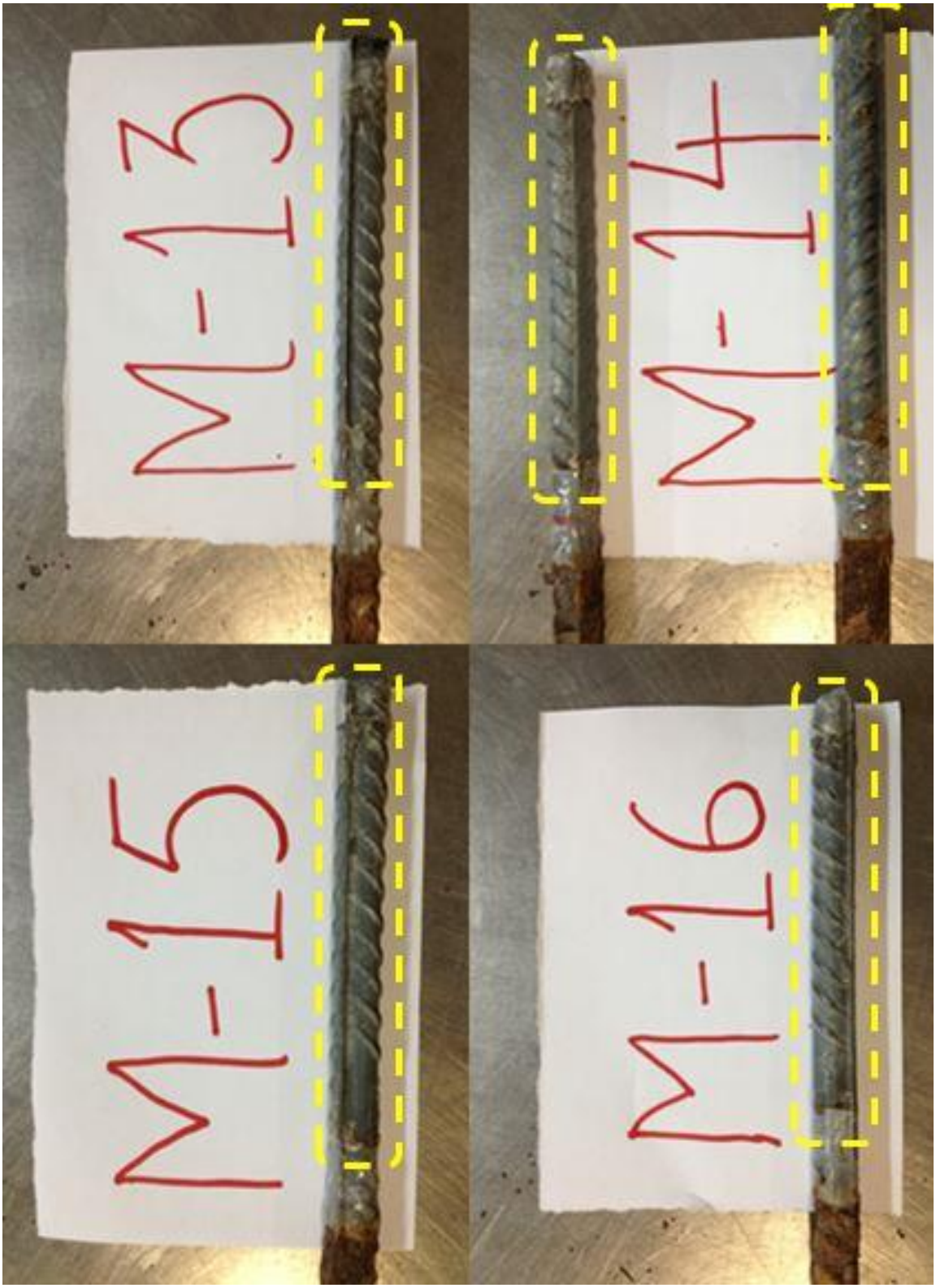

Figure 4.58: Highlighted portion of the rebar was embedded in concrete (Mixes no.13 to 16)

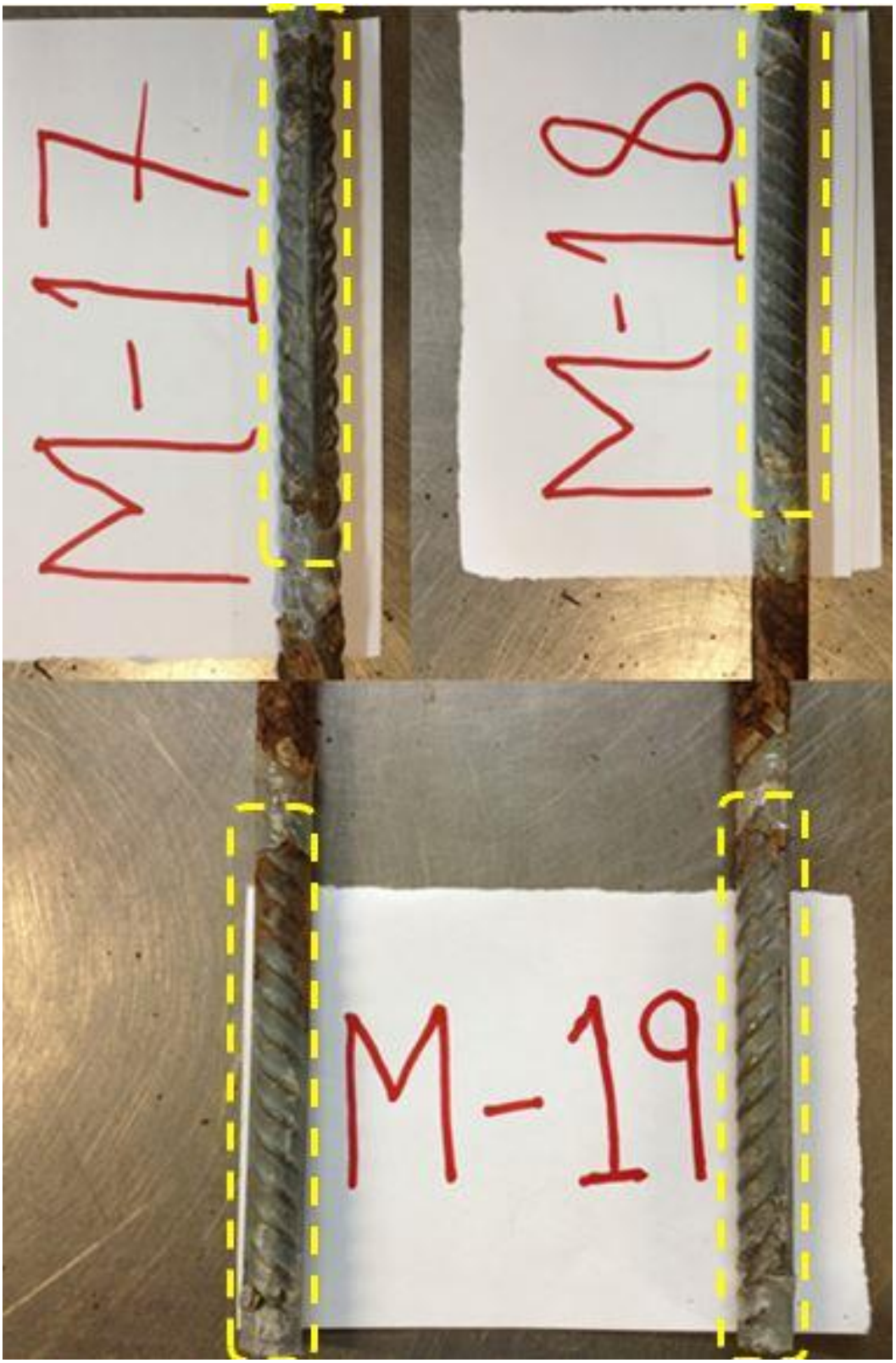

Figure 4.59: Highlighted portion of the rebar was embedded in concrete (Mixes no.17 to 19)

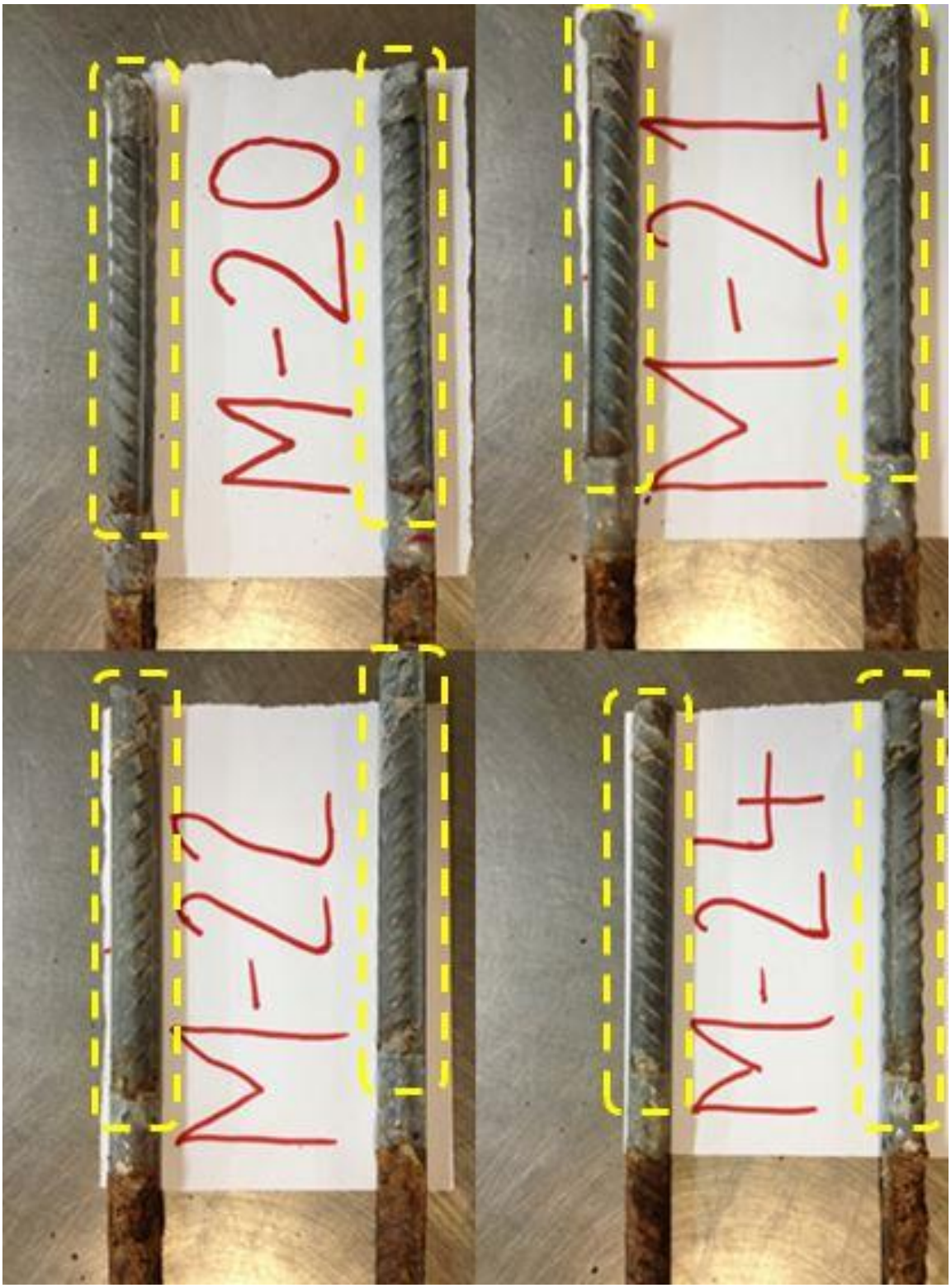

Figure 4.60: Highlighted portion of the rebar was embedded in concrete (Mixes no.20 to 24)

Figure 4.61: Highlighted portion of the rebar was embedded in concrete (Mixes no.25 to 27)

4.9 INDIRECT ASSESSMENT OF PERFORMANCE OF THE UHPC MIXTURES AGAINST REBAR CORROSION

The minimum and maximum values of electrical resistivity, pH and chloride concentration on the rebar surface are presented in **Table 4-11** for the indirect assessment of performance of the UHPC mixtures against rebar corrosion.

Table 4-11: Indirect assessment of performance of the UHPC mixtures against rebar corrosion.

Corrosion indicator	Minimum	Maximum	Remarks
Electrical resistivity (kΩ-cm)	26.7	78.8	Even minimum value is much higher than the limit for **very low risk of rebar corrosion** (i.e., > 20 K-Ω-cm)
pH	12.4	13.0	Even minimum value is much higher than the limit for corrosion initiation (pH >10), so **negligible chances of corrosion initiation** unless a high concentration of chloride ions is built-up on rebar surface to an extent that the Cl^-/OH^- ratio would exceed the threshold value of 0.60.
Chloride concentration at rebar surface (% by wt. of cement) after six months of exposure	0.039	0.200	Less than the threshold value of 0.4%, **so low chances of corrosion initiation**.

As can be observed from the remarks presented in **Table 4-11**, each parameters related to reinforcement corrosion indicates that the rebar corrosion is not initiated almost in any of 27 mixtures of UHPC. This indirect assessment of reinforcement corrosion is in agreement with the direct assessment of reinforcement corrosion made using I_{corr} measurement and visual inspection of the extracted rebars.

4.10 SELECTION OF BEST PERFORMING UHPC MIXTURE

Table 4-12 shows the selection of a best performing mixture among the set of 27 UHPC mixtures based on strength and durability properties.

Table 4-12: Best performing mixture of UHPC

Property	Best performing UHPC mixture
Compressive strength	M9 (has strength of 137 MPa, closure to the highest value of 139 MPa)
Water Penetration Depth (WPD)	M9 (has lowest WPD of 3.3 mm)
Chloride Permeability (CP)	M9 (has lowest CP of 20 Coulombs)
Electrical Resistivity (ER)	M9 (has highest ER of 78.8 kΩ-cm)
Diffusion coefficient (D)	M9 (has lowest D of 2.6×10^{-8} cm^2/s)
pH	M9 (has pH of 12.72 MPa, closure to the highest value of 13.01 MPa)
Chloride concentration at surface after 6 months of exposure (Cl)	M9 (has lowest Cl concentration of 0.039% by wt. of cement, about one-tenth of threshold concentration)

Based on the observations made from **Table 4-12**, it can be stated that the UHPC mixture –M9 (with w/b = 0.15; CC = 1200 kg/m^3 and SF = 25%) is the "best performing mixture" because it showed to have overall best performance (i.e., strength as well as durability).

4.11 SELECTION OF MOST ECONOMICAL UHPC MIXTURE

For picking up a most economical mixture out of 27 mixtures of UHPC, the strength and durability properties of three mixtures of UHPC M1, M10 and M19, having lowest cement and silica fume contents of 1000 kg/m3 and 15%, respectively, were compared in **Table 4-13**. Based on the comparison of strength and durability properties, the mixture M10 (with w/b ratio = 0.175, CC = 1000 kg/m^3 and SF = 15%) can be selected as economical mixture because it has strength and durability properties closure to the mixture M1 but M10 has a w/b ratio of 0.175 which is more than the w/b ratio of 0.15 for M1 that would reduce the required dosage of superplasticizer reducing the cost significantly. **Table 4-13** shows the most economical mixture among the set of 27 UHPC mixtures.

Table 4-13: Most economical mixture

Mix with least CC and SF	Compressive strength (MPa)	Water penetration depth (mm)	Chloride permeability (Coulombs)	Electrical resistivity (KΩ-cm)	Diffusion coefficient (x 10^{-8} cm^2/sec)
M1	132	8.3 (low)	81 (neg.)	44.5 (V. low probability of corrosion)	26.6
M10	129	10.7 (low)	140 (V. low)	37.0 (V. low probability of corrosion)	34.0
M19	121	13.3 (low)	242 (V. low)	27.0 (V. low probability of corrosion)	33.0

Table 4-14: Combined results of all the tests conducted on 27 UHPC mixtures

Mix ID	w/b	Cementing Blend		WPD (mm)	CP	ER (kΩ-cm)	pH	SDF (%)	$D_e \times 10^{-8}$ (cm^2/sec)
		Cement (kg/m^3)	SF (%)						
M-1	0.15	1000	15	8.3	Negligible	44.5	12.829	3.71	26.65
M-2	0.15	1000	20	6.3	Negligible	54.7	12.708	3.18	12.84
M-3	0.15	1000	25	4.7	Negligible	63.4	12.547	2.73	8.81
M-4	0.15	1100	15	6.7	Negligible	55.5	12.935	8.27	10.67
M-5	0.15	1100	20	3.7	Negligible	63.5	12.789	8.3	5.64
M-6	0.15	1100	25	4.7	Negligible	67.5	12.613	6.23	2.88
M-7	0.15	1200	15	5.3	Negligible	60	13.012	5.99	4.19
M-8	0.15	1200	20	4.7	Negligible	66.4	12.936	4.15	3.95
M-9	0.15	1200	25	3.3	Negligible	78.8	12.721	5.04	2.46
M-10	0.175	1000	15	10.7	very low	36.9	12.758	4.66	33.99
M-11	0.175	1000	20	9.7	very low	39.7	12.602	6.25	13.9
M-12	0.175	1000	25	7.7	very low	41	12.425	5.48	9.86
M-13	0.175	1100	15	8.7	very low	37.4	12.854	9.17	17.85
M-14	0.175	1100	20	7	Negligible	44.3	12.741	9.76	9.37
M-15	0.175	1100	25	5.7	Negligible	45.5	12.467	7.47	4.99
M-16	0.175	1200	15	8.3	Negligible	38	12.892	6.49	3.56
M-17	0.175	1200	20	5.3	Negligible	45	12.775	5.37	4.2
M-18	0.175	1200	25	5.7	Negligible	67.7	12.615	6.67	2.6
M-19	0.2	1000	15	13.3	very low	26.7	12.715	9.81	32.38
M-20	0.2	1000	20	11.3	very low	28.7	12.614	7.79	18.21
M-21	0.2	1000	25	9.7	very low	29.9	12.412	5.28	13.26
M-22	0.2	1100	15	12.7	very low	31.8	12.768	7.35	18.02
M-23	0.2	1100	20	9.7	very low	37.3	12.674	5.32	14.73
M-24	0.2	1100	25	8.7	very low	39.9	12.462	8.78	11.43
M-25	0.2	1200	15	10.3	very low	35.2	12.764	7.3	4.07
M-26	0.2	1200	20	9	Negligible	42.5	12.732	5.78	4.48
M-27	0.2	1200	25	7.7	Negligible	62.9	12.543	2.71	3.74

CHAPTER 5

CONCLUSIONS AND RECOMMENDATIONS

5.1 CONCLUSIONS

The following conclusions can be drawn based on the data developed in this study:

- The local fine quartz sand with its natural grading is suitable for the manufacture of UHPC.
- Optimum superplasticizer dosage was 3.6% for a w/b of 0.15, 1.5%-2% for a w/b of 0.175 and 1%-1.5% for a w/b of 0.20.
- The water penetration depth decreased with decrease in w/b ratio and with increase in the silica fume content and cement content. However, w/b ratio was found to be most significant factor. The water penetration depth for all the mixtures was in the low permeability range.
- Like water penetration depth, the chloride permeability decreased with decrease in w/b ratio and with increase in the silica fume content and cement content. However, w/b ratio was found to be most significant factor. The silica fume content showed more significant effect on chloride permeability at a higher w/b ratio. The chloride permeability for all the mixtures was in very low or negligible range.

- The electrical resistivity for all the UHPC mixtures was very high and thus the risk of corrosion was in the negligible range. Electrical resistivity increased with increase in the silica fume content and cement content but decreased with an increase in w/b ratio.
- The pH value decreased with increase in the silica fume content and w/b ratio but pH increased with increase in the cement content. Although the mixtures had high dosages of silica fume which reduces the pH of concrete, the pH values for all the UHPC mixtures were found to be in a higher range of 12.4 to 13.01 (due to high dosages of cement content) indicating a high resistance of chloride-induced reinforcement corrosion.
- No clear trend of the variation of strength deterioration factor was observed due to short period of sulfate exposure.
- Chloride diffusion coefficients of the UHPC mixtures were found to be in the range similar to that for normal concrete although the water and chloride permeabilities were much lesser for UHPC mixtures than that for the normal concrete. The reason behind unexpected higher diffusion coefficient of UHPC mixtures may be attributed to the inaccuracy in measuring chloride concentration at concrete due to corrosion of the portions of fibers extended outside concrete.
- The I_{corr} values monitored over a period for 15 months for all 27 mixtures of UHPC were found to be less than the threshold limit of 0.3 $\mu A/cm^2$ for initiation of active reinforcement corrosion. The absence of active reinforcement corrosion in case of almost all 27 mixtures of UHPC was confirmed through visual

inspection of extracted bars and also through indirect assessment made based on electrical resistivity, pH value and chloride concentration on the rebar surface.

- The mixture M9 was found to be best-performing UHPC mixture and mixture M10 was found to be most economical UHPC mixture.

5.2 RECOMMENDATIONS

- There is a need to explore the possibility of developing UHPC using industrial waste materials for achieving economy.
- The type of exposure and testing technique (i.e. spectrophotometry) for chloride diffusion was found to be unsuitable due to inaccuracy in measuring chloride concentration at concrete surface. So, there is a need to develop a new method of exposure or/and testing technique.
- There is a need to study the effect of cyclic exposure on UHPC considering the fluctuations in local temperature, humidity and moisture conditions.

REFERENCES

1. Yanni, V.Y.G., *"Multi-scale Investigation of Tensile Creep of Ultra High Performance Concrete for Bridge Applications"*. 2009, Georgia Institute of Technology.
2. VandeVoort, T., M. Suleiman, and S. Sritharan, *"Design and Performance Verification of UHPC Piles for Deep Foundations"*, in *'Use of Ultra-High Performance Concrete in Geotechnical and Substructure Applications'*. 2008.
3. Richard, P. and M. Cheyrezy, *"Composition of reactive powder concretes"*. Cement and Concrete Research, 1995. **25**(7): p. 1501-1511.
4. Skazlic´, M. and D. Bjegovic´, *"Toughness Testing of Ultra-high Performance Fibre Reinforced Concrete".* Materials and Structures/Materiaux et Constructions, 2009. **42**: p. 1025-1038.
5. Graybeal, B.A., *"Material Property Characterization of Ultra-High Performance Concrete"*, in *FHWA-HRT-06-103*, F.H. Administration, Editor. 2006: Washington, D.C.
6. Graybeal, B.A., *"Characterization of the Behavior of Ultra-High Performance Concrete"*. 2005, Faculty of the Graduate School of the University of Maryland.
7. Ma, J. and H. Schneider, *"Properties of Ultra-High Performance Concrete"*. LACER, No.7, 2002: p. 25-32.
8. Vagelis G, P., *"Experimental investigation and theoretical modeling of silica fume activity in concrete"*. Cement and Concrete Research, 1999. **29**(1): p. 79-86.
9. Shah, S.P. and W.J. Weiss. *"Ultra High strength concrete; looking toward the future"*. in *ACI Special Proceedings from the Paul Zia Symposium*. 1998. Atlanta.
10. Long, G., X. Wang, and Y. Xie, *"Very-high-performance concrete with ultrafine powders"*. Cement and Concrete Research, 2002. **32**(4): p. 601-605.
11. Yazici, H., et al., *"Mechanical properties of reactive powder concrete containing high volumes of ground granulated blast furnace slag"*. Cement and Concrete Composites, 2010. **32**(8): p. 639-648.
12. de Larrard, F. and T. Sedran, *"Optimization of ultra-high-performance concrete by the use of a packing model"*. Cement and Concrete Research, 1994. **24**(6): p. 997-1009.
13. Konstantin, S., *"The development of a new method for the proportioning of high-performance concrete mixtures"*. Cement and Concrete Composites, 2004. **26**(7): p. 901-907.
14. Acker, P. and M. Behloul. *"Ductal Technology: a large spectrum of properties, a wide range of applications"*. in *Proceedings of the International Symposium on Ultra Reactive Powder Concrete*. 2004: Kassel University Press, Kassel, Germany, pp. 11-24.
15. Chan, Y.-W. and S.-H. Chu, *"Effect of silica fume on steel fiber bond characteristics in reactive powder concrete"*. Cement and Concrete Research, 2004. **34**(7): p. 1167-1172.

16. Hajar, Z., et al. *"Design and constrution of the world first ultra-high performance road bridges"*. in *Proceedings of the Interantional Symposium on Ultra Reactive Powder Concrete*. 2004: Kassel University Press, Kassel, Germany.
17. Kaufmann, J., F. Winnefeld, and D. Hesselbarth, *"Effect of the addition of ultrafine cement and short fiber reinforcement on shrinkage, rheological and mechanical properties of Portland cement pastes"*. Cement and Concrete Composites, 2004. **26**(5): p. 541-549.
18. Liu, J., S. Song, and L. Wang, *"Durability and micro-structure of reactive powder concrete"*. Journal Wuhan University of Technology, Materials Science Edition, 2009. **24**(3): p. 506-509.
19. Matte, V. and M. Moranville, *"Durability of reactive powder composites: Influence of silica fume on the leaching properties of very low water/binder pastes"*. Cement and Concrete Composites, 1999. **21**(1): p. 1-9.
20. Mazanec, O., D. Lowke, and P. Schiel, *"Mixing of high performance concrete: Effect of concrete composition and mixing intensity on mixing time"*. Materials and Structures/Materiaux et Constructions, 2010. **43**(3): p. 357-365.
21. Ng, K.M., C.M. Tam, and V.W.Y. Tam, *"Studying the production process and mechanical properties of reactive powder concrete: A Hong Kong study"*. Magazine of Concrete Research, 2010. **62**(9): p. 647-654.
22. Shmidt, M. and E. Fehling, *"Ultra-High Performance Concrete: Research. Development and Application in Europe"*, in *International Symposium on UHPC*. 2004: Kassel.
23. Tam, C.M., V.W.Y. Tam, and K.M. Ng, *"Optimal conditions for producing reactive powder concrete"*. Magazine of Concrete Research, 2010. **62**(10): p. 701-716.
24. Yazici, H., et al., *"Utilization of fly ash and ground granulated blast furnace slag as an alternative silica source in reactive powder concrete"*. Fuel, 2008. **87**(12): p. 2401-2407.
25. Garas, V.Y., L.F. Kahn, and K.E. Kurtis, *"Short-term tensile creep and shrinkage of ultra-high performance concrete"*. Cement and Concrete Composites, 2009. **31**(3): p. 147-152.
26. Tam, C.M., V.W.Y. Tam, and K.M. Ng, *"Assessing drying shrinkage and water permeability of reactive powder concrete produced in Hong Kong"*. Construction and Building Materials, 2012. **26**(1): p. 79-89.
27. Loukili, A., A. Khelidj, and P. Richard, *"Hydration Kinetics, Change of Relative Humidity, and Autogenous Shrinkage of Ultra-High-Strength Concrete",*. Cement and Concrete Research, 1999. **29**(4, April): p. 577-584.
28. Graybeal, B.A. and J.L. Hartmann, *"Strength and Durability of Ultra-High Performance Concrete"*, in *Concrete Bridge Conference*. 2003, Portland Cement Association.
29. Gilliland, S.K. *"Reactive Powder Concrete (UHPC), A New Material for Prestressed Concrete Bridge Girders"*. in *Structures Congress – Proceedings, Building an International Community of Structural Engineers*. 1996.
30. Buitelaar, P. *"Heavy Reinforced Ultra-Reactive Powder Concrete"*. in *Proceedings of the International Symposium on Ultra Reactive Powder Concrete*. 2004: Kassel University Press, Kassel, Germany.

31. ASTM, *"Standard specification for steel fiber reinforced concrete"*, in *ASTM A 820-90*. 1990.
32. ASTM, *"Standard Test Method for Flow of Hydraulic Cement Mortar"*, in *ASTM C1437 - 07* 2007.
33. Jenq, Y. and S.P. Shah, *"Two Parameter Model for Concrete".* Journal of Engineering Mechanics, 1985. **111**(10): p. 1227-1241.
34. *ASTM C 39, "Standard Test Method for Compressive Strength of Cylindrical Concrete Specimens"*. Annual Book of ASTM Standards. Vol. 4.02. 2005, Philadelphia: American Society for Testing and Materials.
35. Gowripalan, N. and R.I. Gilbert, *"Design Guidelines for UHPC Prestressed Concrete Beams"*. 2000, The University of New South Wales.
36. ACI, *"Building Code Requirements for Reinforced Concrete (ACI 318M-95) and Commentary (ACI 318RM-95),"* in *Committe 318*. 1995. p. 371 pp.
37. Acker, P. and Behloul, M., "Ductal technology: a large spectrum of properties, a wide range of applications,", *Proceedings of the International Symposium on Ultra Reactive Powder Concrete*, Kassel University Press, Kassel, Germany, 2004, pp. 11-24.
38. Buitelaar, P., "Heavy reinforced ultra-Reactive Powder Concrete," *Proceedings of the International Symposium on Ultra Reactive Powder Concrete*, Kassel University Press, Kassel, Germany, 2004.
39. Hajar, Z., Simon, A., Lecointre, D., and Petitjean, J., "Design and construction of the world first ultra-high performance road bridges", *Proceedings of the International Symposium on Ultra Reactive Powder Concrete*, Kassel University Press, Kassel, Germany, 2004, pp. 39-48.
40. Larrard, F. and Sedran, T., "Optimization of ultra-high-performance concrete by the use of a packing model", *Cement and Concrete Research*, 24(6), 1994, pp. 997-1009.
41. Long, G., Wang, X., and Xie, Y., "Very-high-performance concrete with ultrafine powders", *Cement and Concrete Research*, 32, 2002, pp. 601-605.
42. Ma, J. and Schneider, H., "Properties of ultra-high-performance concrete", *LACER*, No.7, 2002, pp. 25-32.
43. Papadakis, V., "Experimental investigation and theoretical modeling of silica fume activity in concrete", *Cement and Concrete Research*, 29, 1999, pp. 79-86.
44. Richard, P. and Cheyrezy, M., "Composition of reactive powder concretes" *Cement and Concrete Research*, 25(7), 1995, pp. 1501-1511.
45. Schmidt, M., Fehling, E., Teichmann, T., Bunje, K., and Bornemann, R., "Ultra Reactive Powder Concrete: Perspective for the precast concrete industry", *Beton und Fertigteil-Technik*, 3, 2003, pp. 16-29.
46. Shah, S.P. and Weiss, W.J., "Ultra high strength concrete; looking toward the future", *ACI special proceedings from the Paul Zia symposium*, Atlanta, 1998.
47. Sobolev, K., "The development of a new method for the proportioning of high-performance concrete mixtures", *Cement & Concrete Composites*, 26, 2004, pp. 901-907.
48. Stern, M. and Geary, A.L. "Electrochemical polarization-a theoretical analysis of the shape of polarization curves", *Journal of the Electrochemical Society*, 104, 1957, pp. 56-63.

49. Habib. M. Zein Al-Abidien "Aggregates in Saudi Arabia: A survey of their properties and suitability for concrete", Materials and Structures, 1987, 20, 260-264.
50. Vernet, C.P., "Ultra-durable concretes: structure at the micro-and nanoscale", *Materials Research Society*, 29(5), 2004, pp. 324-327.
51. Maslehuddin, M., Rasheeduzzafar, Page, C. L. Al-Mana, A. I., "Influence of Some Parameters Relevant to Arabian Gulf Environment on Reinforcement Corrosion," *Arabian Journal for Science and Engineering*: Theme Issue on Corrosion and its Prevention, April 1995, pp. 239-257.
52. N. Roux, C. Andrade and M. A. Sanjuan, "Experimental study of durability of Reactive Powder Concrete" *Journal of materials in civil engineering,* 1996.
53. Semion Zhutovsky, Konstantin Kovler, "Effect of internal curing on durability-related properties of high performance concrete" *Cement and Concrete Research,* 2011.
54. Amr S. El-Dieb "Mechanical, durability and microstructural characteristics of Ultra-high strength self-compacting concrete incorporating steel fibers" *Materials and Design*, 2009.
55. R.D. Toledo Filho, E.A.B. Koenders, S. Formagini, E.M.R. Fairbairn, "Performance assessment of Ultra High Performance Fiber Reinforced Cementitious Composites in view of sustainability" *Materials and Design*, 2012.
56. C.M. Tam, Vivian W.Y. Tam, K.M. Ng, "Assessing drying shrinkage and water permeability of reactive powder concrete produced in Hong Kong" *Construction and Building Materials*, 2012.
57. Benjamin A. Graybeal, Joseph L. Hartmann, "Strength and Durability of Ultra-High Performance Concrete", *Concrete bridge Conference,* 2003.
58. Benjamin A. Graybeal, Jussara Tanesi, "Durability of Ultra–High Performance Concrete", *Journal of materials in Civil Engineering*, 2007.
59. LIU Juanhong, SONG Shaomin, WANG Lin, "Durability and Micro-structure of Reactive Powder Concrete", *Journal of Wuhan University of Technolotgy-Mater. Sci. Ed.,* June 2009.
60. The Concrete Society, *Permeability testing of site concrete- A review of methods and experience,* in *technical report No.31*, 1987, p.75.
61. Ahmad, S., *Reinforcement Corrosion in Concrete Structures, Its Monitoring and Service Life Prediction—a Review*. Cement and Concrete Composites, 2003. **25**(4–5): p. 459-471.
62. Broomfield, J.P., *Corrosion of Steel in Concrete: Understanding, Investigation and Repair*. 2003: Spoon Press.
63. American Society for Testing and Materials, *Standard Test Method for Electrical Indication of Concrete's Ability to Resist Chloride Ion Penetration*, in *ASTM C 426, Annual Book of ASTM Standards, Vol. 4.01*. 1997.
64. American Society for Testing and Materials, *Standard Test Method for Electrical Indication of Concrete's Ability to Resist Chloride Ion Penetration*, in *ASTM C 1202, Annual Book of ASTM Standards, Vol. 4.02*. 1994: Philadelphia.
65. Bungey, J.H., *The testing of concrete in structures.* 1989, London: Surrey University Press, London.

66. ASTM C 876, *"Standard Test Method for Half-cell Potentials of Uncoated Reinforcing Steel in Concrete"*. Annual Book of ASTM Standards, Vol. 4.02, American Society for Testing and Materials, West Conshohocken, 2005.
67. Stern, M. and A.L. Geary, *A Theoretical Analysis of the Slope of the Polarization Curves.* Journal of Electrochemical Society, 1957. **104**: p. 56.
68. Lambert, P., C.L.Page and P.R.W. Vassie, *Investigations of reinforcement corrosion: Electrochemical monitoring of steel in chloride contaminated concrete.* Materials and Structures, 1991. 24: p.351-358.
69. Saheed K.A., A Study on Developing SCC Utilizing Indigenous Natural and Industrial Waste Materials, MS Thesis, KFUPM.
70. Azhar M., Evaluation of ternary cements for improving concrete durability, MS Thesis, KFUPM.
71. Zubair A., A study on mechanical properties of UHPC utilizing local quartz sand, MS Thesis, KFUPM.
72. Najamuddin S.K., Production of medium to low strength concrete utilizing indigenous waste products, MS Thesis, KFUPM.
73. Salami B.A., Self-compacting concrete utilizing local materials, MS Thesis, KFUPM.
74. Moinuddin M.K., Mechanical Properties and Durability of Quaternary Cement Concretes, MS Thesis, KFUPM.
75. Al Kutti W.A., Compliance Criteria for quality concrete, MS Thesis, KFUPM.
76. S.T. Lee, H.Y. Moon and R.N. Swamy, "Sulfate attack and role of silica fume in resisting strength loss", *Cement and Concrete Composites*, 2003.

APPENDIX

```
In[1]:= data1 = {{M1, 0.343, 0.231, 0.152, 0.1, 0.055},
        {M2, 0.325, 0.15, 0.073, 0.067, 0.055}, {M3, 0.32, 0.128, 0.065, 0.05, 0.04},
        {M4, 0.276, 0.11, 0.065, 0.05, 0.04}, {M5, 0.276, 0.086, 0.05, 0.035, 0.028},
        {M6, 0.3, 0.061, 0.039, 0.03, 0.025}, {M7, 0.348, 0.081, 0.072, 0.057, 0.051},
        {M8, 0.278, 0.065, 0.053, 0.042, 0.031},
        {M9, 0.266, 0.045, 0.039, 0.035, 0.021},
        {M10, 0.377, 0.263, 0.18, 0.13, 0.085}, {M11, 0.38, 0.163, 0.091, 0.085, 0.073},
        {M12, 0.39, 0.147, 0.084, 0.075, 0.067}, {M13, 0.31, 0.16, 0.092, 0.075, 0.05},
        {M14, 0.324, 0.11, 0.077, 0.059, 0.055}, {M15, 0.349, 0.09, 0.072, 0.06, 0.055},
        {M16, 0.387, 0.083, 0.076, 0.061, 0.053}, {M17, 0.292, 0.071,
         0.056, 0.046, 0.031}, {M18, 0.287, 0.051, 0.044, 0.036, 0.017},
        {M19, 0.455, 0.291, 0.2, 0.15, 0.109}, {M20, 0.423, 0.178, 0.128, 0.102, 0.089},
        {M21, 0.45, 0.17, 0.117, 0.094, 0.091}, {M22, 0.425, 0.19, 0.13, 0.099, 0.085},
        {M23, 0.4, 0.15, 0.107, 0.093, 0.081}, {M24, 0.414, 0.15, 0.1, 0.087, 0.075},
        {M25, 0.444, 0.101, 0.091, 0.083, 0.074}, {M26, 0.38, 0.092,
         0.078, 0.066, 0.058}, {M27, 0.36, 0.081, 0.068, 0.059, 0.05}};
    d = Table[-7.5 + 10 i, {i, 1, 5}]

Out[2]= {2.5, 12.5, 22.5, 32.5, 42.5}

In[3]:= Do[ExpData[i] = Table[{d[[k]], data1[[i, k + 1]]}, {k, 1, 5}], {i, 1, 27}]
    Model0 = c0 (1 - Erf[x / (2 Sqrt[180 Dc])]);
    FindFit[ExpData[1], Model0, {c0, Dc}, x]

Out[5]= {c0 → 0.361549, Dc → 2.30275}

In[6]:= Do[sol = FindFit[ExpData[i], Model0, {c0, Dc}, x];
     Model[i] = Model0 /. sol;
     Print["Model No: ", data1[[i, 1]]];
     Print["Estimated C_o = ", c0 /. sol, "% wt of cement"];
     Print["Estimated D_C = ", (Dc / 24 / 3600) /. sol, " mm^2/sec"];
     Print[TableForm[{{"Depth(mm)", "C-experimental", "C-computed"}}]];
     Print[TableForm[Table[{d[[k]], "      ",
         data1[[i, k + 1]], "    ", Model[i] /. {x → d[[k]]}}, {k, 1, 5}]]];
     p1[i] = ListPlot[ExpData[i], PlotStyle → PointSize[0.02],
       DisplayFunction → Identity];
     p2[i] = Plot[Model[i], {x, 0, 42.5}];
     Print["**********************************************"], {i, 1, 27}]

Model No: M1

Estimated C_o = 0.361549% wt of cement

Estimated D_C = 0.0000266522 mm^2/sec

Depth(mm)    C-experimental    C-computed

2.5              0.343           0.336533
12.5             0.231           0.240135
22.5             0.152           0.157104
32.5             0.1             0.0936381
42.5             0.055           0.0505874

**********************************************

Model No: M2
```

Estimated C_o = 0.341153% wt of cement

Estimated D_C = 0.0000128382 mm^2/sec

Depth(mm)	C-experimental	C-computed
2.5	0.325	0.307188
12.5	0.15	0.181364
22.5	0.073	0.0887622
32.5	0.067	0.0354348
42.5	0.055	0.0114067

****

Model No: M3

Estimated C_o = 0.349947% wt of cement

Estimated D_C = 8.81243×10^{-6} mm^2/sec

Depth(mm)	C-experimental	C-computed
2.5	0.32	0.307944
12.5	0.128	0.157561
22.5	0.065	0.0609395
32.5	0.05	0.0173722
42.5	0.04	0.00358941

****

Model No: M4

Estimated C_o = 0.292552% wt of cement

Estimated D_C = 0.0000106718 mm^2/sec

Depth(mm)	C-experimental	C-computed
2.5	0.276	0.260622
12.5	0.11	0.144127
22.5	0.065	0.0634375
32.5	0.05	0.0217802
42.5	0.04	0.0057524

****

Model No: M5

Estimated C_o = 0.316734% wt of cement

Estimated D_C = 5.64257×10^{-6} mm^2/sec

Depth(mm)	C-experimental	C-computed
2.5	0.276	0.269326
12.5	0.086	0.1094
22.5	0.05	0.0283273
32.5	0.035	0.00448443
42.5	0.028	0.000423267

****

Model No: M6

Estimated C_o = 0.376936% wt of cement

Estimated D_C = 2.88625×10^{-6} mm^2/sec

Depth(mm)	C-experimental	C-computed

2.5	0.3	0.298493
12.5	0.061	0.0705164
22.5	0.039	0.00662037
32.5	0.03	0.000227419
42.5	0.025	2.74159×10^{-6}

****

Model No: M7

Estimated C_o = 0.412316% wt of cement

Estimated D_C = 4.19034×10^{-6} mm^2/sec

Depth(mm)	C-experimental	C-computed
2.5	0.348	0.340847
12.5	0.081	0.112792
22.5	0.072	0.0200975
32.5	0.057	0.00182107
42.5	0.051	0.0000812739

****

Model No: M8

Estimated C_o = 0.332761% wt of cement

Estimated D_C = 3.9543×10^{-6} mm^2/sec

Depth(mm)	C-experimental	C-computed
2.5	0.278	0.273413
12.5	0.065	0.0864164
22.5	0.053	0.0141352
32.5	0.042	0.00112615
42.5	0.031	0.0000422647

****

Model No: M9

Estimated C_o = 0.342035% wt of cement

Estimated D_C = 2.45701×10^{-6} mm^2/sec

Depth(mm)	C-experimental	C-computed
2.5	0.266	0.265042
12.5	0.045	0.0522467
22.5	0.039	0.0034407
32.5	0.035	0.0000687701
42.5	0.021	3.98308×10^{-7}

****

Model No: M10

Estimated C_o = 0.391018% wt of cement

Estimated D_C = 0.0000339888 mm^2/sec

Depth(mm)	C-experimental	C-computed
2.5	0.377	0.367053
12.5	0.263	0.273966
22.5	0.18	0.191183
32.5	0.13	0.124158
42.5	0.085	0.0747526

****

Model No: M11

Estimated C_o = 0.38909% wt of cement

Estimated D_C = 0.000013904 mm^2/sec

Depth(mm)	C-experimental	C-computed
2.5	0.38	0.351859
12.5	0.163	0.213138
22.5	0.091	0.108664
32.5	0.085	0.0459507
42.5	0.073	0.0159473

****

Model No: M12

Estimated C_o = 0.414968% wt of cement

Estimated D_C = 9.86446×10^{-6} mm^2/sec

Depth(mm)	C-experimental	C-computed
2.5	0.39	0.367873
12.5	0.147	0.197303
22.5	0.084	0.0825635
32.5	0.075	0.0263665
42.5	0.067	0.00632983

****

Model No: M13

Estimated C_o = 0.317887% wt of cement

Estimated D_C = 0.0000178548 mm^2/sec

Depth(mm)	C-experimental	C-computed
2.5	0.31	0.29103
12.5	0.16	0.189402
22.5	0.092	0.107985
32.5	0.075	0.0533612
42.5	0.05	0.0226711

****

Model No: M14

Estimated C_o = 0.343938% wt of cement

Estimated D_C = 9.36791×10^{-6} mm^2/sec

Depth(mm)	C-experimental	C-computed
2.5	0.324	0.30389
12.5	0.11	0.159585
22.5	0.077	0.0644764
32.5	0.059	0.0195761
42.5	0.055	0.00439639

****

Model No: M15

Estimated C_o = 0.403341% wt of cement

Estimated D_C = 4.99708×10^{-6} mm^2/sec

Depth (mm)	C-experimental	C-computed
2.5	0.349	0.339237
12.5	0.09	0.12747
22.5	0.072	0.0286833
32.5	0.06	0.00368564
42.5	0.055	0.000263017

****

Model No: M16

Estimated C_o = 0.469873% wt of cement

Estimated D_C = 3.56163×10^{-6} mm^2/sec

Depth (mm)	C-experimental	C-computed
2.5	0.387	0.381654
12.5	0.083	0.110412
22.5	0.076	0.0152896
32.5	0.061	0.000947438
42.5	0.053	0.0000253405

****

Model No: M17

Estimated C_o = 0.346295% wt of cement

Estimated D_C = 4.22074×10^{-6} mm^2/sec

Depth (mm)	C-experimental	C-computed
2.5	0.292	0.286483
12.5	0.071	0.095332
22.5	0.056	0.0171631
32.5	0.046	0.00157953
42.5	0.031	0.0000719841

****

Model No: M18

Estimated C_o = 0.365823% wt of cement

Estimated D_C = 2.59956×10^{-6} mm^2/sec

Depth (mm)	C-experimental	C-computed
2.5	0.287	0.285705
12.5	0.051	0.0601751
22.5	0.044	0.00451495
32.5	0.036	0.000110167
42.5	0.017	8.36008×10^{-7}

****

Model No: M19

Estimated C_o = 0.460504% wt of cement

Estimated D_C = 0.0000323788 mm^2/sec

Depth (mm)	C-experimental	C-computed

2.5	0.455	0.431589
12.5	0.291	0.319435
22.5	0.2	0.220271
32.5	0.15	0.140815
42.5	0.109	0.0831213

****

Model No: M20

Estimated C_o = 0.415855% wt of cement

Estimated D_C = 0.0000182107 mm^2/sec

Depth(mm)	C-experimental	C-computed
2.5	0.423	0.381065
12.5	0.178	0.249277
22.5	0.128	0.143246
32.5	0.102	0.0715589
42.5	0.089	0.0308324

****

Model No: M21

Estimated C_o = 0.456339% wt of cement

Estimated D_C = 0.0000132642 mm^2/sec

Depth(mm)	C-experimental	C-computed
2.5	0.45	0.411637
12.5	0.17	0.245641
22.5	0.117	0.122289
32.5	0.094	0.0500084
42.5	0.091	0.0166128

****

Model No: M22

Estimated C_o = 0.423335% wt of cement

Estimated D_C = 0.0000180237 mm^2/sec

Depth(mm)	C-experimental	C-computed
2.5	0.425	0.387737
12.5	0.19	0.252962
22.5	0.13	0.144768
32.5	0.099	0.0719111
42.5	0.085	0.0307585

****

Model No: M23

Estimated C_o = 0.398205% wt of cement

Estimated D_C = 0.0000147307 mm^2/sec

Depth(mm)	C-experimental	C-computed
2.5	0.4	0.361182
12.5	0.15	0.222693
22.5	0.107	0.116751
32.5	0.093	0.0513421
42.5	0.081	0.0187513

****

Model No: M24

Estimated C_o = 0.42779% wt of cement

Estimated D_c = 0.0000114274 mm^2/sec

Depth(mm)	C-experimental	C-computed
2.5	0.414	0.382661
12.5	0.15	0.217025
22.5	0.1	0.0995455
32.5	0.087	0.0362482
42.5	0.075	0.0103435

****

Model No: M25

Estimated C_o = 0.528012% wt of cement

Estimated D_c = 4.07301×10^{-6} mm^2/sec

Depth(mm)	C-experimental	C-computed
2.5	0.444	0.435201
12.5	0.101	0.14085
22.5	0.091	0.0240807
32.5	0.083	0.00205055
42.5	0.074	0.0000841733

****

Model No: M26

Estimated C_o = 0.445976% wt of cement

Estimated D_c = 4.47713×10^{-6} mm^2/sec

Depth(mm)	C-experimental	C-computed
2.5	0.38	0.371151
12.5	0.092	0.129102
22.5	0.078	0.0252262
32.5	0.066	0.00262497
42.5	0.058	0.000141113

****

Model No: M27

Estimated C_o = 0.434205% wt of cement

Estimated D_c = 3.7437×10^{-6} mm^2/sec

Depth(mm)	C-experimental	C-computed
2.5	0.36	0.354654
12.5	0.081	0.107122
22.5	0.068	0.0160924
32.5	0.059	0.00112769
42.5	0.05	0.0000356027

****

VITAE

Name : Ahmed Yousuf Shareef

Nationality : Indian

Date of Birth : 26th November, 1988

Permanent Address : H. No.: 8-1-366/A/35

Janaki Nagar Colony, Tolichowki,

Hyderabad – 500008, Andhra Pradesh, INDIA

Email : yousuf_shareef01@yahoo.co.in

Phone : +966-536342278

Degrees:

Bachelor of Engineer in Civil Engineering from Osmania University (Sept. 2006 – April 2010).

Experience:

Research Assistant in Civil Engineering Department of King Fahd University of Petroleum & Minerals (KFUPM) (Feb 2011 – Sep 2013).**)**